NUREG/CR-6773
LA-UR-02-6786

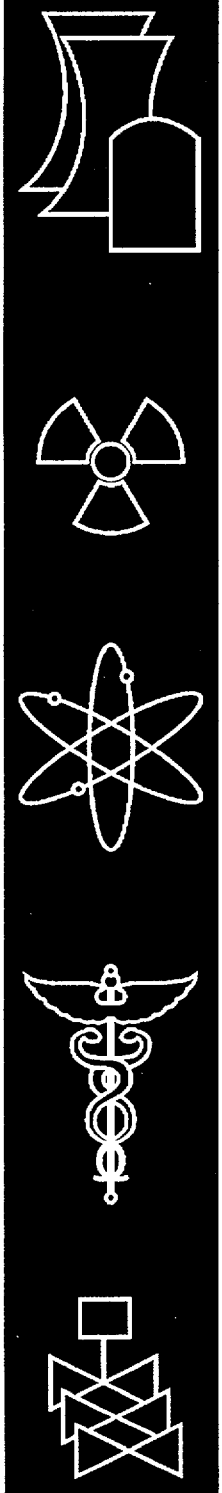

GSI-191: Integrated Debris-Transport Tests in Water Using Simulated Containment Floor Geometries

Los Alamos National Laboratory

U.S. Nuclear Regulatory Commission
Office of Nuclear Regulatory Research
Washington, DC 20555-0001

AVAILABILITY OF REFERENCE MATERIALS IN NRC PUBLICATIONS

NRC Reference Material

As of November 1999, you may electronically access NUREG-series publications and other NRC records at NRC's Public Electronic Reading Room at http://www.nrc.gov/reading-rm.html. Publicly released records include, to name a few, NUREG-series publications; *Federal Register* notices; applicant, licensee, and vendor documents and correspondence; NRC correspondence and internal memoranda; bulletins and information notices; inspection and investigative reports; licensee event reports; and Commission papers and their attachments.

NRC publications in the NUREG series, NRC regulations, and *Title 10, Energy*, in the Code of *Federal Regulations* may also be purchased from one of these two sources.

1. The Superintendent of Documents
   U.S. Government Printing Office
   Mail Stop SSOP
   Washington, DC 20402–0001
   Internet: bookstore.gpo.gov
   Telephone: 202-512-1800
   Fax: 202-512-2250
2. The National Technical Information Service
   Springfield, VA 22161–0002
   www.ntis.gov
   1–800–553–6847 or, locally, 703–605–6000

A single copy of each NRC draft report for comment is available free, to the extent of supply, upon written request as follows:

Address: Office of the Chief Information Officer,
Reproduction and Distribution
Services Section
U.S. Nuclear Regulatory Commission
Washington, DC 20555-0001
E-mail: DISTRIBUTION@nrc.gov
Facsimile: 301–415–2289

Some publications in the NUREG series that are posted at NRC's Web site address http://www.nrc.gov/reading-rm/doc-collections/nuregs are updated periodically and may differ from the last printed version. Although references to material found on a Web site bear the date the material was accessed, the material available on the date cited may subsequently be removed from the site.

Non-NRC Reference Material

Documents available from public and special technical libraries include all open literature items, such as books, journal articles, and transactions, *Federal Register* notices, Federal and State legislation, and congressional reports. Such documents as theses, dissertations, foreign reports and translations, and non-NRC conference proceedings may be purchased from their sponsoring organization.

Copies of industry codes and standards used in a substantive manner in the NRC regulatory process are maintained at—

The NRC Technical Library
Two White Flint North
11545 Rockville Pike
Rockville, MD 20852–2738

These standards are available in the library for reference use by the public. Codes and standards are usually copyrighted and may be purchased from the originating organization or, if they are American National Standards, from—

American National Standards Institute
11 West 42nd Street
New York, NY 10036–8002
www.ansi.org
212–642–4900

Legally binding regulatory requirements are stated only in laws; NRC regulations; licenses, including technical specifications; or orders, not in NUREG-series publications. The views expressed in contractor-prepared publications in this series are not necessarily those of the NRC.

The NUREG series comprises (1) technical and administrative reports and books prepared by the staff (NUREG–XXXX) or agency contractors (NUREG/CR–XXXX), (2) proceedings of conferences (NUREG/CP–XXXX), (3) reports resulting from international agreements (NUREG/IA–XXXX), (4) brochures (NUREG/BR–XXXX), and (5) compilations of legal decisions and orders of the Commission and Atomic and Safety Licensing Boards and of Directors' decisions under Section 2.206 of NRC's regulations (NUREG–0750).

NUREG/CR-6773
LA-UR-02-6786

GSI-191: Integrated Debris-Transport Tests in Water Using Simulated Containment Floor Geometries

Manuscript Completed: November 2002
Date Published: December 2002

Prepared by
D. V. Rao, C. Shaffer,* B. C. Letellier,
A. K. Maji,** L. Bartlein

Los Alamos National Laboratory
Los Alamos, NM 87545

Subcontractors:
*ARES Corporation
851 University Blvd. S.E.
Suite 100
Albuquerque, NM 87106

**University of New Mexico
Department of Civil Engineering
Albuquerque, NM 87110

B. P. Jain and M. L. Marshall, NRC Project Managers

Prepared for
Division of Engineering Technology
Office of Nuclear Regulatory Research
U.S. Nuclear Regulatory Commission
Washington, DC 20555-0001
NRC Job Code Y6041

ABSTRACT

This report documents the results of experiments conducted to examine insulation debris transport under flow and geometry configurations typical of those found in pressurized water reactors (PWRs). This work was part of a comprehensive research program to support the resolution of Generic Safety Issue (GSI)-191. GSI-191 addresses the potential for debris accumulation on PWR sump screens and consequent loss of the emergency core cooling system pump net positive suction head following a loss-of-coolant accident. Among the GSI-191 program research tasks is the development of a method to estimate debris transport in PWR containments and the quantity of debris that would accumulate on the sump screen for use in plant-specific evaluations. Predicting the transport of debris within the sump pool is an essential part of that methodology.

The analytical method proposed by the Los Alamos National Laboratory to predict debris transport within the pool is to use computational fluid dynamics combined with experimental debris transport data to predict debris transport and accumulation on the screen. The three-dimensional tank tests were conducted to test debris transport under conditions that simulate flow regimes relevant to a typical PWR plant. These tests provided insights into the relative importance of the various debris-transport mechanisms and are directly applicable to creating or validating models capable of estimating debris transport within a PWR plant containment sump.

CONTENTS

Figures

Tables

EXECUTIVE SUMMARY

Experiments were conducted to examine insulation debris transport under flow conditions and geometric configurations typical of those found in pressurized water reactors (PWRs). This work was part of a comprehensive research program to support the resolution of Generic Safety Issue (GSI) 191. GSI-191 addresses the potential for debris accumulation on the PWR sump screens and consequent loss of the emergency core cooling system pump net positive suction head following a loss-of-coolant accident. Among the GSI-191 program research tasks is the development of a method for estimating debris transport in PWR containments to estimate the quantity of debris that would accumulate on the sump screen for use in plant-specific evaluations. Predicting the transport of debris within the sump pool is a major part of that methodology. The analytical method proposed by Los Alamos National Laboratory to predict debris transport within the pool is to use computational fluid dynamics (CFD) combined with experimental debris-transport data to predict debris transport and accumulation on the screen. CFD simulations of actual plant containment designs would provide flow data for a postulated accident in that plant, e.g., three-dimensional patterns of flow velocities and flow turbulence. Small-scale experiments would determine parameters defining the debris-transport characteristics for each type of debris.

Based on a determination of the physical processes governing the transport of debris on the containment floor, two types of small-scale tests were conducted to support the analytical methods: (1) separate-effects tests [4] and (2) three-dimensional (3-D) tank tests (reported here). These tests were conducted at the University of New Mexico Open-Channel Hydrology Laboratory. The separate-effects tests, which were conducted primarily in a large linear flume, measured several specific transport properties for a variety of insulation debris. The primary goal of the flume tests was to measure the minimum flow velocities required to initiate specific types of motion for each debris type. The 3-D tank tests were conducted in a large tank with provisions to simulate a variety of PWR containment and sump features. In this manner, debris transport was studied in such a way that all the separate effects studied in the separate-effects testing could be integrated into tests that were more typical of PWR geometries. The important physical processes that took place in the 3-D tank tests included settling of debris in turbulent pools, tumbling/sliding of settled debris along the floor, reentrainment of debris from the containment floor, lifting of debris over structural impediments, retention of debris on vertical screens, and the further disintegration of debris as a result of sump-pool dynamics. The integrated phenomena included early debris transport as the sump filled and later debris transport after a steady-state flooded condition was achieved.

The flow regimes established during the tests included quiescent, turbulent, and rotational flow in geometries comparable to the complexity of PWR containment floors. The tests provided insights into the relative importance of the various debris-transport mechanisms and are directly applicable to creating or validating models capable of estimating debris transport within a PWR plant containment sump. Further, these tests provided debris particle tracks and bulk debris transport data that are necessary to validate CFD code applications to estimate debris transport within a PWR plant containment sump.

ACKNOWLEDGEMENT

The US Nuclear Regulatory Commission, Office of Nuclear Regulatory Research, sponsored the work reported here. Dr. Bhagwat Jain and Mr. Michael Marshall, RES/DET, were the NRC Project Managers for this task. They provided critical technical direction and provided continuing review of the progress of work documented in this report.

The authors would particularly like to acknowledge the contributions of Dr. Ashok Ghosh and Mr. Thomas Escobedo of the University of New Mexico (UNM). These individuals helped design, construct, and conduct the debris-transport tests at UNM and assess the importance of the various debris-transport mechanisms and mapped the flow velocities within the tank for a variety of conditions.

The authors would also like to acknowledge the work of Ms. Juanita Lujan, and Ms. Mary Timmers of Los Alamos National Laboratory for their valuable contribution in preparation and production of this report. Finally, Ms. Nancy Butner (ARES) provided the program coordination necessary to ensure that tests were performed within the resources allocated and that all program deadlines are met.

ABBREVIATIONS

AJITs	Air Jet Impact Tests
BWROG	Boiling Water Reactor Owners' Group
CEESI	Colorado Engineering Experiment Station, Inc.
CFD	Computational Fluid Dynamics
CS	Containment Spray
ECCS	Emergency Core Coolant System
GSI	Generic Safety Issue
LANL	Los Alamos National Laboratory
LDFG	Low-Density Fiberglass
LOCA	Loss-of-Coolant Accident
NPSH	Net Positive Suction Head
NRC	U. S. Nuclear Regulatory Commission
PIRT	Phenomena Identification and Ranking Table
PWR	Pressurized Water Reactor
RMI	Reflective Metallic Insulation
SS	Stainless Steel
UNM	University of New Mexico

UNITS FORMULA

Convert From	To	First Add	Multiply By
ft	m	0	3.048E-01
ft^3	m^3	0	2.831E-02
in.	m	0	2.540E-02
gallon	m^3	0	3.785E-03
gpm	m^3/min	0	3.785E-03
ft/s	m/s	0	3.048E-01
°F	°C	-32	5.556E-01

1.0 INTRODUCTION

1.1 Background

In the event of a loss-of-coolant accident (LOCA) within the containment of a pressurized water reactor (PWR), thermal insulation and other materials (e.g., coatings and concrete) in the vicinity of the break will be damaged and dislodged. Some of this material will be deposited in the pool of water that would accumulate on the containment floor by the steam/water flows induced by the break and the containment sprays. Within this pool of water, debris transport would be governed by various physical processes, including the settling of debris in agitated pools, tumbling/sliding of settled debris along the floor, reentrainment of debris from the containment floor, lifting of debris over structural impediments, retention of debris on vertical screens, and destruction of debris as a result of sump-pool flow dynamics, thermal effects, and chemical effects. As a result of these processes, a fraction of the deposited debris ultimately would be transported to the recirculation (or emergency) sump and accumulate on the screen. The excessive head loss caused by the debris bed buildup could exceed the net positive suction head (NPSH) margin of the emergency core coolant system (ECCS) or containment spray (CS) pumps. For sump screens that are only partially submerged by water on the containment floor, excessive head loss across the debris bed could prevent water from entering the sump. Generic Safety Issue (GSI)-191 titled "Assessment of Debris Accumulation on PWR Sump Performance" addresses the issue of debris generation, transport, and accumulation on the PWR sump screen and its subsequent effect on ECCS performance. Los Alamos National Laboratory (LANL) has been supporting the US Nuclear Regulatory Commission (NRC) in the resolution of GSI-191.

A parametric evaluation was performed [1] as part of the GSI-191 study to demonstrate the credibility of recirculation sump clogging for operating PWRs. For each of the 69 representative models of domestic PWRs, the minimum amount of debris accumulation on the sump screen needed to exceed the required NPSH margin for the ECCS and CS pumps was determined using a mixture of generic and plant-specific data. The generic transport fractions used in that evaluation were based on existing research [2]. The integrated tests reported here were underway when the parametric evaluation was initiated, and preliminary integrated testing provided insights into PWR sump-pool debris-transport fractions for the parametric evaluation.

Among the GSI-191 program research tasks is the development of a method for estimating debris transport in PWR containments. The NRC sponsored the formation of a Phenomena Identification and Ranking Table (PIRT) panel to identify and rank the phenomena and processes associated with the transport of debris in a PWR containment following the initiation of one or more accident sequences. The PIRT [3] has been used to support decision-making regarding analytical, experimental, and modeling efforts related to debris transport within PWR containments. One aspect of the panel's evaluation was the identification of the phenomena and processes pertinent to the transport of debris in the containment sump pool during each phase (blowdown, post-blowdown, and sump operation) of the accident scenario. The thermal-hydraulic processes affecting debris transport in the sump pool and the debris-transport/deposition processes identified by the panel are shown in Figures 1-1 and 1-2, respectively. The panel was consulted to support the design of the test apparatus used to conduct the integrated tests.

Consistent with PIRT panel recommendations, the NRC first conducted a series of separate-effects tests to study debris behavior when it is subjected separately to the various physical processes governing the transport of debris on the containment floor [4]. The separate-effects tests were conducted primarily in a large linear flume in which flow uniformity and turbulence were controlled. Several specific transport characteristics, such as the minimum flow velocity required to initiate specific types of motion, were measured for a variety of insulation debris. The separate effects data were pertinent to understanding the debris transport encountered in the integrated debris-transport tests.

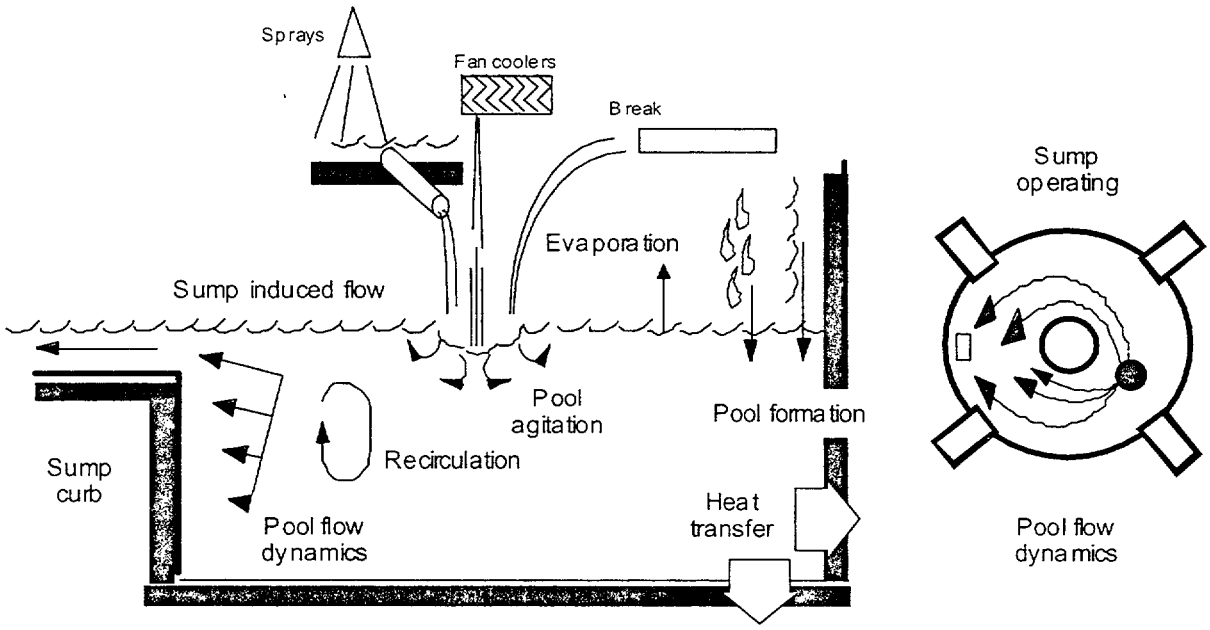

Figure 1-1 Thermal-Hydraulic Processes Affecting Debris in the Sump Pool

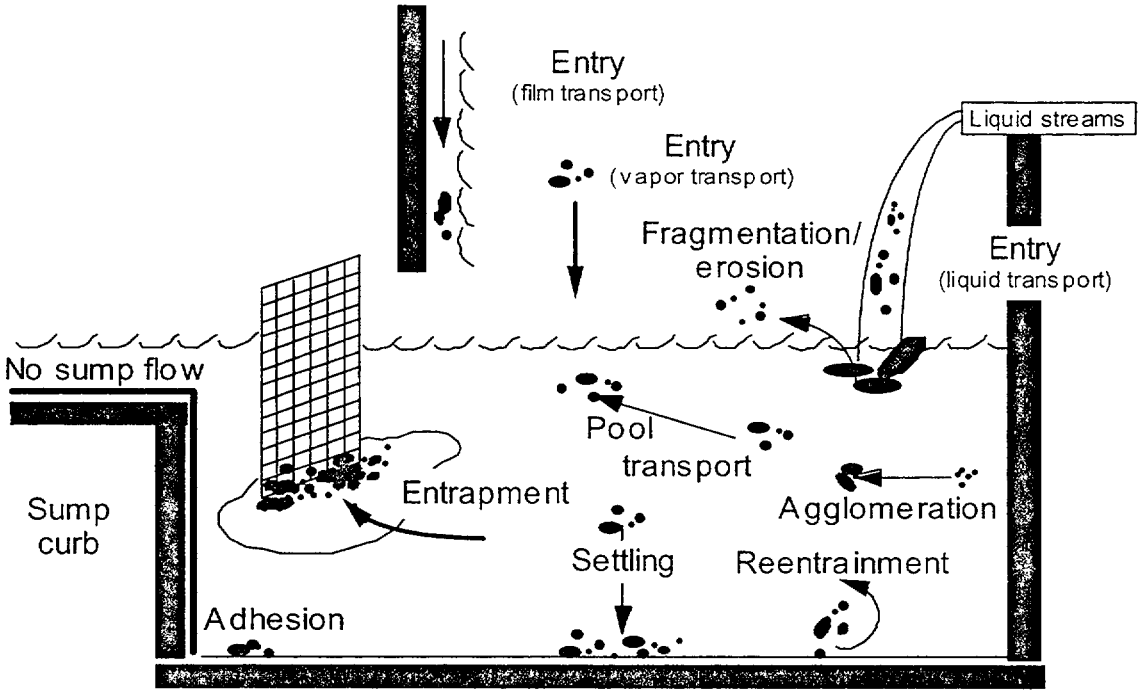

Figure 1-2 Transport/Deposition Processes for Debris in the Sump Pool

The debris-transport methodology developed by LANL for estimating debris transport in PWR containments relies on an approximate method for coupling the results of computational fluid dynamics (CFD) simulations with the experimental debris-transport data to predict debris transport and accumulation on the screen. CFD simulations of actual plant containment designs would provide flow data for a postulated accident in that plant, e.g., three-dimensional (3-D) patterns of flow velocities that would exist on the containment floor following a LOCA. The separate-effects tests provide data regarding the debris-transport characteristics for each type of debris, e.g., how each type of debris would behave when it is subjected to a particular water flow velocity. The containment floor transport methodology will merge debris-transport characteristics with CFD results to provide a reasonable estimate of debris transport within the containment floor pool and subsequent accumulation of debris on the sump screen. Experimental data obtained from the integrated three-dimensional tank tests would provide the data necessary to benchmark the methodology, i.e., validate various approximations used to couple CFD results with the debris-transport test data. The experiments described in this report are designed to generate the data necessary to validate the debris-transport methodology.

1.2 Test Objectives and Scope

The experimental program described here is designed to complement the CFD simulations by providing the integrated three-dimensional small-scale test data required to benchmark the CFD simulation results. The test program has three objectives.

- Provide debris-transport data and "qualitative" particle tracking data that can be used to benchmark CFD simulations pertaining to 3-D transport phenomena in water pools formed on PWR containment floors; including accumulation on the sump screen.
- Identify the features of the containment layout and sump positioning that could affect debris transport and accumulation on the sump screen. Of particular interest are the physical features close to the sump screen, such as debris curbs.
- Provide insights that could be used to develop a simple method (or criteria) that could be used for each plant-specific configuration to "conservatively" attest to their safety. Such methods potentially could be used in lieu of complex analyses (e.g., CFD) and may consist of performing small-scale experiments and/or one-dimensional (1-D) flow calculations (similar to those suggested in NUREG-0897 [5]).

The integrated testing was performed using a large tank with provisions to simulate a variety of PWR containment/sump features. The test program was designed to explore the effect of various containment internal structures on debris transport and from that draw inferences on the features of the containment that could affect debris transport significantly. These tests were not planned to be "scaled" tests;[1] instead, the focus was to simulate the sequential progression of various phases of accident progress and examine the overall effect on debris transport. The integrated phenomena included debris transport during the fill-up phase (i.e., while the sump and tank were being filled) and after steady-state conditions were achieved (i.e., water flow from the break is equal to the flow out the sump). The tests provided visual records (video clips) of debris movement/location during and after pool fill-up and during the ECCS recirculation phase. Quantitative measurements included (a) the amount of debris added to the tank and the fraction that reached the sump screen and (b) the location of the remaining debris on the tank floor. Qualitative velocity mapping included local velocity measurements during steady state.

The debris used in the test program included primarily fiberglass debris of different sizes and shapes and reflective metallic insulation (RMI) debris of different sizes and shapes. The debris was of sufficiently small size not to be affected by the scaling issues.

1.3 Report Organization

The debris-transport test facility and apparatus are described in Section 2. Section 3 describes the test procedures, including the preparation of

[1] In other words, these tests may not provide data that are directly scalable to the actual plants, but they will provide data that can be used to validate any debris-transport methodology that may be developed.

the simulated insulation debris. Section 4 describes the tests conducted and the test results. Section 5 describes the CFD simulation results and compares those results with tank test results. Section 6 contains a summary, conclusions, and recommendations and includes general observations about the debris that were compiled during the testing. Appendix A provides flowmeter calibration data, and Appendix B describes the results of spherical tracer movement tests.

2.0 DEBRIS-TRANSPORT TEST FACILITY DESCRIPTION

The debris-transport tests were conducted at the University of New Mexico (UNM) Open-Channel Hydrology Laboratory. The test apparatus consisted of a shallow circular steel tank with internal structures designed to simulate the structural features of a typical PWR plant. The UNM hydrology laboratory contains the equipment necessary to supply a steady flow of water to the tank and to drain water from the tank.

2.1 Test Tank Description

The test tank, which is shown in Figure 2-1, is 13 ft in diameter, 2.5 ft deep, and open at the top. The floor of the steel tank was covered with high-strength concrete and leveled. The floor and the tank inner surfaces then were coated with an epoxy paint typical of that used in PWRs.

An outlet box designed to simulate a PWR containment recirculation sump was installed as shown in Figure 2-2 to drain water from the tank. The outlet box is 30 in. long, 14.5 in. wide, and 20 in. deep with a volume of 5.3 ft^3 (approximately 40 gal.).

Water was introduced into the tank by an overhead pipe and (in some tests) through a coarse diffuser, which also is shown in Figure 2-1. Figure 2-3 is a schematic of the test loop used in these tests. Water was supplied to the test tank from a below-floor reservoir by a 2500-gpm-capacity pump via an overhead 6-in.-diam pipe. The pump was a variable-speed centrifugal pump that allowed the pump flow to be regulated by adjusting the motor frequency. In addition, a butterfly valve in the overhead piping was available to finely regulate the supply flow. A calibrated flow meter (Hoffer Model HIT-2-2-A-X-F) located in the main piping monitored the flow rate (in gallons per minute). The calibration of the flow meter was checked periodically (see Appendix A).

The tank was drained at the outlet box after water flowed through the outlet screen that was used to collect debris transported to the outlet box. The tank outflow was carried through two 8-in.-diam pipes that connect to the side of the outlet box underneath the outlet screen (Figure 2-2). One of these pipes has a butterfly valve; the other pipe has an 8-in. gate-slide valve. These valves were used to regulate the outflow of the tank and hence the water level in the tank. The butterfly valve was used when fine-tuning of the water level in the tank was required. The drainage water was returned to the below-floor reservoir, where it was available for pumping back to the tank.

2.2 Test Configurations

A survey of operating US PWR plants was conducted as part of the resolution of NRC GSI-191 to compile plant-specific data relative to the resolution of GSI-191 [6]. A portion of these data pertained to the design of the recirculation sumps in each PWR plant surveyed. The sumps were found to vary widely in their design, size, and screen arrangement; there is no standard sump design. The sump-screen arrangements included vertical, horizontal, and slanted screen orientations. Examples of vertical- and horizontal-oriented sump screens are shown in Figure 2-4. In some cases, nonhorizontal screens would not be submerged completely during pump operation. In some plants, the containment drawings indicated that the sump could be influenced strongly by break-flow turbulence (referred to as "exposed sump"). The break flows in other containments would be remote from the sumps (referred to as "remote sump"). For many plants, it could not be determined whether the sump would be exposed directly to break-flow turbulence.

Internal structures were used in the tank to simulate this type of variability in PWR containment sump geometries—ranging from a fully exposed sump to a remote sump and from a horizontal sump screen to a vertical sump screen. The location of the inlet pipe, one of the primary test parameters, was varied during the course of testing, resulting in three test configurations, A, B, and C, as shown in Figures 2-5, 2-6, and 2-7, respectively. In the latter tests, the interior walls nearest to the outlet box were removed to simulate an exposed-sump condition, resulting in Configuration D as shown in Figure 2-8.

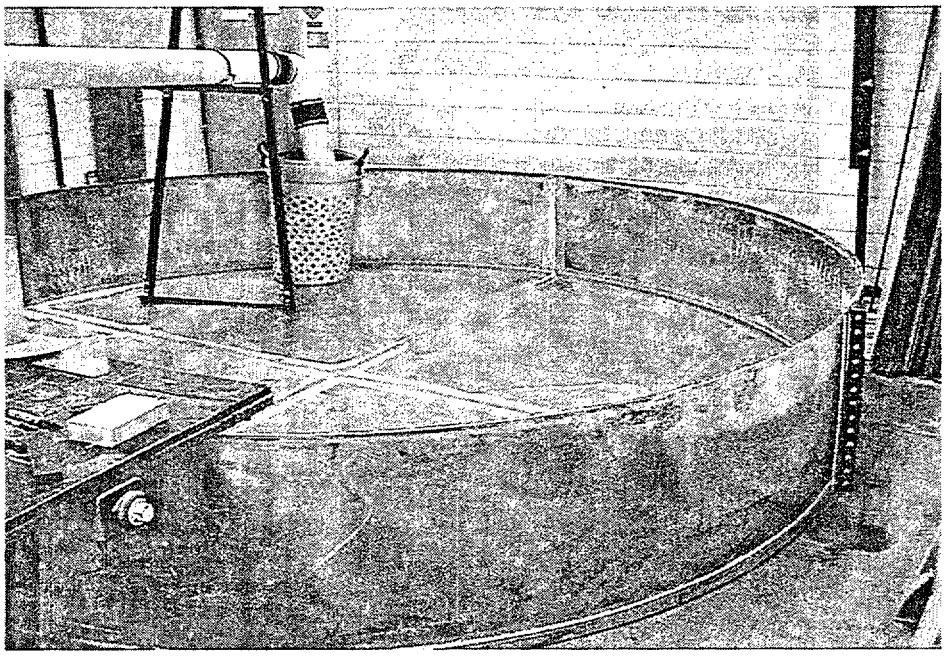

Figure 2-1 Photo of Steel Tank

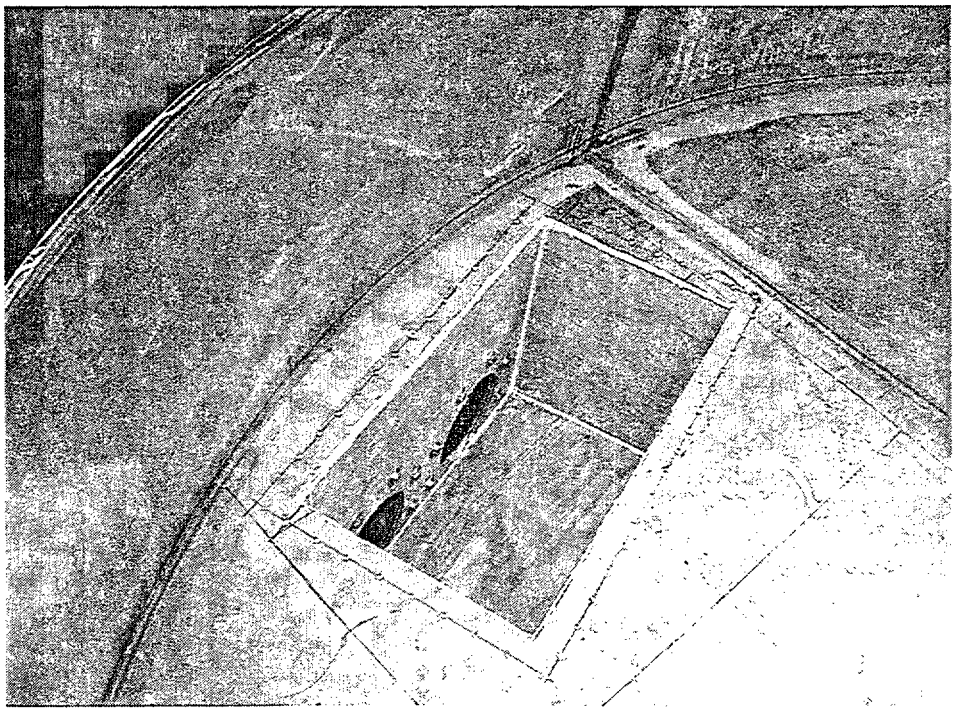

Figure 2-2 Test Tank Outlet Box

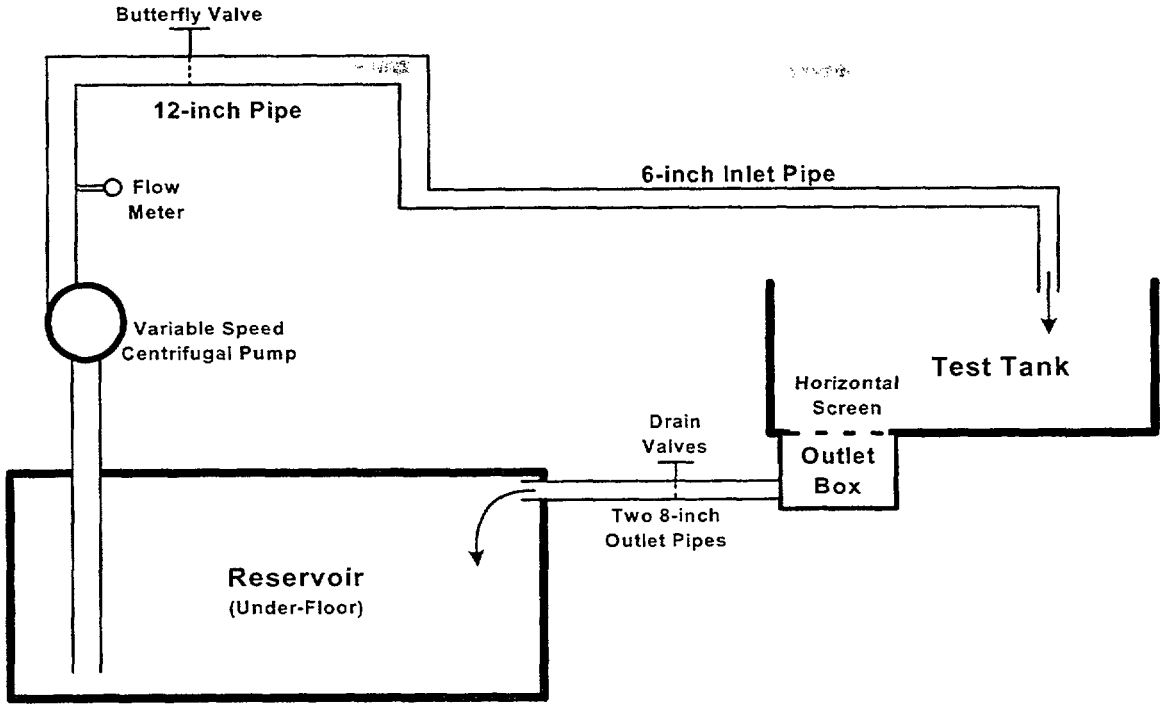

Figure 2-3 Schematic of the Test Loop

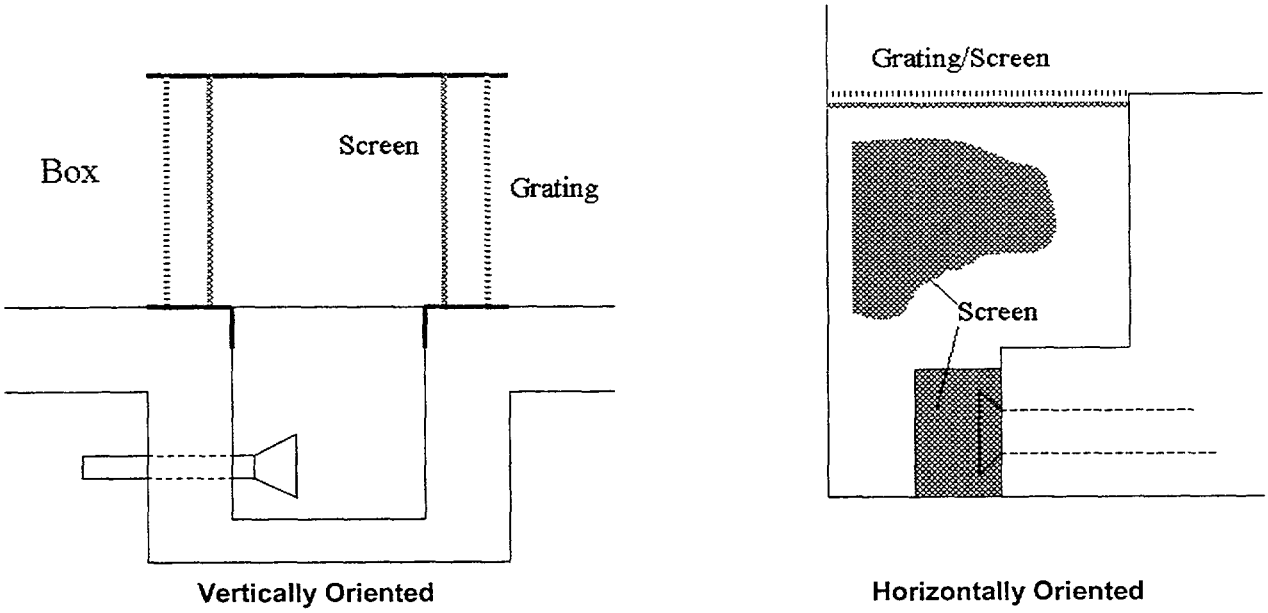

Figure 2-4 Schematics of Selected PWR Sump Arrangements

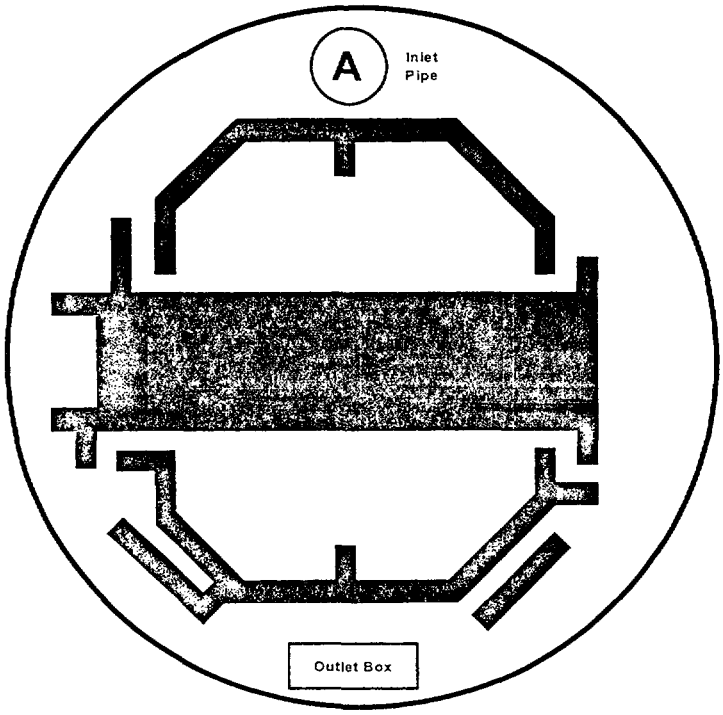

Figure 2-5 Test Configuration A

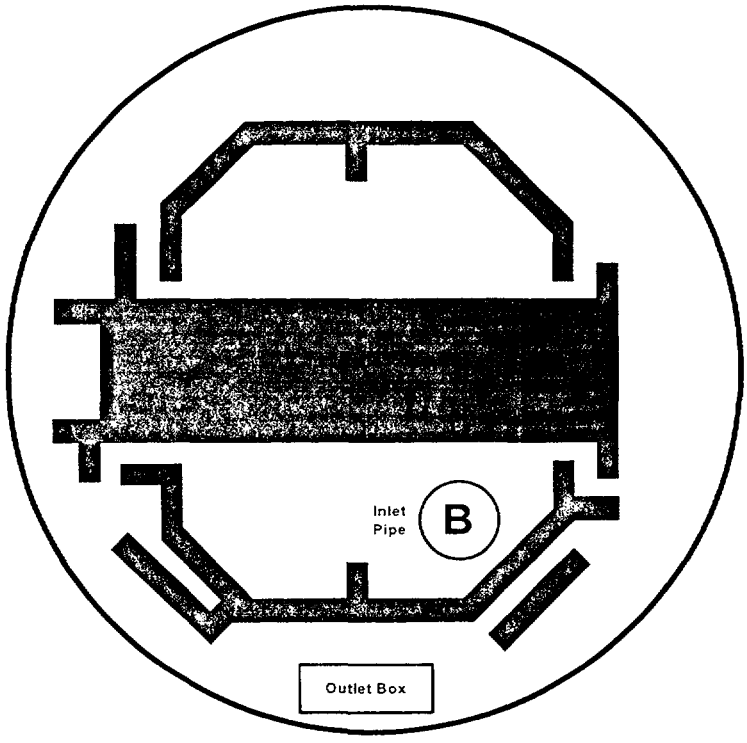

Figure 2-6 Test Configuration B

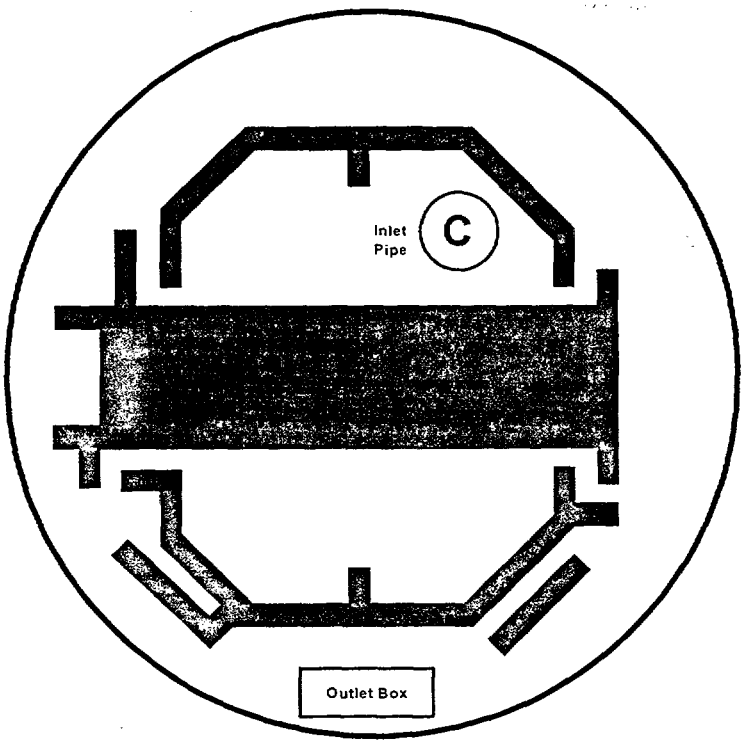

Figure 2-7 Test Configuration C

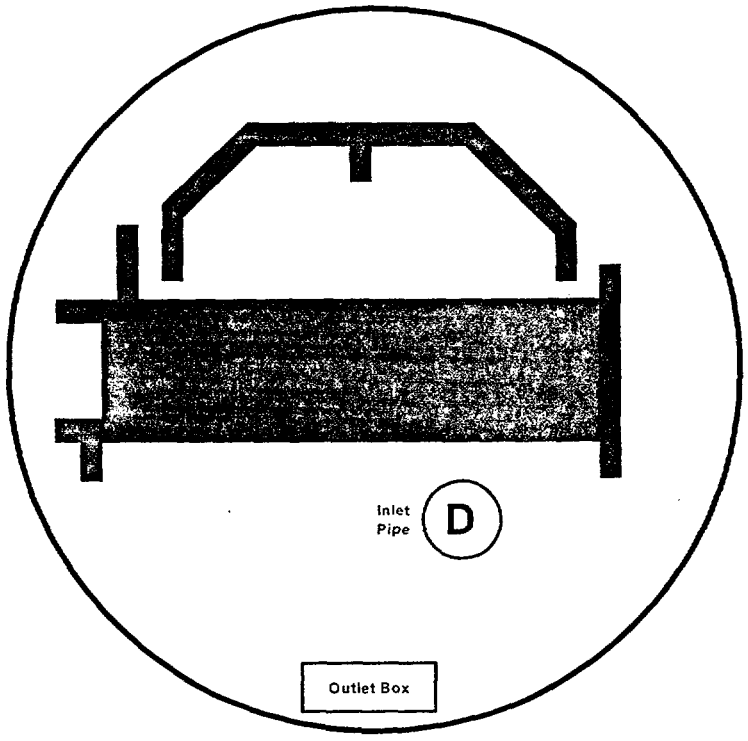

Figure 2-8 Test Configuration D

Two outlet screen orientations were used in these tests. A screen was fitted horizontally over the outlet box as shown in Figure 2-9; the screen dimensions are 28.5 in. by 13 in. A 1-in.-high curb was constructed around the screen to preclude debris from simply rolling into the sump screen. The transport fractions are based on debris flowing over the curb.

In the vertical mode, the screen was mounted into the side of a box that was placed over the tank outlet box as shown in Figure 2-10. The screen open-area dimensions are 26 in. by 13.75 in., and the bottom of the screen is closed to flow to simulate a 1.5-in.-high curb.

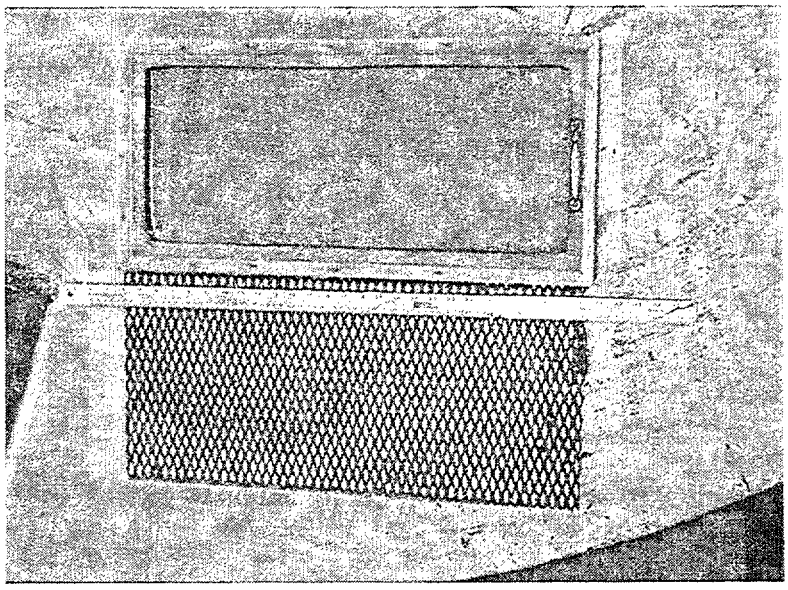

Figure 2-9 Outlet Box Horizontal Screen

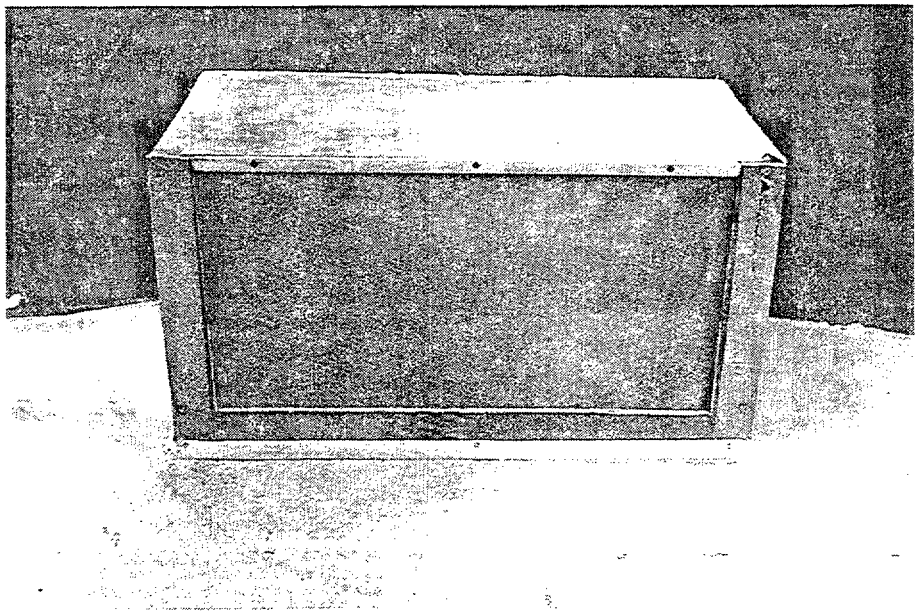

Figure 2-10 Outlet Box Vertical Screen

3.0 DEBRIS-TRANSPORT TEST PROCEDURES

Scoping tests were conducted to support the development of appropriate testing procedures and to help select appropriate test parameters. The test procedures described include the preparation of the debris test samples, their insertion into the experiment, the removal and processing of the debris, and the selection of test flow conditions.

3.1 Debris Preparation

Three types of debris were tested in the integrated tank tests: (1) calibrated tracers, (2) low-density fiberglass (LDFG) insulation, and (3) RMI. Both the stainless-steel (SS) and aluminum (Al) types of RMI were tested. Precharacterized "spheres" (referred to as "tracers") were used to generate transport data suitable for the benchmarking CFD simulations[2] (the characterization of the tracers is discussed in Appendix B).

A commercially available leaf shredder processed large mats of fibrous insulation into simulated LDFG insulation debris. The leaf-shredding process generated LDFG debris that had properties akin to debris that has been generated by impact jet testing.[3] A typical sample of LDFG debris is shown in Figure 3-1. Before testing, this debris was pretreated to simulate expected containment conditions following a LOCA, i.e., when LDFG insulation debris is dropped into water at the temperatures expected in a PWR sump pool following a LOCA, that debris would saturate rapidly with water, allowing it to sink.[4] When LDFG is dropped into the room-temperature water of the integrated tank tests, most of it would float for hours. Therefore, before the LDFG was suitable for testing in cold water, it was prepared by being immersed into a container of hot (80°C) water for a minimum of 5 min to remove all the air trapped in the fibers. The simulated debris was introduced into each test while it was still immersed in the water.

Al-RMI was obtained from an insulation vendor in small pieces that were approximately 0.5-in.- and 2-in.-square and1.5-mil thick. These pieces were subjected to air jets to produce crumpled samples of simulated debris. A sample of this debris is shown in Figure 3-2.

To prepare SS-RMI debris, sheets of 24-gage 304 stainless-steel foils were cut into 2-in.-square and 0.5-in.-square pieces. These pieces were processed by hand to make three categories of debris: crumpled, semi-crumpled, and flat. A sample of this debris is shown in Figure 3-3.

3.2 Debris Insertion

Debris-transport testing was performed in two transport phases. The first transport phase, referred to as the fill-up phase, examined debris transport when the debris was on the tank floor before the tank was filled with water. The second transport phase, referred to as the steady-state phase, examined how debris would transport when it was dropped into the pool after steady-state flow patterns were established.

The PIRT panel chose to examine each LOCA accident scenario in three accident phases: (1) the blowdown phase, (2) the post-blowdown phase, and (3) the sump-operation phase. The sump would begin to fill with water during the blowdown and still could be filling during the sump-operation phase because the recirculation pumps could activate before the pool reaches its maximum height. The steady-state-transport phase corresponds to the sump-operation accident phase after the pool has reached its approximate maximum depth. In the testing reported here, the fill-up transport phase began with the first water pouring into the tank and ended when the outlet flow approximately equaled the inlet flow. The steady-state transport phase then began.

In the fill-up phase tests, the individual debris pieces (or small conglomerates of debris pieces) were placed at several locations on the floor before the pump was turned on. Debris typically

[2]The tracers were suitable for debris-transport testing because the tracers were spherical and uniform and could be visualized clearly.

[3]This process also was used in the NUREG/CR-6224 study [7].

[4]Note that very fine debris, such as individual fibers, would remain suspended with even low levels of turbulence at both cold and hot water temperatures.

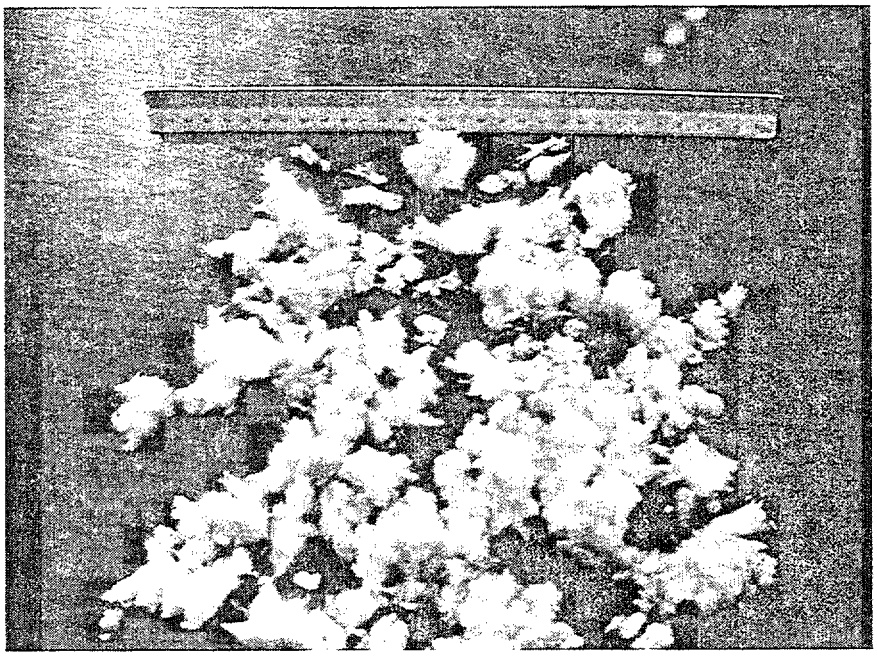

Figure 3-1 Typical Sample of LDFG Insulation Debris Prepared for Testing

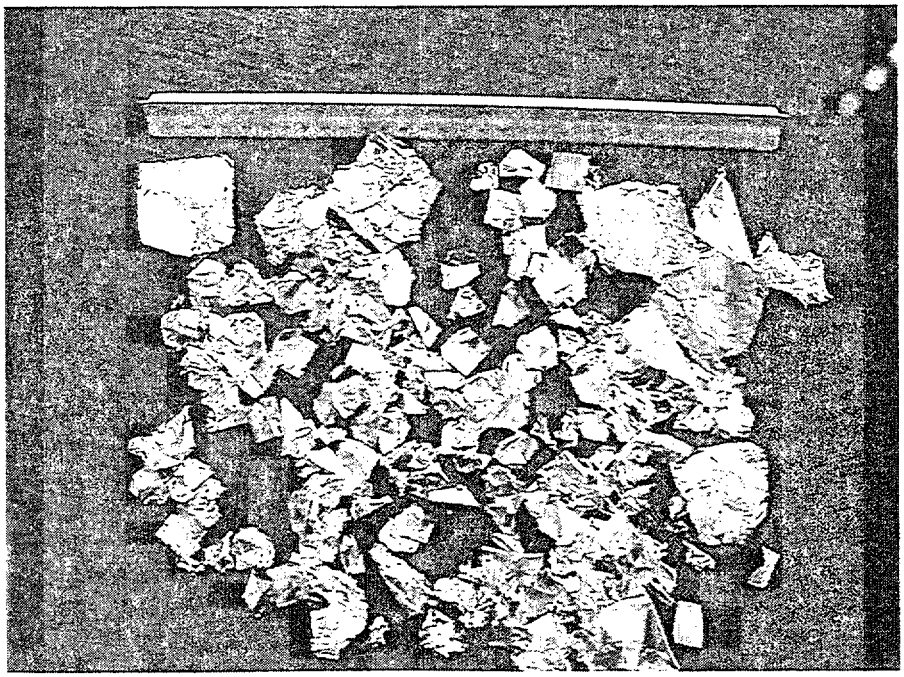

Figure 3-2 Typical Sample of Al-RMI Debris Prepared for Testing

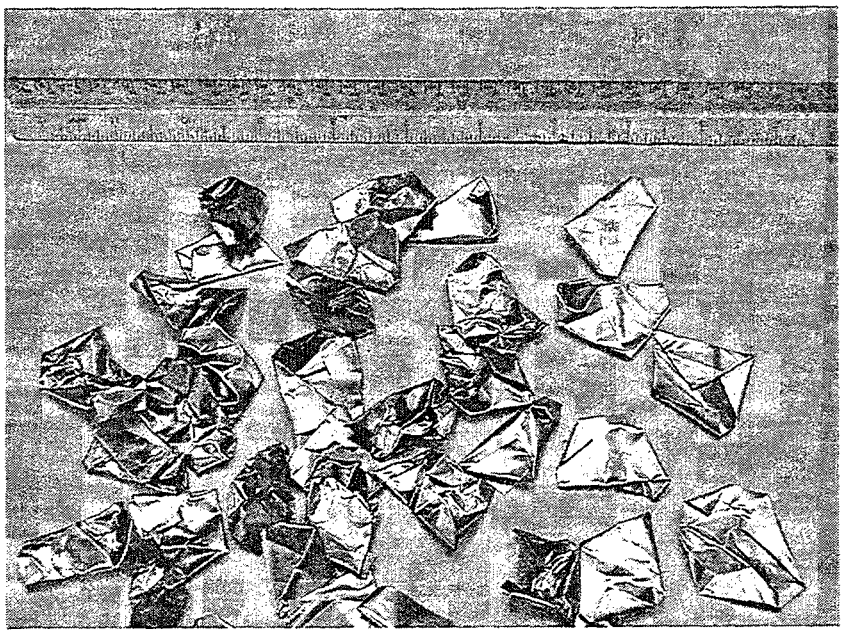

Figure 3-3 Typical Sample of SS-RMI Debris Prepared for Testing

was placed either directly under the pipe inlet or near it. Alternately, debris occasionally was placed at other locations per testing specifications. A typical placement of LDFG debris on the floor before the tank is filled is shown in Figure 3-4.

For testing debris transport under steady-state flow conditions, the debris either was inserted onto the floor of the tank using a PCV pipe[5] or simply was dropped into the pool from above, depending on the objectives of the test. To insert debris directly onto the tank floor, a large-diameter, vertically oriented PCV pipe was lowered to the tank floor, and the debris sample was dropped through the pipe to the floor. After the sample was sufficiently settled to the bottom, the pipe was slowly removed with a minimum of flow disturbance, leaving the sample on the floor with no initial momentum. The size of the pipe depended on the size of the debris sample. Placing the debris onto the pool surface allowed the debris to also transport horizontally while it settled slowly to the floor of the tank.

Because the primary objective of the debris-transport tests was to determine the fraction of debris transported to the outlet-box screen, the sample size needed to be large enough for statistical considerations but small enough not to overwhelm the outlet screen. For LDFG debris, the sample sizes were typically 200 g (dry). This sample size allowed pieces of debris to interact and then to move as a group, whereas each piece of debris would move independently in a sparse sample.

3.3 Debris Removal and Processing

Debris that transported to the outlet-box screen was removed from the screen and handled separately from the other debris in the tank. In some tests, the outer screen where the debris collected (the first of two screens) simply was removed from the tank, and the debris was removed from the screen. During tank cleanup after the tank was drained, all of the remaining debris in the tank was washed to the inner, second outlet-box screen using a water hose, where it also was removed. In other tests involving LDFG, the debris was removed periodically from the outer screen both to provide time-dependent data and to prevent a blockage of the screen that would terminate the test prematurely. LDFG debris was removed periodically while the test was still underway by carefully hand-scraping the layer of debris from the screen. Debris that was piled at the base of the screen also was removed. This had to be

[5]The same procedure was used in the separate-effects testing; it is described in detail in that report [4].

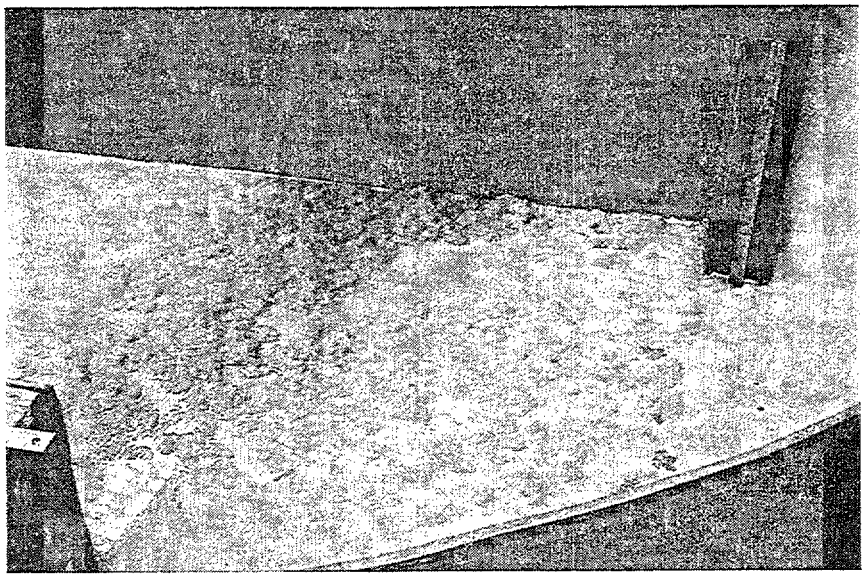

Figure 3-4 Typical Placement of Debris on Floor Before the Tank Is Filled

done carefully to prevent pieces of the debris from escaping back into to the bulk tank. All removed LDFG debris was dried thoroughly and weighed.

3.4 Selection of Test Flow Conditions

From the separate-effects tests, it was clear that debris transport is influenced most by water velocity and flow "turbulence" in the tank. Exploratory 3-D tank tests confirmed this finding. For example, Tests S8 through S12 (presented in Appendix-B) demonstrated that RMI and LDFG debris dropped in any active part of the tank would be swept up and transported to the screen at an inlet flow rate of 440 gpm. On the other hand, at an inlet flow rate of 50 gpm, debris transport is limited to a few locations of the tank. Experiments (discussed in Section 4) were performed between these two extremes.

During the exploratory testing, the flow velocities were estimated at two selected locations (reference locations) for a range of pump flow rates to be used as a guide in specifying pump flow rates for testing. These velocities are listed in Table 3-1, and the two reference locations are shown in Figure 3-5. With the flow introduced into the tank on the opposite side from the outlet box, the entire flow had to pass through one of the two reference locations for which the flow area was a function of the pool depth and the annulus gap width. Note that Reference Location 1 was significantly wider than Reference Location 2. The testing determined the distribution of flow between the two reference locations with the pool in Configuration A (see Figure 2-5). These flow velocities would differ somewhat from the Table 3-1 velocities when the test configuration was not that of Configuration A.

The more important velocity was the outlet-box screen-approach velocity, which was based on the area of the submerged vertical screen, i.e., the pump volumetric flow divided by the submerged screen area. Because this velocity can strongly affect the formation of the debris bed as well as, the head loss across the debris bed, it was important that the screen-approach velocity was representative of typical approach velocities that would exist at PWR sump screens. A pump flow rate of 150 gpm provided a screen-approach velocity in the general range considered typical of PWR sump screen. Note that the screen-approach velocity was only dependent on the pump flow rate and pool depth and, as such, was not dependent on the configuration of the test. When the horizontal screen was used, it was always submerged completely, so the approach velocity was approximately that of the 16-in.-depth vertical screen-approach velocities.

Table 3-1 Bulk Flow Annulus Velocities (ft/s) at Reference Locations as a Function of Inlet Flow Rate and Pool Depth								
Inlet Flow (gpm)	Velocity at Reference Location 1 vs Pool Depth			Velocity at Reference Location 2 vs Pool Depth			Velocity at Vertical Screen	
	2 in.	9 in.	16 in.	2 in.	9 in.	16 in.	9 in.	16 in.
51	0.15	0.05	0.02	0.40	0.14	0.05	0.07	0.05
75	0.22	0.08	0.03	0.59	0.21	0.08	0.10	0.07
85	0.25	0.09	0.03	0.67	0.23	0.09	0.12	0.08
100	0.29	0.10	0.04	0.79	0.28	0.10	0.14	0.09
120	0.35	0.12	0.05	0.94	0.33	0.12	0.16	0.11
130	0.38	0.13	0.05	1.02	0.36	0.13	0.18	0.12
150	**0.44**	**0.15**	**0.06**	**1.18**	**0.41**	**0.15**	**0.21**	**0.14**
170	0.49	0.17	0.06	1.34	0.47	0.18	0.23	0.16
180	0.52	0.18	0.07	1.41	0.50	0.19	0.25	0.17
200	0.58	0.20	0.08	1.57	0.55	0.21	0.27	0.19
230	0.67	0.23	0.09	1.81	0.63	0.24	0.32	0.22
250	0.73	0.25	0.10	1.97	0.69	0.26	0.34	0.24
300	0.87	0.31	0.11	2.36	0.83	0.31	0.41	0.28
440	1.28	0.45	0.17	3.46	1.21	0.45	0.60	0.42

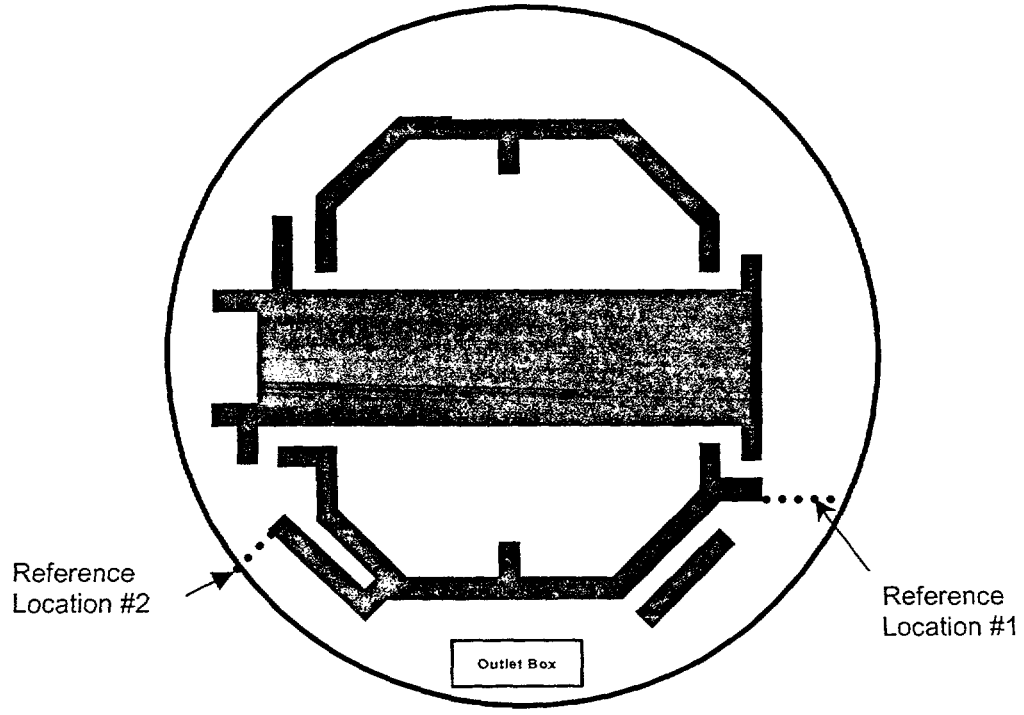

Figure 3-5 Reference Points for Velocity Measurements

4.0 DEBRIS-TRANSPORT TEST RESULTS

A total of 32 tests were carried out during the test program.[6] These tests can be divided broadly into three groups. The first set of tests specifically examined debris transport in the tank during the fill-up phase for a variety of insulation debris types. These tests also examined pool transport using spherical nylon tracer particles as a surrogate for actual debris (see Sec. 4.1 and Appendix B). These tests typically lasted 5–10 min, and their emphasis was to track the transport of individual pieces of debris. Tests in the second group were designed to provide insights into short-term transport. These tests were carried out over a period of 30 min and measured the fraction of debris that reached the outlet at the end of the test. Several parameters were varied in the conduct of these tests, which allowed test-to-test comparison in which a single specific variable was altered (see Sec. 4.2). The third group of tests was carried out over a much longer time period (extending up to 6 h) to study the long-term transport of debris. Of particular interest is the transport of "fine" debris. These long-term tests also provided time-dependent transport data (see Sec. 4.3).

4.1 Debris Transport During the Fill-Up Phase

Following a postulated LOCA in a PWR plant, some of the insulation debris is expected to accumulate on the sump-pool floor before significant water accumulates. Subsequently, the overflow from the break and CS drainage would start to fill the sump floor with water, and the water spreading across the sump floor would push debris across the floor. Understanding this mode of debris transport is essential to the overall evaluation of debris transport in a PWR plant.

The fill-up transport phase began with water pouring into the tank and ended when steady state conditions were established after the tank water height reached the specified test depth of 9 in. for these tests and the outlet flow was adjusted to maintain this outlet depth. In the fill-up-phase tests, the screen was in a horizontal mode, and the curb around the screen was approximately 1 in. high. Debris or the spherical nylon tracer particles (debris surrogate) were placed on the floor of the integrated test tank first; then pump flow was initiated, and the subsequent movement of the debris was recorded. The fraction of the debris transported to the sump screens was measured and provided for each test. An assortment of debris types and the tracer particles was used to examine tank fill-up debris transport. The tests conducted are shown in Table 4-1. During a series of preliminary tests documented in Appendix B, the motion of the spherical tracers across the floor was recorded for different test conditions.

Test F1. Test F1, was conducted with the inlet pipe located in the annulus, i.e., Configuration A (see Figure 2-5). Ninety 0.75-in.-diam spherical nylon tracers initially were distributed randomly in four general locations within the tank. The pump flow was initiated at the rate of 130 gpm, and the movement of the tracers as the water spread across the floor was observed. When the water level within the tank was approximately 9 in. deep at about 4 min, the outlet box drain valves were opened sufficiently to keep the level steady at this depth. The positions of the tracers were recorded as steady state was achieved, and the test was terminated. The initial positions and the results of Test F1 are shown in Figure 4-1. In this figure (and in subsequent figures), the boxes denote the number of tracers initially placed in each region. The circles show the approximate locations where the tracers were located at the end of the test.

It can be seen from Figure 4-1 that all of the tracers were relocated at the end of the test. Many of the tracers had been pushed into an interior region or into dead (or inactive) zones.[7] Other tracers had been pushed around the annulus to the outlet-box screen; in fact, 39 of the 90 tracers were transported to the outlet area. This translates into a pool fill-up transport

[6] Before these tests were conducted, preliminary testing was performed to determine appropriate test procedures, such as controlling the water flow rate and pool depth and the introduction and removal of debris. Some initial debris-transport behavior also was observed during this test procedure development period.

[7] A dead zone was a region where debris tended to remain in place because there was little or no flow and the pool turbulence was relatively low.

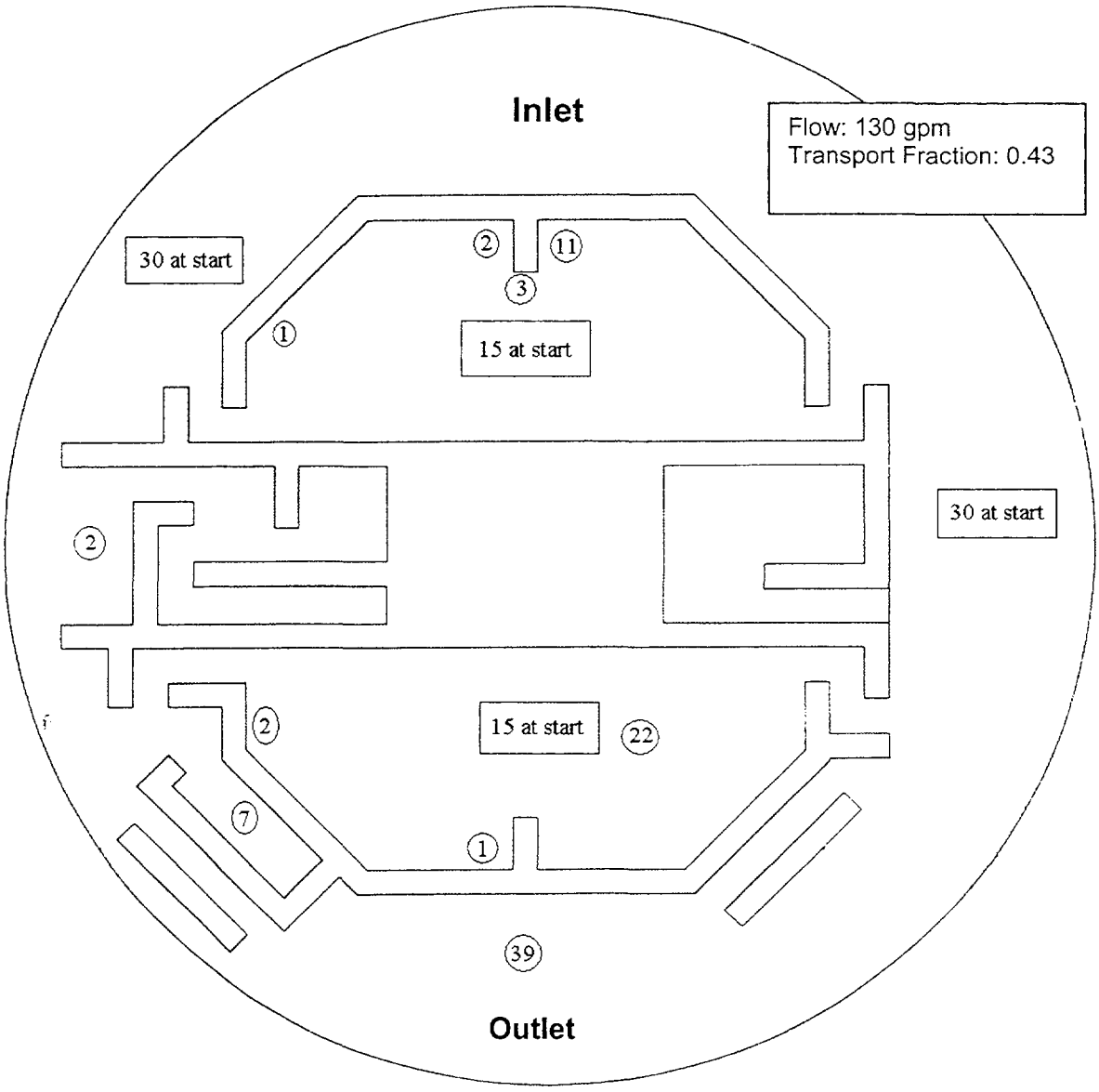

Figure 4-1 Nylon Tracer Transport Results for Fill-Up Transport Test F1[8]

[8]The boxes denote the number of tracers initially placed in each region, and the circles show the approximate locations where the tracers were located at the end of the test.

Table 4-1 Fill-Up Transport-Phase Debris-Transport Test Matrix				
Test Number	**Test Debris**	**Special Condition**	**Test Configuration**	**Pump Flow (gpm)**
F1	Nylon Tracers	—	A	130
F2	Nylon Tracers; LDFG; SS-RMI	Barriers	A	85–130
F3	Nylon Tracers	—	B	51
F4	Nylon Tracers	—	B	78
F5	LDFG	Presaturated	A	109
F6	AL-RMI	—	A	72
F7	SS-RMI	—	A	108
F8	Intact SS-RMI Cassette	Dry	A	120
F9	Intact SS-RMI Cassette	Prefilled	A	270
F10	Intact Thermal-Wrap Pillow	Dry	A	120
F11	Intact Thermal-Wrap Pillow	Presaturated	A	300

fraction of 0.43. This test demonstrates that some of the debris could be transported into the inactive zones of the containment sump during the fill-up transport phase and may not be available for transport to the sump screen. Furthermore, some material may reach the sump even before the ECCS is switched over. Similar results also were observed for debris fragments.

Test F2. Test F2 was designed to study the effectiveness of physical barriers (e.g., floor curbs) in limiting or redirecting debris transport. PWR plants frequently have such features; these could be curbs specifically designed to stop debris from reaching the outlet screens or the barrier could be an equipment support structure or a conduit. For Test F2, two 2-in.-high barriers were placed in the annulus to obstruct the tracers. One of these obstructions is shown in Figure 4-2, and the locations of the barriers are shown as dashed lines in Figure 4-3, which also shows the results of test F2. The pump flow rate was 85 gpm, and the inlet flow was placed at Configuration A.

In the base test, 25 nylon tracers were placed in each of two annulus regions, 15 tracers were placed in each of the inner compartments, and 5 tracers were placed just downstream of each one of the obstructions. In this test, only the 10 tracers placed downstream of the obstructions reached the outlet screen. All of the other tracers were diverted into either an inner compartment or an inactive region.

Variations of Test F2 were conducted at flow rates ranging from 85 to 130 gpm for fiberglass, aluminum RMI (Al-RMI), and stainless-steel RMI (SS-RMI) fragments to examine the effect of the curbs on the transportability of these debris types. In these variations, 25 pieces of each type of debris were placed upstream of each curb, the water was turned on, and the test was carried on through the fill-up phase. The numbers of debris pieces transported over the barrier were counted to determine the fraction transported. The following insights were gained.

(a) At 85 gpm, approximately 90% of the fiberglass and 100% of the Al-RMI fragments placed upstream of Barrier #2 were lifted and transported past the barrier. On the other hand, only a small fraction (approximately 10–15%) of the fiberglass and Al-RMI placed upstream of Barrier #1 was transported past the barrier. SS-RMI did not make it past either of the barriers.
(b) At 130 gpm, almost all the fiberglass and RMI fragments placed upstream of both barriers made it past the barriers. Only 10–25% of the SS-RMI pieces made it past Barrier #2, and none made it past Barrier #1.
(c) It took approximately 440 gpm for a majority of SS-RMI pieces to be transported to the screen, and even then, 60% of the SS-RMI pieces placed upstream of Barrier #1 did not move past that barrier.

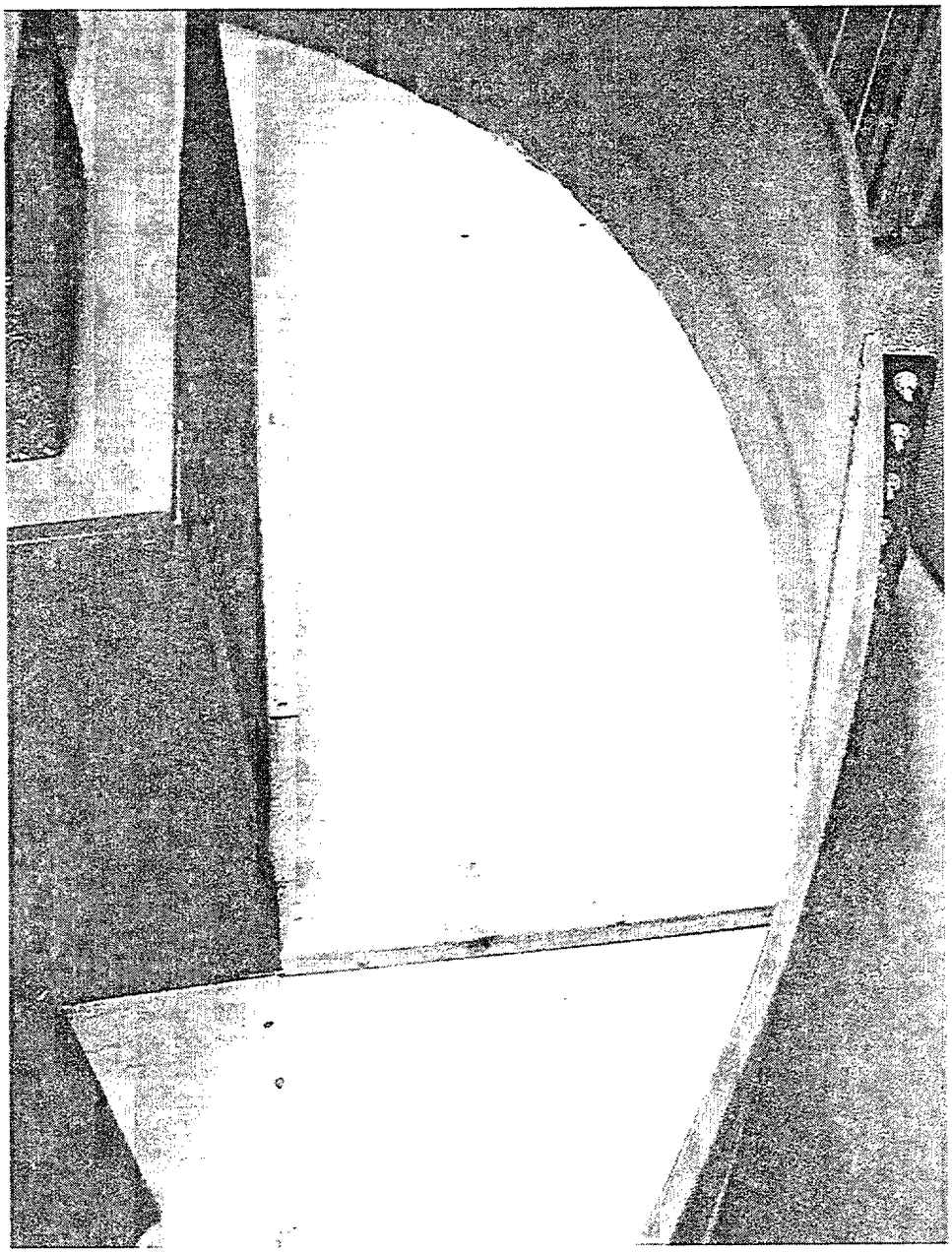

Figure 4-2 Debris-Transport Obstruction

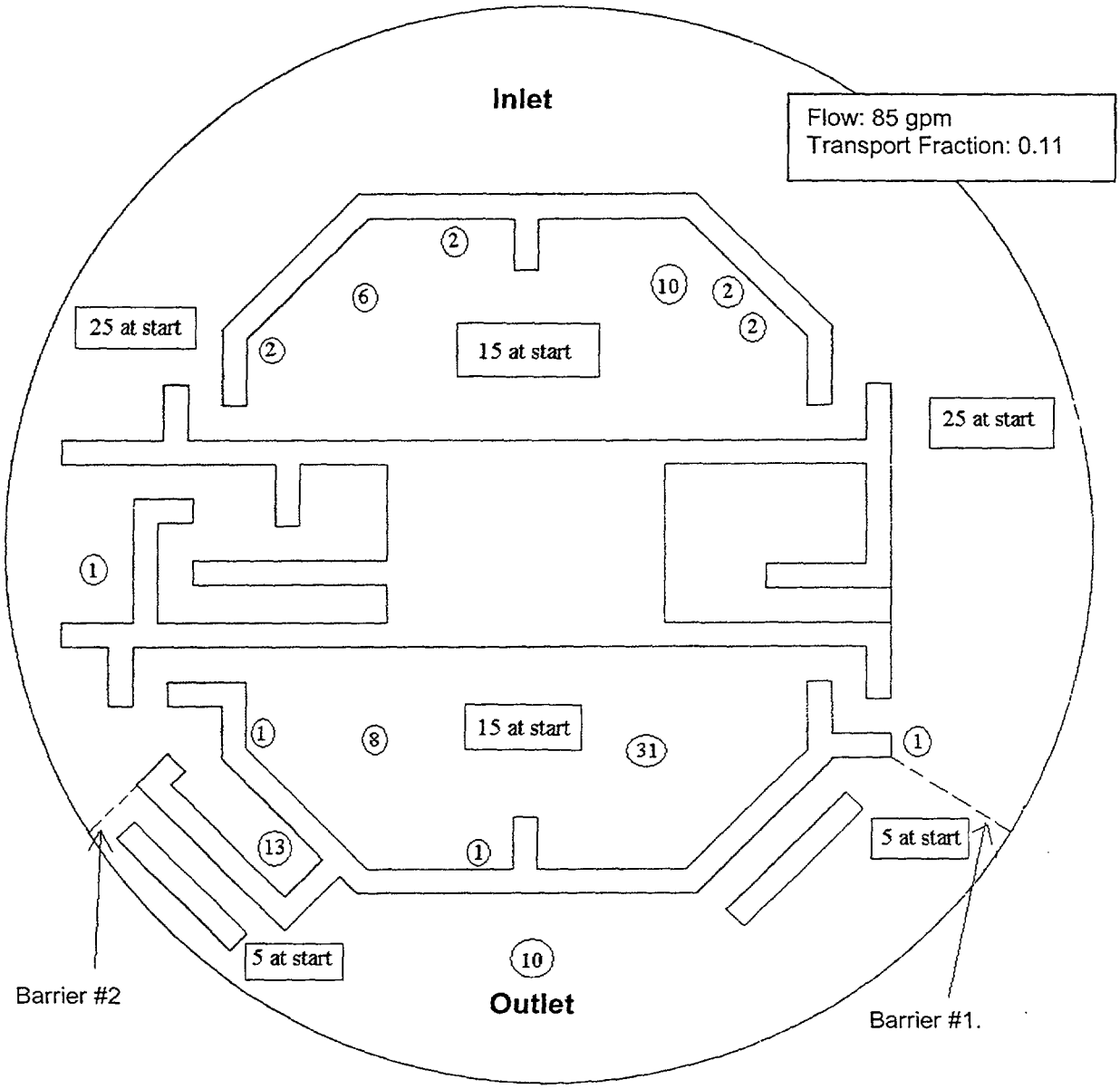

Figure 4-3 Nylon Tracer Transport Results for Fill-Up Transport Test F2[9]

[9]The boxes denote the number of tracers initially placed in each region, and the circles show the approximate locations where the tracers were located at the end of the test.

These tests clearly demonstrate that (1) barriers could provide an effective means for capturing certain types of debris (e.g., SS-RMI) and (2) the barriers' effectiveness is a function both of the debris type and of the flow velocity past the curb.

Tests F3 and F4. Two tests were conducted with the inlet pipe located in the inner compartment (designated Configuration B). These tests were conducted in a manner similar to that of Tests F1 and F2. The primary difference between Tests F3 and F4 was the initial location of the spherical nylon tracers. In Test F3, the tracers were placed randomly in the annulus and the two inner compartments, whereas in Test F4, the tracers were all placed in the inner compartment where the inlet pipe was located. The locations of the initial placement of the tracers, as well as the results of the tests, are shown in Figures 4-4 and 4-5 for Tests F3 and F4, respectively. Most, but not all, of the tracers initially placed in the inner compartment with the inlet pipe were pushed out of that inner compartment. A few tracers that were pushed against an inner compartment wall found relatively small quiescent regions that trapped them in that compartment. A substantial number of tracers were pushed toward the side of the tank opposite from the outlet box, where those tracers likely would have remained during a long-term steady-state phase. The transport fractions to the outlet box screen were 0.12 and 0.40 for Tests F3 and F4, respectively.

Test F5. One fill-up test, Test F5, was conducted to test the transport of pretreated LDFG debris. (The pretreatment process is described in Section 3.1.) The test was conducted in Configuration A with a pump flow rate of 109 gpm. The initial placement of the debris and the results for Test F5 are shown in Figure 4-6. The debris initially was placed in the annulus, well away from the outlet, with approximately half of the debris randomly distributed on either side of the inlet pipe. The positioning of LDFG after the water level reached a depth of 9 in. is shown in the circled numbers in Figure 4-6. About 30% of the LDFG debris was on the outlet-box screen at the end of the fill-up phase, i.e., a transport fraction of 0.3. Approximately half of the debris was pushed into the two inner compartments, where most of it likely would have remained during long-term transport because these inner compartments were inactive zones from the perspective of water flow in these tests. Test F5 was repeated at an initial flow rate of 145 gpm, and the measured transport fraction was 0.45.

Test F6. One fill-up test in this series, Test F6, was conducted to test the transport of Al-RMI debris. The test was conducted in Configuration A with a pump flow rate of 72 gpm. Again, steady state was established at a tank water level of 9 in. The initial placement of the debris and the results for Test F6 are shown in Figure 4-7. About 80% of the debris initially was placed in the annulus, well away from the outlet box, such that approximately half of this amount was distributed randomly on either side of the inlet pipe. The remaining 20% was distributed within the two inner compartments. The positioning of the debris after the water level reached a depth of 9 in. is shown in the circled numbers in Figure 4-7. About 30% of the Al-RMI debris was on the outlet box screen at the end of the fill-up phase. The transport fraction was 0.3. The quantities of debris trapped within the two inner compartments increased from the initial 20% to 50% by the end of the fill-up phase, where the debris was likely to remain during long-term transport.

Test F7. One fill-up test, Test F7, was conducted in this series that tested the transport of SS-RMI debris. The test was conducted in Configuration A with a pump flow rate of 108 gpm. The initial placement of the debris and the results for Test F7 are shown in Figure 4-8. Note that in this figure, the region containing the initial placement of debris is designated "Zone A." Approximately 70 pieces of debris were used in the test. The positioning of SS-RMI debris after the water level reached a depth of 9 in. also is shown in the boxes in Figure 4-8. Most of the debris in this test (about 90%) found its way to the outlet-box screen. Note that the transport fraction of 0.9 for the SS debris was substantially higher than that for the Al debris. The reasons for this difference are not clear. The flow rate in Test F7 was substantially higher than that for Test F6. In addition, the stainless steel is heavier than aluminum.

Tests F8, F9, F10, and F11. The transport of large, intact insulation components was examined briefly in Tests F8 through F11. An intact stainless-steel cassette measuring 1 ft by 1 ft and an intact pillow of thermal wrap insulation (also 1 ft by 1 ft) were tested. These two objects were tested in both dry and presaturated conditions. The test arrangement

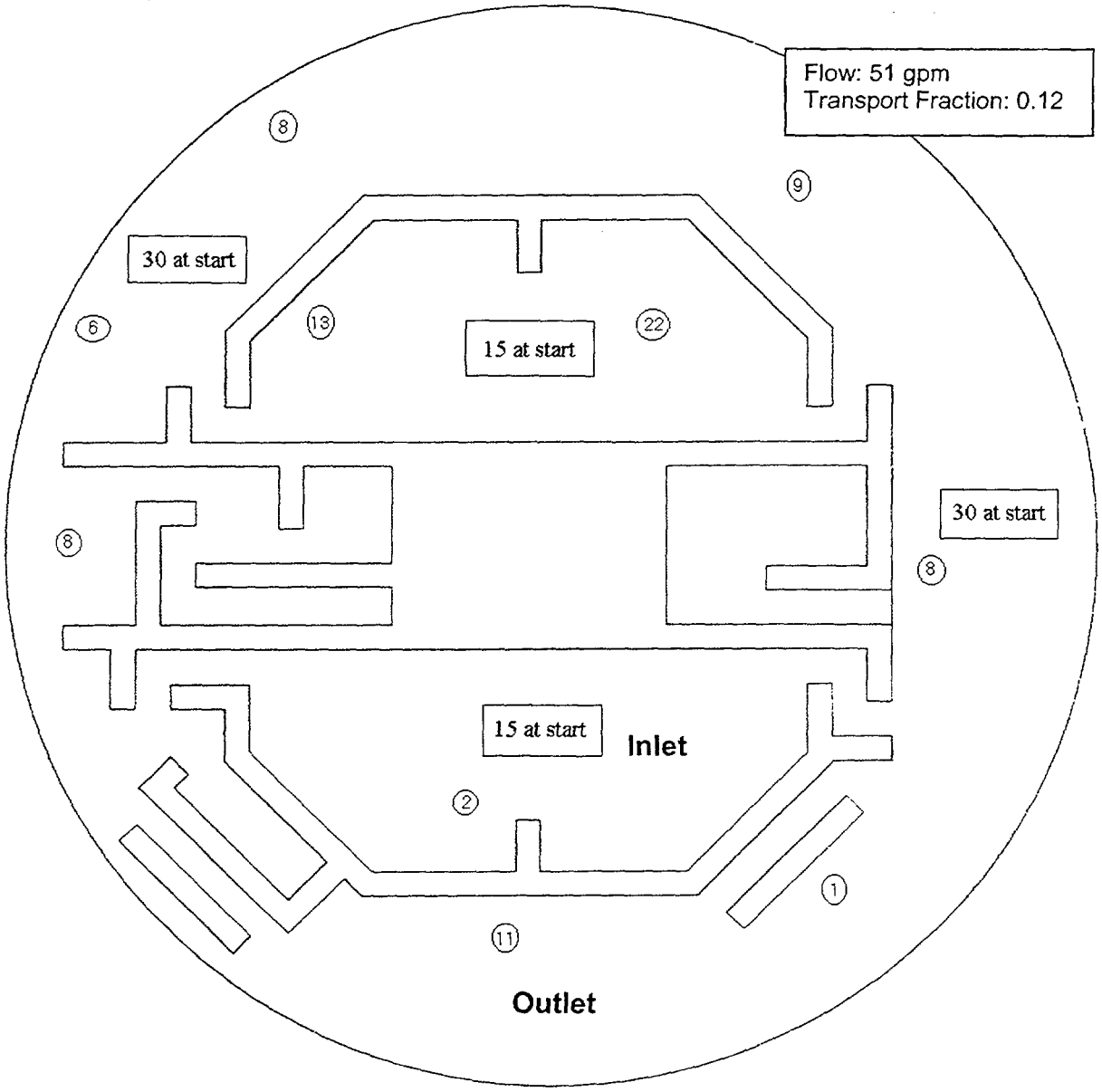

Figure 4-4 Nylon Tracer Transport Results for Fill-Up Transport Test F3[10]

[10]The boxes denote the number of tracers initially placed in each region, and the circles show the approximate locations where the tracers were located at the end of the test.

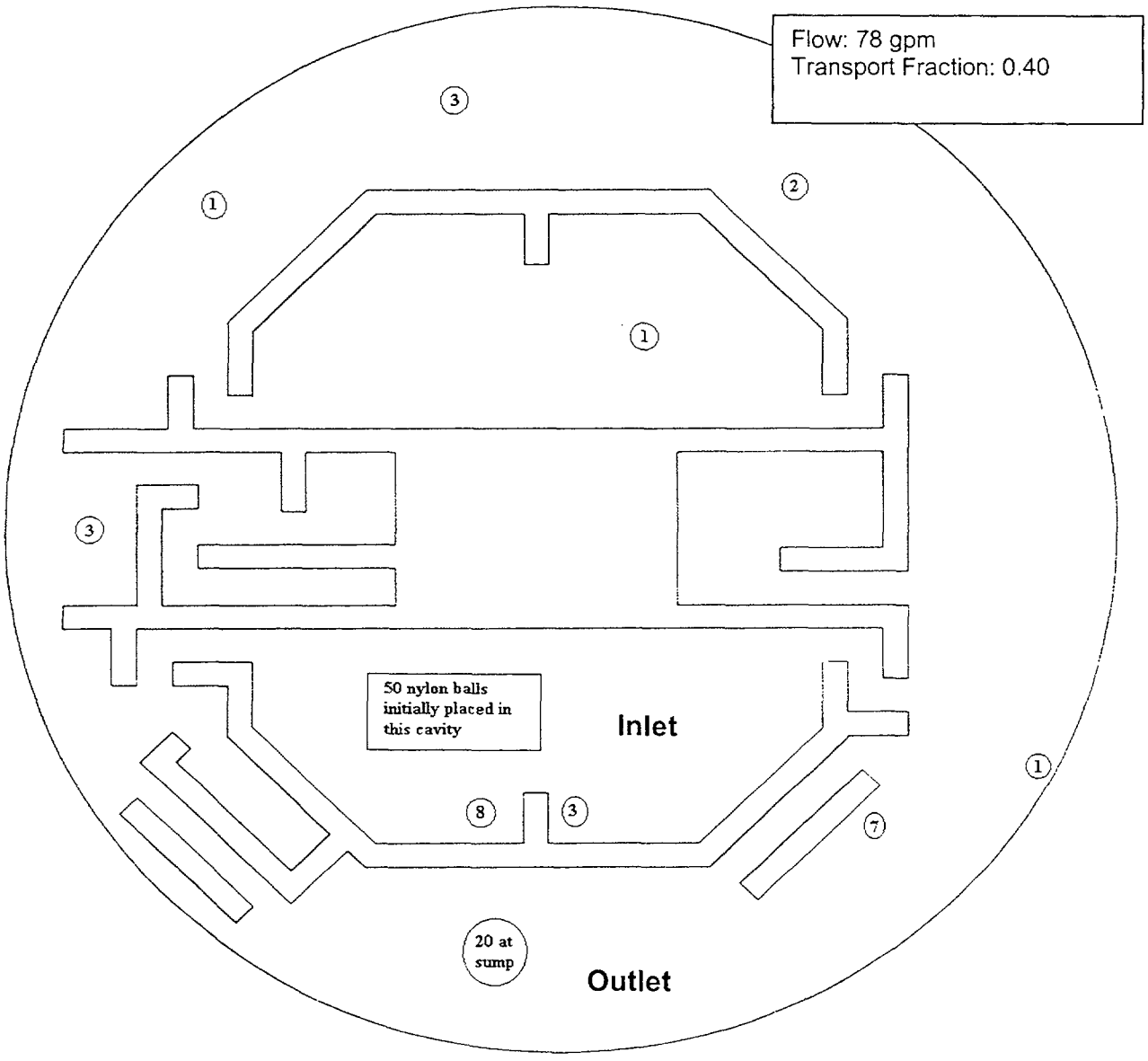

Figure 4-5 Nylon Tracer Transport Results for Fill-Up Transport Test F4[11]

[11]The boxes denote the number of tracers initially placed in each region and the circles show the approximate locations where the tracers were located at the end of the test.

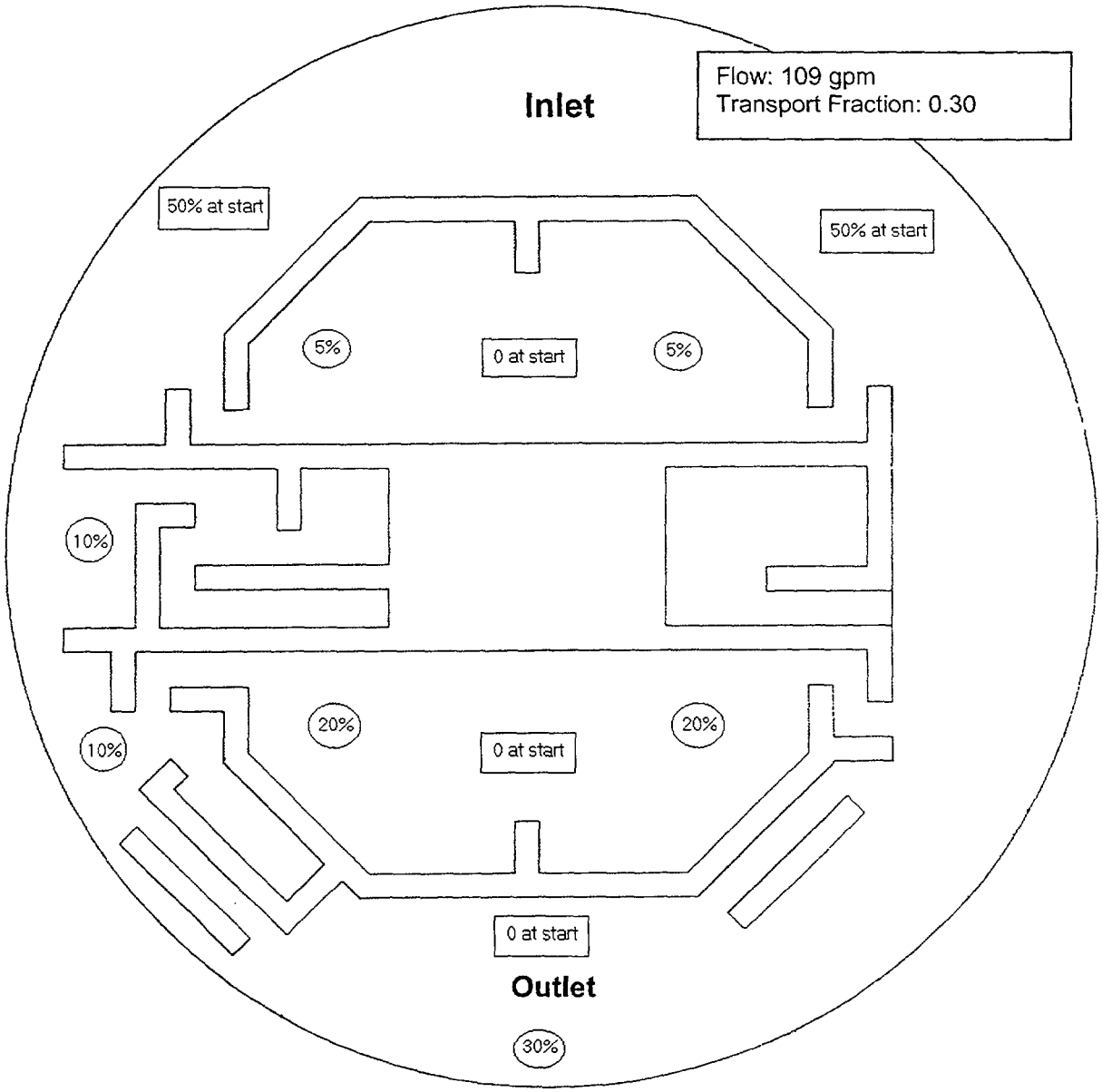

Figure 4-6 LDFG Transport Results for Fill-Up Transport Test F5[12]

[12]The boxes denote the initial placement of the LDFG debris, and the circles show the approximate locations where the pieces of debris were located at the end of the test.

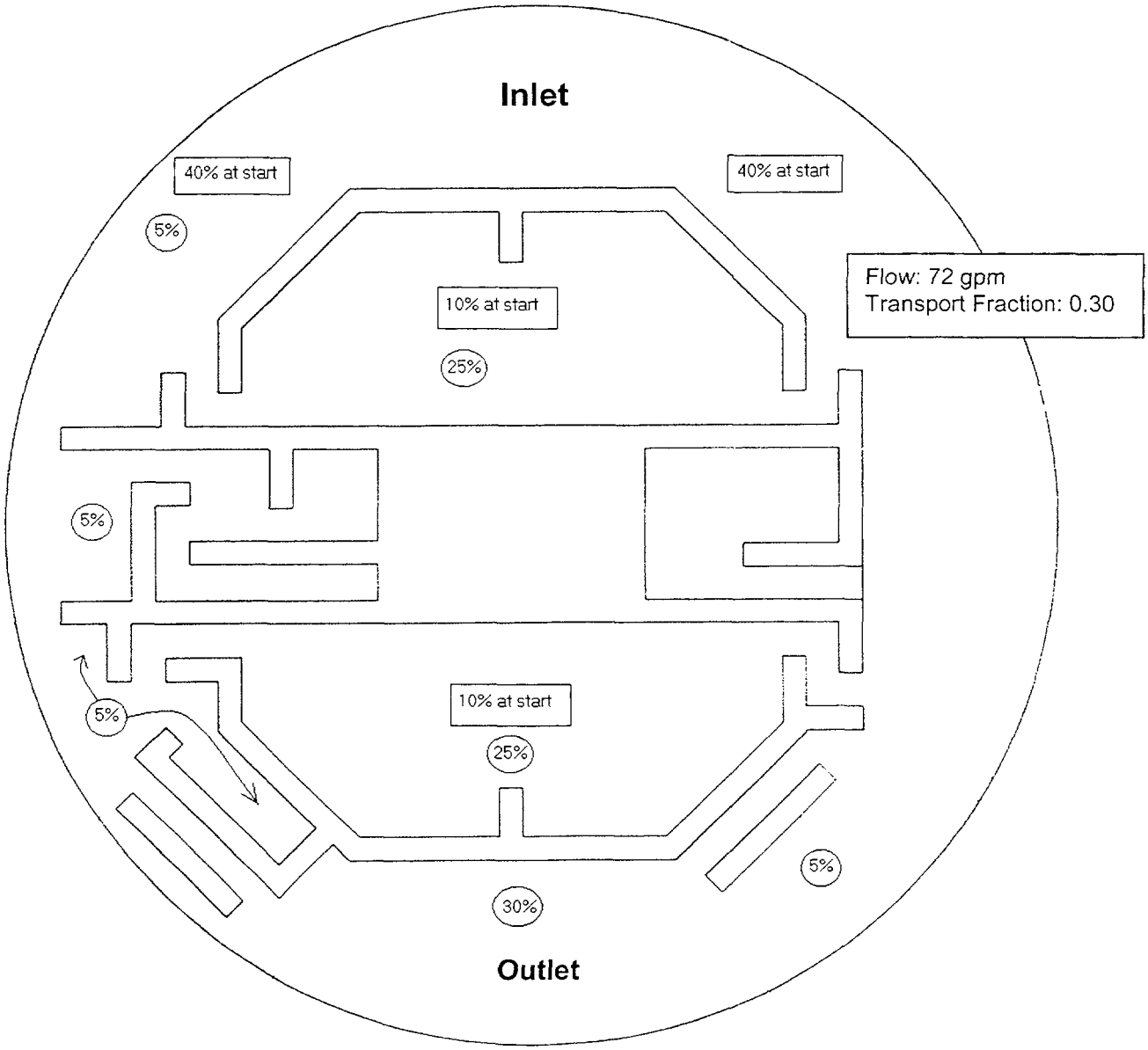

Figure 4-7 Al-RMI Transport Results for Fill-Up Transport Test F6[13]

[13]The boxes denote the initial placement of the Al-RMI debris, and the circles show the approximate locations where the pieces of debris were located at the end of the test.

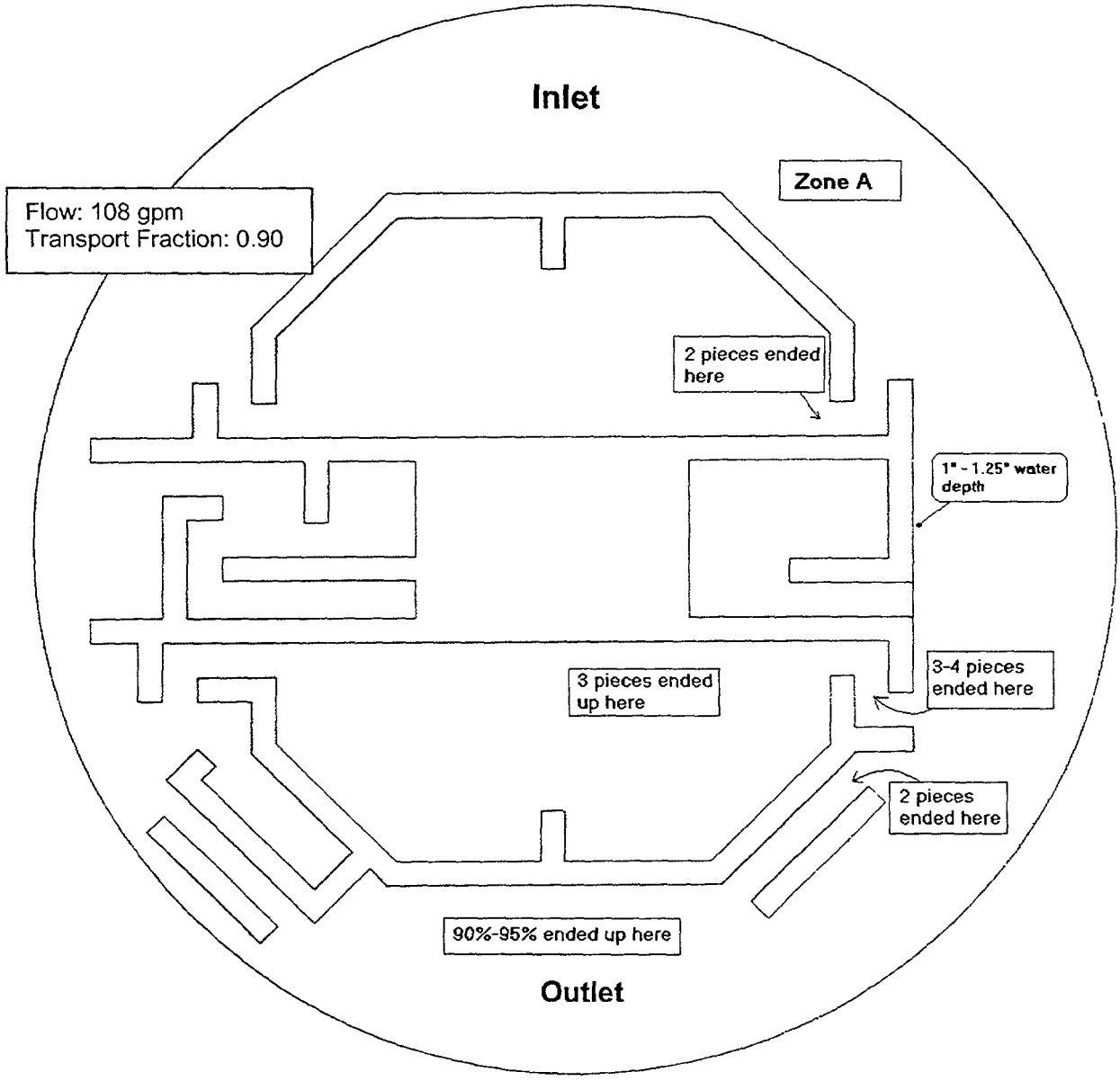

Figure 4-8 SS-RMI Transport Results for Fill-Up Transport Test F7[14]

[14]The SS-RMI debris initially was placed in each region designated as Zone A in the figure, and the other boxes show the approximate locations where the pieces of debris were located at the end of the test.

for these four tests is shown in Figure 4-9. In these tests, the test object was placed in the annulus near the inlet flow. The pump flow was initiated, and it was determined whether the object would move down the annulus toward the outlet box. The pump flow was increased incrementally until the object moved. The result of the test was the pump flow rate that would move the object along the annulus to the outlet box. The pump flow rates listed in Table 4-1 are the rates that moved the object. When the objects were dry, they transported relatively easily at a pump flow rate of about 120 gpm. However, these objects generally were not submerged completely during transport, although water flowed over the objects at times because of the action of waves. However, when the objects were water-saturated and on the floor, it took a substantially higher flow rate to move them; in fact, it took nearly 300 gpm to move the saturated objects.

4.2 Short-Term Transport Tests

The short-term transport tests focused primarily on the transport of LDFG debris. The emphasis of this group of tests was measuring bulk transport fractions rather than tracking the movement of individual debris pieces (which was the focus of the previous group of tests).

This test series consisted of 17 tests. The parameters of the tests conducted in this series are shown in Table 4-2. In 10 of the tests, the debris was placed on the floor of the tank, and its subsequent transport behavior was observed through the fill-up transport phase and the steady-state conditions afterward. In Table 4-2, these tests are shown as "Fill-Up" tests. In the other seven tests, which are marked as steady-state tests, the debris was introduced into the pool water after steady-state pool conditions were achieved (also near the location of the inlet pipe). All LDFG debris was pretreated in hot water as described in Section 3.1 to removed trapped air from the fibers. The quantity of debris transported to the outlet box-screen was collected and weighed so that a transport fraction for that test could be calculated (i.e., the dry mass collected on the outlet box screen divided by the dry mass introduced into the tank).

Three locations for the inlet pipe were tested in this series: Configurations B, C, and D. Most of these tests were conducted with a simple horizontal screen used to collect the debris from the drainage flow. The last four tests were conducted with the vertical-screen apparatus installed to examine how debris would accumulate on a vertically oriented screen. In three of the tests, the flow diffuser was placed under the inlet pipe to reduce the effect of flow agitation caused by the flow plummeting onto the floor. The diffuser is shown in Figure 4-10.

The test combinations in Table 4-2 were selected based on the following rationale.

- No tests were conducted in Configuration A because a combination of tests F2, F5, F10, F11 (Table 4-1), and S8 through S12 (Table B-4, Appendix B) provided the necessary data for this configuration. The F-series of tests studied fill-up-phase transport under Configuration A, and the S-series of tests studied steady-state transport.
- The inlet flow rates were varied between 40 and 200 gpm. This range was selected for examination because debris transport is negligible below 40 gpm, except during the fill-up phase, and debris transport remains unchanged beyond 200 gpm.
- Most of the tests were conducted using a horizontal-screen setup with a 1-in. curb; very few tests were performed using vertical screens, except in Configuration D. This has little significance for the test objectives, which were to measure transport fractions but not accumulation patterns.

The debris masses and the transport fractions for each of the tests in this test group are summarized in Table 4-3. The transport fractions were affected by the parameters of the tests—some parameters more than others. Comparing tests in which a particular parameter, such as the pump flow rate, was varied shows the relative effect of that test parameter. These comparisons are discussed in the following paragraphs.

Effect of the Inlet Flow Diffuser. The use of the diffuser under the inlet pipe reduced inlet flow agitation, reduced the quantities of debris in suspension near the inlet, and possibly reduced the disintegration of the debris caused by agitation. The diffuser did not appear to alter flow velocity patterns in the annulus, although it is possible.

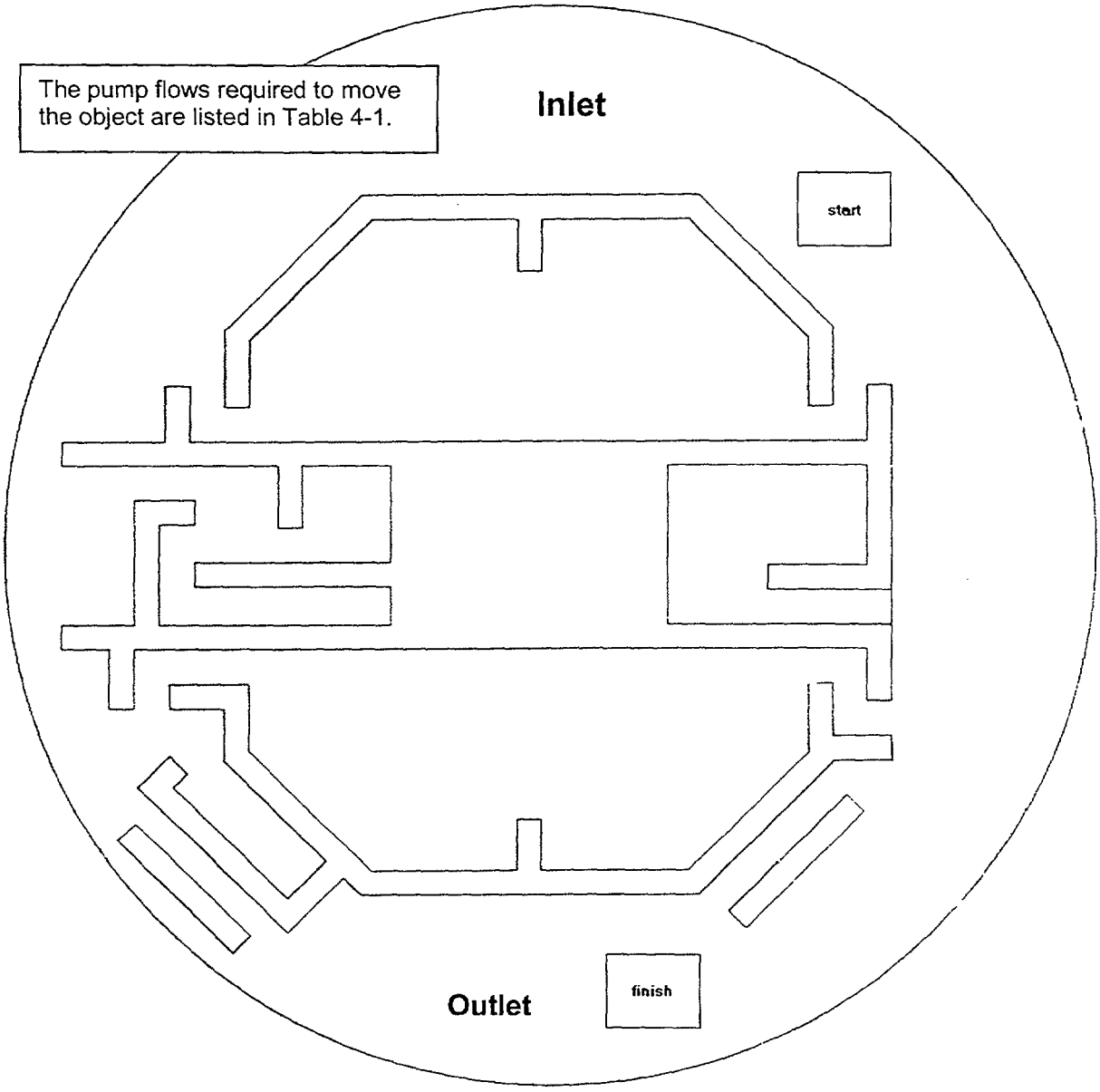

Figure 4-9 Large Insulation Transport Results for Tests F8, F9, F10, and F11[15]

[15]Boxes indicate the initial and final positions of the insulation components for each test.

Table 4-2 Matrix of Short-Term Debris-Transport Tests							
Test No.	Phase Tested	Test Configuration	Screen Orientation	Diffuser	Flow (gpm)	Depth (in.)	Duration (min)
ST1	Fill-Up	B	H	Off	130	9	15
ST2	Fill-Up	B	H	Off	145	9	20
ST3	Fill-Up	B	H	On	150	9	30
ST4	Steady	B	H	Off	140	9	30
ST5	Steady	B	H	Off	200	9	30
ST6	Fill-Up	C	H	On	130	9	30
ST7	Steady	C	H	On	140	9	30
ST8	Steady	C	H	Off	130	9	15
ST9	Fill-Up	C	H	Off	40	9	30
ST10	Steady	C	H	Off	40	9	30
ST11	Fill-Up	D	H	Off	135	9	39
ST12	Fill-Up	D	H	Off	60	9	38
ST13	Fill-Up	D	H	Off	150	16	30
ST14	Fill-Up	D	V	Off	140	9	30
ST15	Fill-Up	D	V	Off	140	17	30
ST16	Steady	D	V	Off	140	9	30
ST17	Steady	D	V	Off	108	9	30

Figure 4-10 Flow Diffuser

Table 4-3 Summary of Debris-Transport Characterization Test Results			
Test Number	**Source Mass (g)**	**Mass Collected on Screen (g)**	**Transport Fraction**
ST1	185	78.8	0.43[+]
ST2	250	124.8	0.50[+]
ST3	200	95.8	0.48
ST4	200	61.1	0.31
ST5	200	103.0	0.52
ST6	200	76.0	0.38
ST7	200	55.4	0.27
ST8	200	59.3	0.30[+]
ST9	100	9.4	0.09
ST10	100	0.6	0.01
ST11	200	45.6	0.23
ST12	200	19.5	0.10
ST13	200	15.5	0.08
ST14	200	39.2	0.20
ST15	200	20.5	0.10
ST16	200	134.2	0.67
ST17	200	146.1	0.75
[+]These tests were terminated before transport was complete because of excessive head loss. Actual transport may slightly exceed these reported values.			

The transport fraction was reduced whenever the diffuser was placed under the inlet pipe. This is illustrated by comparing the transport fractions for tests with and without the diffuser as shown in Table 4-4. Considering that ST2 and ST8 were terminated before accumulation was completed, the comparison could be much worse.

Phase of Debris Transport. As already noted, the debris was introduced into a few tests only after a steady-state pool was achieved rather than onto the tank floor before pump flow was initiated. This provided debris-transport information relevant to each of the two transport phases. The transport fractions are compared in Table 4-5.

Debris transport during the fill-up phase was very dramatic. The following discussion applies to Configurations A through C. During the fill-up phase, the debris literally was pushed by the spread of water throughout the tank. In fact, as discussed in Section 4.1, the debris was likely to move well away from the inlet area where it was introduced. However, during steady state, debris transport tended to follow the flow from the inlet to the outlet only if the local water velocity was sufficiently large. Otherwise, the debris tended to settle out in the quiescent areas. The fill-up-phase transport fractions for this series of tests were substantially higher than the corresponding transport fractions for the steady-state phase. A phenomenological explanation for this observation is given below.

(a) *Volume of the sump pit.* As discussed in Section 2, the volume of the sump-pit used in the present set of tests was approximately 40 gal. As a result, the sump acted as a sink for water flow and provided strong directionality for debris movement. To examine this effect systematically, ST2 and ST6 were repeated with the sump pit filled before the water was turned on. This cut down the transport fraction to 25%. (Very little of this debris was directly on the screen; instead, it was located in close proximity and was brought to the screen during the brief interval when the sump was turned on to establish steady state.)

(b) *Inlet Flow Rates.* The flow rates used in this series of tests resulted in low steady-state water velocities. It is possible that increasing the flow velocity may either reverse the trend or make the distinction insignificant. For example, the transport fractions associated with ST2 and ST5 are approximately the same value.

Table 4-4 Test Comparison Showing the Effect of the Diffuser				
Test	Diffuser	Inlet Location	Duration (min)	Transport Fraction
Fill-Up-Phase Transport				
ST3	On	B	30	0.48
ST2	Off	B	20	0.50[+]
Steady-State-Phase Transport				
ST7	On	C	30	0.27
ST8	Off	C	15	0.30[+]
[+]These tests were terminated before transport was complete because of excessive head loss. Actual transport may slightly exceed these reported values.				

Table 4-5 Test Comparison for the Debris-Transport Phase*					
Test	Phase Tested	Inlet Location	Flow (gpm)	Duration (min)	Transport Fraction
First Comparison					
ST2	Fill-Up	B	145	20	0.50[+]
ST4	Steady	B	140	30	0.31
Second Comparison					
ST6	Fill-Up	C	130	30	0.38
ST7	Steady	C	140	30	0.27
Third Comparison					
ST9	Fill-Up	C	40	30	0.09
ST10	Steady	C	40	30	0.01
Fourth Comparison					
ST14	Fill-Up	D	140	30	0.20
ST16	Steady	D	140	30	0.67
*A horizontal screen was used in all these tests.					

However, with Configuration D, this trend is reversed because the initial water flow tended to move debris away from the sump; in this case, most of debris settled in quiescent regions away from the sump. On the other hand, debris introduced during steady state remained near the break and tended to accumulate on the sump screen.

These discussions are presented to establish that the test data presented in Table 4-5 should not be used to draw conclusions regarding the relative importance of the fill-up phase *vis-à-vis* the steady-state phase for generic applications. Rather, these discussions provide insights into phenomena and processes that must be considered when estimating the transport of debris within a sump pool.

Influence of Flow Rate. As expected, the flow velocities had a strong influence on debris transport. Obviously, the higher the inlet pump flow rate, the faster the water flowed throughout the tank; therefore, the greater the debris transport, the larger would be the transport fraction. The transport fractions of tests where the pump flow rate varied are compared in Table 4-6. The corresponding data for Configurations A through C are shown in Figure 4-11. (Figure 4-11 also includes data points from Tests F5 and S8.) Although the figure displays an almost linear relationship, it is not clear that such a relationship is generic. It is also possible that the transport fraction would reach a maximum in the case of the fill-up phase, perhaps around 50%.

Table 4-6 Comparison of Tests with Different Pump Flow Rates						
Test	Phase Tested	Inlet Location	Diffuser	Flow (gpm)	Duration (min)	Transport Fraction
First Comparison						
ST5	Steady	B	Off	200	30	0.42
ST4	Steady	B	Off	140	30	0.31
Second Comparison						
ST11	Fill-Up	D	Off	135	39	0.23
ST12	Fill-Up	D	Off	60	38	0.10
Third Comparison						
ST6	Fill-Up	C	On	130	30	0.38
ST9	Fill-Up	C	Off	40	30	0.09
Fourth Comparison						
ST8	Steady	C	Off	130	15	0.30
ST10	Steady	C	Off	40	30	0.01

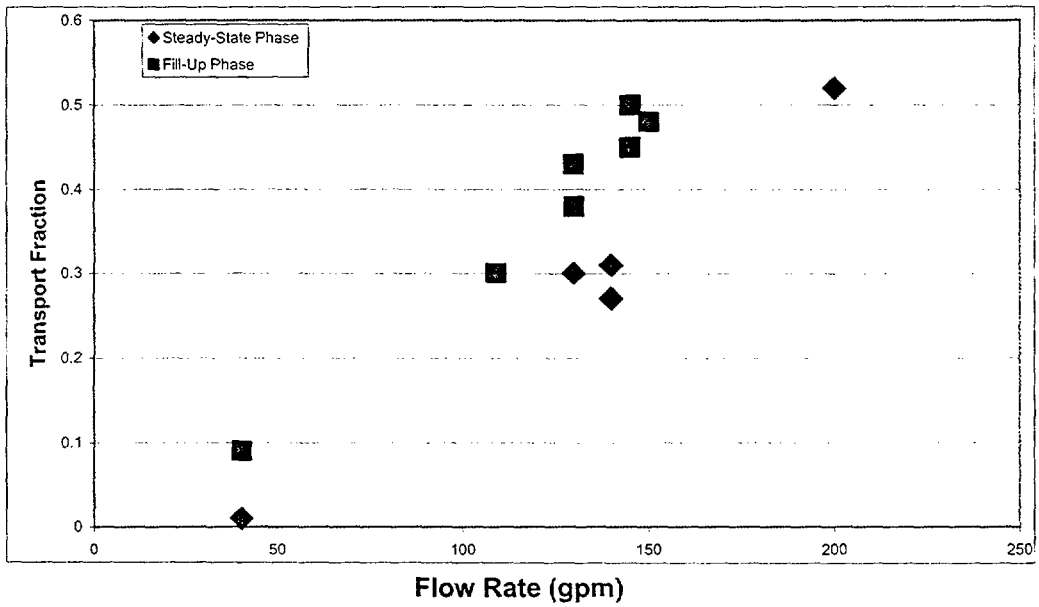

Figure 4-11 Effect of Inlet Flow Rate on Debris Transport

Comparison of Inlet Locations. It was expected that the location of the inlet pipe would have a substantial effect on the debris-transport fractions. The test comparisons are shown in Table 4-7; the primary difference between the two tests was the configuration. The transport fractions were essentially identical for the first two comparisons, which compared tests conducted in Configuration B with tests conducted in Configuration C (one for the fill-up phase and one for the steady-state phase). However, a significant difference is shown in the third comparison, which compares a Configuration B test (Test ST2) with a Configuration D test (Test ST11). In the Configuration D test, more debris was transported away from the outlet box during fill-up than was transported in the Configuration B test, and this debris tended to remain in the relatively quiescent side of the tank diagonally across from the sump. This comparison helps make the point that fill-up-phase transport can either reduce or enhance debris transport substantially, depending on the relative orientation of the inlet pipe and the outlet box.

Table 4-7 Test Comparison Showing the Effect of Inlet Pipe Location					
Test	Phase Tested	Inlet Location	Diffuser	Duration (min)	Transport Fraction
First Comparison					
ST3	Fill-Up	B	On	30	0.38
ST6	Fill-Up	C	On	30	0.38
Second Comparison					
ST4	Steady	B	Off	30	0.31
ST8	Steady	C	Off	15	0.30
Third Comparison					
ST2	Fill-Up	B	Off	20	0.50
ST11	Fill-Up	D	Off	39	0.23

Effect of Screen Orientation. Two comparisons (shown in Table 4-8) demonstrate that the orientation of the outlet-box screen had little, if any, effect on the debris-transport fraction. This conclusion is not necessarily applicable to a PWR plant sump or even to all test configurations of the integrated tank tests. A particular PWR plant sump could have a feature that would enhance debris capture, such as a sump that is below the floor.

Repeatability. Experimental variability resulting from the variability and uncertainty in test parameters is inherent to these tests. Although the pump flow rate and pool depth were controlled reasonably well, these parameters still had some variability and uncertainty associated with them. The preparation and introduction of the LDFG debris sample into the test inherently varied somewhat from test to test. Specifically, there was no guarantee that each debris sample had the same exact debris-size distribution. For example, one sample could have had a little more fine debris than another sample. However, every effort was made to prepare debris samples in a consistent manner. There was almost certainly some error associated with debris collection as debris was removed by hand from the screen. In some cases, a piece or two of debris that was deposited onto the screen might have drifted back into the bulk pool. Thus, there is some variability associated with these debris-transport numbers, and the magnitude of that variability was not something that could be deduced readily. The uncertainty associated with the experimental variability was considered small enough that the overall transport results and test conclusions are valid. These transport fractions demonstrate the relative importance of parameters that affect pool debris transport.

4.3 Long-Term Debris-Transport Tests

The 30-min time period of the short-term transport tests conducted in Configurations A through C was sufficient for the purposes of those tests because within that short duration, debris moved away more readily from the inlet toward the outlet or into various quiescent regions. However, in Configuration D, debris seemed to undergo a more continuous process of being resuspended by water eddies, being drawn closer to the inlet, and then being moved away from the inlet. This raised the concern that long-term transport testing may increase debris transport. Four long-term tests, LT1 through LT4, were conducted to address this issue.

All of the long-term tests were conducted with the experimental apparatus in Configuration D, with the vertical screen installed, and without the diffuser present. In Configuration D (see Figure 2-8), the front part of the interior wall structure was removed to create a more open approach for the flow approaching the screen. The test parameters for these tests are shown in Table 4-9.

In the first three long-term tests, the debris was placed on the floor of the tank directly below the inlet pipe before pump flow was initiated (as shown in Figure 3-4). In these three tests, debris was transported during the tank fill-up-transport phase as well as during the long-term steady-state-transport phase. For the fourth test, the tank was filled and relatively steady pool conditions were achieved before the debris was introduced into the pool. The debris in Test LT4 was introduced onto the pool surface at four

Table 4-8 Test Comparison Showing the Effect of Screen Orientation				
Test	Screen Orientation	Flow (gpm)	Duration (min)	Transport Fraction
First Comparison (9-in. Depth)				
ST11	Horizontal	135	39	0.23
ST14	Vertical	140	30	0.20
Second Comparison (16-in. Depth)				
ST13	Horizontal	150	30	0.08
ST15	Vertical	140	30	0.10

Table 4-9 Matrix of Long-Term Debris-Transport Tests					
Test Number	Phase Tested	Debris Insertion	Flow (gpm)	Depth (in.)	Duration (h)
LT1	Fill-Up	Floor Below Inlet	140	16	4
LT2	Fill-Up	Floor Below Inlet	140	9	4
LT3	Fill-Up	Floor Below Inlet Enhanced Disintegration	140	16	3
LT4	Steady	Pool Surface at Four Quadrants Enhanced Disintegration	140	16	5

locations in equal portions. The four locations are shown in Figure 4-12. For each of the four tests, 200 g of LDFG debris were introduced.

The time-dependent results for the four long-term tests are shown in Tables 4-10 through 4-13 for Tests LT1, LT2, LT3, and LT4, respectively. These tables list the weight of debris collected from the screen at each 30-min interval, the cumulative weight collected, and the fraction of the weight introduced into the tank that was collected on the screen.

The time-dependency of these results also is shown in Figures 4-13 and 4-14. Figure 4-13 shows the debris weights collected at each 30-min interval. Figure 4-14 shows the fraction of the debris weight introduced into the tank that was collected from the screen.

Approximately three times as much debris was transported to the screen in the LT2 test as was transported in the LT1 test; the only significant difference between the two tests was the pool depth. This difference was a result of the faster flow velocities in LT2, which was conducted with a pool depth of 9 in., compared with the velocities in LT1, which were conducted with a pool depth of 16 in. Faster flow velocities transport more debris than slower flow velocities.

The effect of long-term transport can be assessed by comparing the measurements made during this series of tests with the corresponding short-term tests. This comparison is provided in Table 4-14. As shown in this table, the long-term accumulation contribution is typically within 10–20% of the short-term accumulation. Most of the long-term accumulation is finer debris that remains in suspension well after 30 min.

Comparing test LT4 with ST16 is not easy because of the differences in the locations where debris was added to the tank.

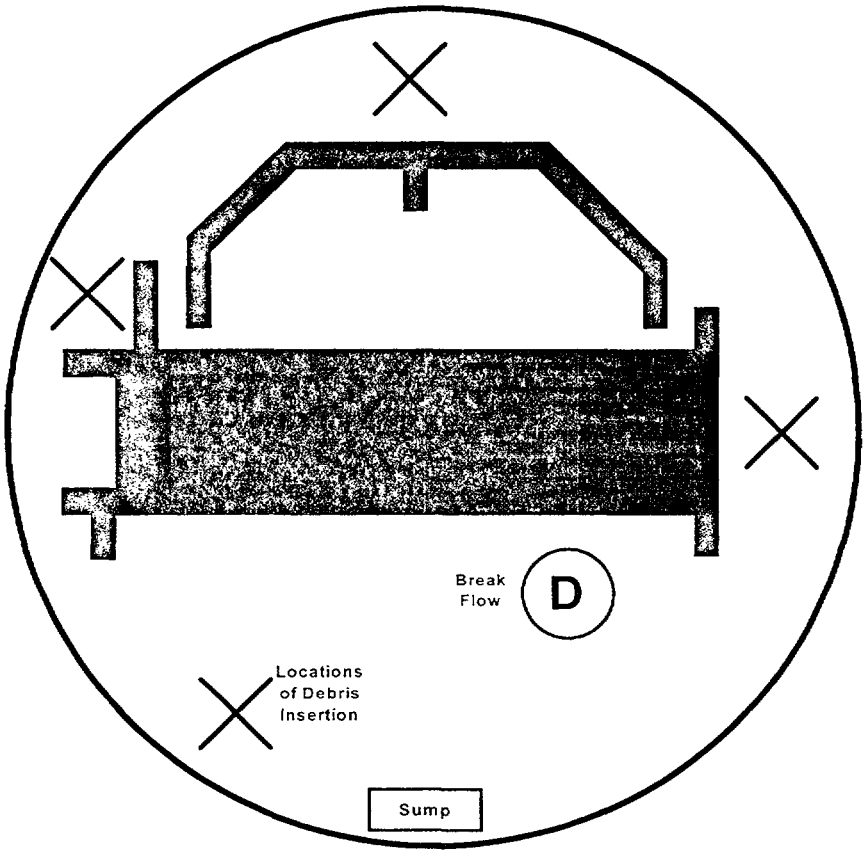

Figure 4-12 Debris-Insertion Locations for Test LT4

Table 4-10 Test Results for LT1			
Time (h)	30-min Collection Weight (g)	Cumulative Weight Collected (g)	Transport Fraction
0.5	9.9	9.9	0.049
1.0	2.5	12.3	0.062
1.5	1.7	14.0	0.070
2.0	0.4	14.5	0.072
2.5	0.5	15.0	0.075
3.0	0.5	15.5	0.077
3.5	0.5	16.0	0.080
4.0	0.3	16.3	**0.082**

Table 4-11 Test Results for LT2			
Time (h)	30-min Collection Weight (g)	Cumulative Weight Collected (g)	Transport Fraction
0.5	26.1	26.1	0.131
1.0	9.7	35.8	0.179
1.5	2.8	38.6	0.193
2.0	2.1	40.7	0.204
2.5	2.1	42.8	0.214
3.0	1.5	44.3	0.222
3.5	2.1	46.4	0.232
4.0	2.1	48.5	**0.243**

Table 4-12 Test Results for LT3			
Time (h)	30-min Collection Weight (g)	Cumulative Weight Collected (g)	Transport Fraction
0.5	16.2	16.2	0.081
1.0	2.5	18.6	0.093
1.5	1.5	20.1	0.101
2.0	0.6	20.7	0.104
2.5	0.3	21.0	0.105
3.0	0.3	21.3	**0.106**

Table 4-13 Test Results for LT4			
Time (h)	30-min Collection Weight (g)	Cumulative Weight Collected (g)	Transport Fraction
0.5	40.4	40.4	0.202
1.0	6.2	46.6	0.233
1.5	9.6	56.2	0.281
2.0	5.4	61.6	0.308
2.5	1.4	63.0	0.315
3.0	4.5	67.5	0.338
3.5	2.2	69.7	0.349
4.0	1.2	70.9	0.355
4.5	0.4	71.3	0.357
5.0	0.5	71.8	0.359
5.5	0.1	71.9	**0.360**

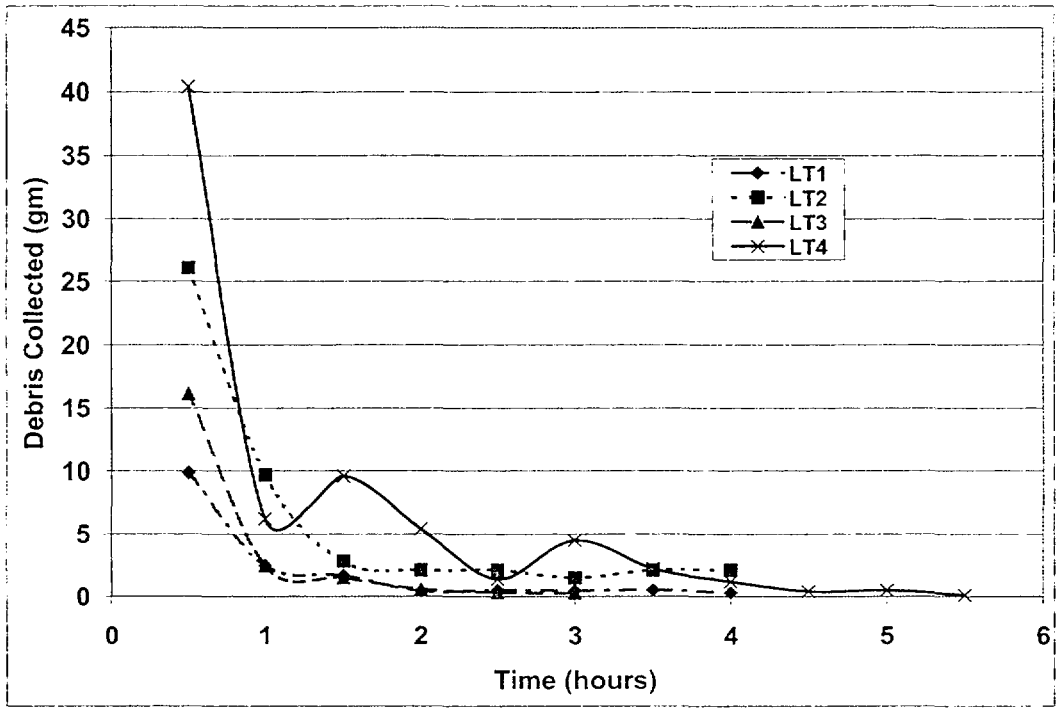

Figure 4-13 Thirty-Minute Collection Masses

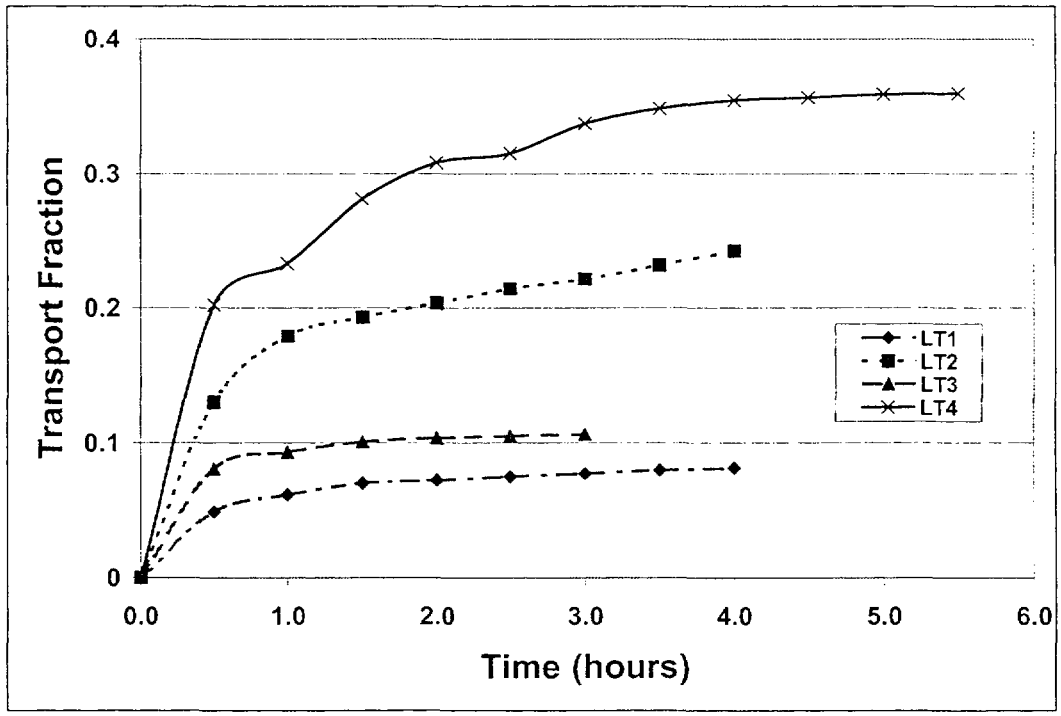

Figure 4-14 Time-Dependent Transport Fraction

Table 4-14 Test Comparison Showing the Effect of Inlet-Pipe Location					
Test	Phase Tested	Inlet Location	Diffuser	Duration (min)	Transport Fraction
First Comparison					
LT1	Fill-Up	D	Off	240	0.08
LT3	Fill-Up	D	Off	180	0.11
ST13	Fill-Up	D	Off	30	0.08
Second Comparison					
LT2	Fill-Up	D	Off	240	0.24
ST14	Fill-Up	D	Off	30	0.20

5.0 COMPUTATIONAL FLUID DYNAMICS FLOW SIMULATIONS

The flows within the integrated tank test apparatus were simulated using the FLOW-3D CFD computer code. The results of these simulations helped the analysts to understand the flow patterns within the tank. Further, these simulations were compared with the test results to gain insights into the adequacy of using CFD calculations to simulate pool-water velocity patterns. The FLOW-3D computer code was designed to produce simulations of fluid flows influenced by a variety of physical processes and is based on the fundamental laws of mass, momentum, and energy conservation. The capabilities of the code are particularly well suited for simulating the flow patterns within the integrated tank.

The geometry of the tank and the internal wall structure, which were described in Section 2, were modeled using the FLOW-3D computer code. The dimensions of the internal structures (shown in Figure 5-1) actually were taken from an AutoCAD drawing of a PWR plant layout and then reduced in scale; i.e., the test tank was one-tenth the size of the PWR containment. The geometry also included a depression in the floor to simulate the recirculation-cooling sump. A total of 120 cells was used to subdivide the geometry in both horizontal directions (x and y); 20 cells were used for the vertical direction (z). The water was sourced into each calculation using a source object located per the A, B, C, and D test configurations (Figures 2-5 through 2-8) at the mass flow rate specified for the calculation. Water was drained from the simulation by another source-object (with a negative mass flow rate) placed in the depressed sump volume. Both steady-state-pool and pool-fill-up simulations were performed.

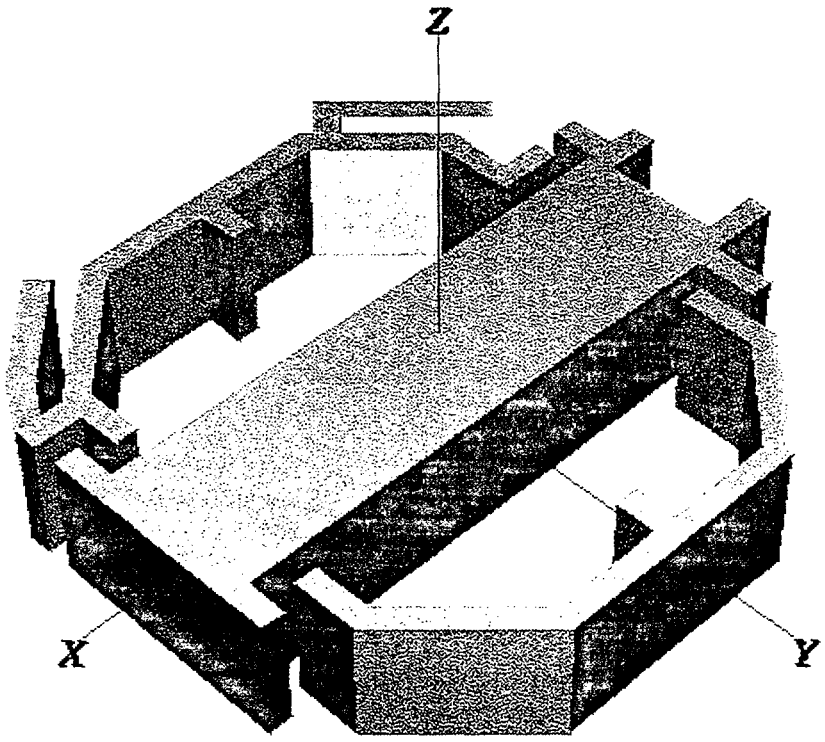

Figure 5-1 Interior Wall Portion of the CFD Model

5.1 Test Configuration A Simulation

Simulations of the tank flow patterns were completed for test Configuration A. The steady-state pool flow velocities for the simulation with the inlet flow set at a rate of 150 gpm and the pool depth at 9 in. are compared in Figure 5-2 with the corresponding tracer motion map from Appendix B (Figure B-2). In the CFD simulation snapshot, the shading indicates the magnitude of the flow velocities near the tank floor. The higher end of the shading bar indicates locations where the flow velocity was at or greater than 0.2 ft/s, and the lower end indicates near-zero velocities. The water flowed in both directions around the annulus from the pipe inlet to the outlet box. There was very little flow through the interior regions.

Exploratory tests (described in detail in Appendix B) were conducted using spherical tracers placed on the pool floor after steady state was achieved. These allowed the flow patterns within the tank to be visualized. After the tracers were placed on the floor of the tank, their motion was observed and charted over a period of time. The process was repeated at numerous locations and for a variety of tank flow conditions. Charts showing multiple individual "motions tracks" effectively demonstrated flow patterns within the tank. These tracks also provided some indication of the velocity of flow; however, these tracers could not be used to determine flow velocities accurately because the velocity of the tracers lags behind that of the flow by an undetermined amount and the measured velocity of the tracers represented an average for the entire track, including the time when a tracer may have stopped.

Several flow measurements were made using a neutrally buoyant balloon while the apparatus was in Configuration A, and the pump flow rate was nominally 150 gpm. The fastest flow velocity measured using this method was about 0.17 ft/s, which was in the annulus near the outer wall. This measurement was in good agreement with the CFD results shown in Figure 5-2. The slower flow velocities nearer the inner annulus walls also were verified. These balloon velocity measurements tended to verify the validity of the analytical CFD results.

As discussed in Appendix B, the spherical tracers were found to start rolling when the local flow velocity near the tracer reached or exceeded a velocity range from 0.22 to 0.27 ft/s. That is, in relatively uniform and nonturbulent flow, some tracers were found to begin to move at a flow velocity of 0.22 ft./s, and all tracers were found to move in bulk at a velocity of 0.27 ft/s (or greater). These threshold velocities were measured in a linear flume in which the flow turbulence had been dampened to low levels. If the flows within the integral test tank were both uniform and nonturbulent, then the tracer should have moved only in the faster regions in Figure 5-2. However, the tracer motion map clearly indicates that the tracers were actually in motion at locations where the flow velocities were substantially less than the threshold velocity of 0.22 ft/s. The tracers apparently were moving when the flow velocities were on the order of about 0.15 ft/s. The most likely reason that the tracers tended to move at flow velocities below the measured threshold velocities required to move them was the additional flow turbulence of the tank tests. It was noted during Configuration A testing that the agitation associated with the inlet flow plummeting into the tank tended to extend around the annulus of the tank. These results clearly indicate that agitation within the pool likely will move debris at lower flow velocities than indicated by the uniform nonturbulent threshold velocities measured for a particular type of debris. In addition, it should be noted that there was significant uncertainty in the measurement of the pump flow rates, so the actual test flow rate may have been somewhat higher than 150 gpm. When models are devised to estimate debris transport within a pool, each model must consider the potential effect of pool agitation on debris transport.

In addition to the tracks showing movement of the tracers in the outer annulus, many of the tracers came to rest when they moved toward the inner spaces, where both the CFD simulations and the balloon velocity measurements showed slower velocities. Test observations, as well as these results, tend to verify the ability of the CFD code to predict the flow velocities' patterns within the tank.

Section 4 discussed the results of Configuration A tests conducted with actual debris, i.e., Figures 4-6, 4-7, and 4-8 for Tests F5, F6, and F7 that used LDFG, Al-RMI, and SS-RMI insulation debris, respectively. Because these tests were fill-up-phase debris-transport tests in which the pool depth and flow velocities were all transient, a direct comparison with a single CFD

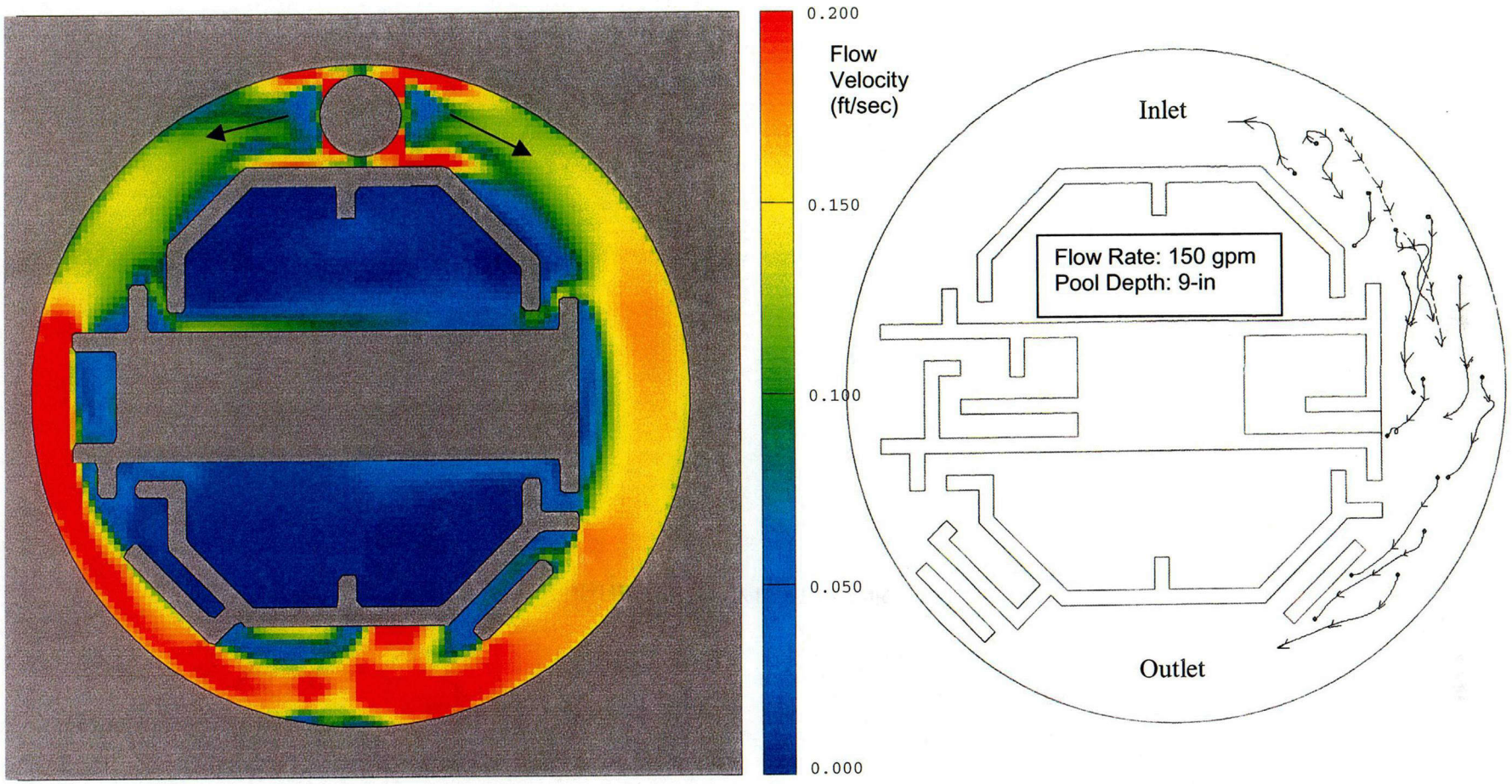

CFD Simulation

Tracer Motion (Ref. Fig. B-2)

Figure 5-2 Comparison of Configuration A CFD Simulation with Tracer Motion Map

C01

INTENTIONALLY LEFT BLANK

velocity map (Figure 5-2) provides only limited insights. However, one can see how flow from the inlet pipe along both sides of the annulus would push debris placed in front of the flow into each of the side compartments as these compartments filled, as well as toward the outlet box.

A few details of the CFD simulation further illustrate the patterns of flow within the tank. The pool velocities did not vary much with pool depth except in the regions near the pipe inlet. A vertical cross section of the annulus midway between the inlet and the outlet (the right side of Figure 5-2) is shown in Figure 5-3. Although there is some 3-D structure to this flow pattern, the velocities on the outer side of the annulus were about 0.15 ft/s; on the inner side, the velocities were less than about 0.05 ft/s. Tracers would stop upon entering the inner, slower flowing side of the annulus. Vertical variations could well occur in deeper pools. (This pool was only 9 in. deep.)

A similar situation was found on the opposite side of the tank as shown in Figure 5-4. In this situation, the annulus flow was forced through a narrower section of the annulus (left side of figure), where its velocity exceeded 0.2 ft/s. Debris did not remain there. However, there was an offset space at this location where the water was relatively quiescent. The horizontal cross section of this space is shown in Figure 5-5. Within this offset, a small, slow-rotating vortex was formed in the CFD simulation, and it was observed during testing that the vortex did trap debris. The photo in Figure 6-6[16] illustrates the debris capture within this offset. Once again, the CFD simulation predicted a feature of the pool that was observed during testing and illustrated a mechanism for trapping debris.

5.2 Test Configuration B Simulation

Simulations of the tank flow patterns also were completed for test Configuration B. The steady-state-pool flow velocities for the simulation with the inlet flow set at a rate of 120 gpm and the pool depth at 9 in. are compared with the corresponding tracer motion map from Appendix B (Figure B-6) in Figure 5-6. The shading scale is the same as that of the preceding figures.

[16]The photo was taken during a Configuration D test.

The input water, which was introduced into the interior compartment, entered the annulus from both sides of that interior compartment.[17] These flows then flowed toward the outlet box; however, the flow exiting on the right side (of Figure 5-6) split such that a portion of that flow passed around the backside of the tank (opposite of the outlet box). These exiting flows are better shown in the blow-up sections in Figures 5-7 and 5-8 for the left and right exits, respectively. In these blow-up sections, vectors indicate the direction of flow. There was very little flow through the other interior regions. Regions of relative quiescence were inter-dispersed with the regions of faster flow.

Comparing the CFD simulation results with the tracer tracks illustrates that, generally speaking, only the tracers in faster flow locations actually moved from their initial positions. This comparison shows that the comparison between the CFD simulation results and the tank test data is good. The CFD code predicted the tank flow patterns indicated by the tracers.

5.3 Test Configuration C Simulation

Simulations of the tank flow patterns were completed for test Configuration C. The steady-state-pool flow velocities for the simulation with the inlet flow set at a rate of 95 gpm and the pool depth at 9 in. are compared with the corresponding tracer motion map from Appendix B (Figure B-8) in Figure 5-9. The shading scale is the same as that of the preceding figures.

The input water, which is introduced into the interior compartment, entered the annulus from both sides of that compartment. These flows then moved toward the outlet box, leaving a relatively quiescent region of the pool in the annulus opposite the outlet box where debris could be retained. These exiting flows are better shown in the blow-up sections shown in Figures 5-10 and 5-11 for the left and right exits, respectively. In these blow-up sections, vectors indicate the direction of flow. There was very little flow through the other interior regions.

[17]These passageways simulated the entrance doorways between the sump annulus and two connecting steam generator compartments in the actual plant.

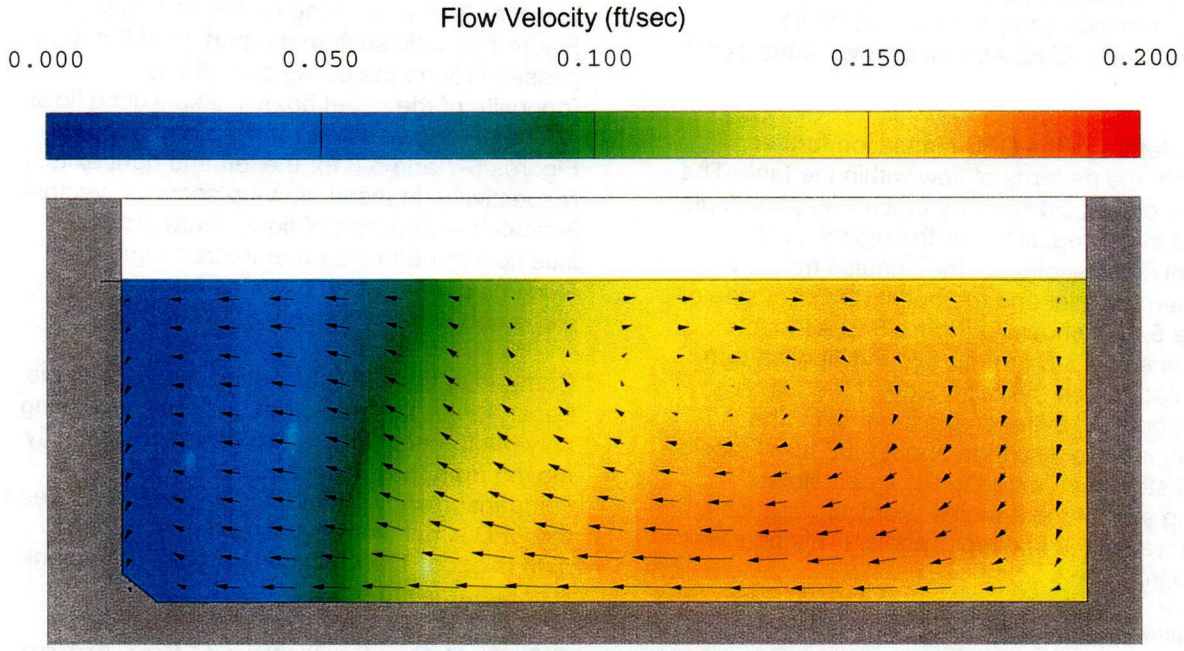

Figure 5-3 Vertical Cross Section of Configuration A CFD Simulation

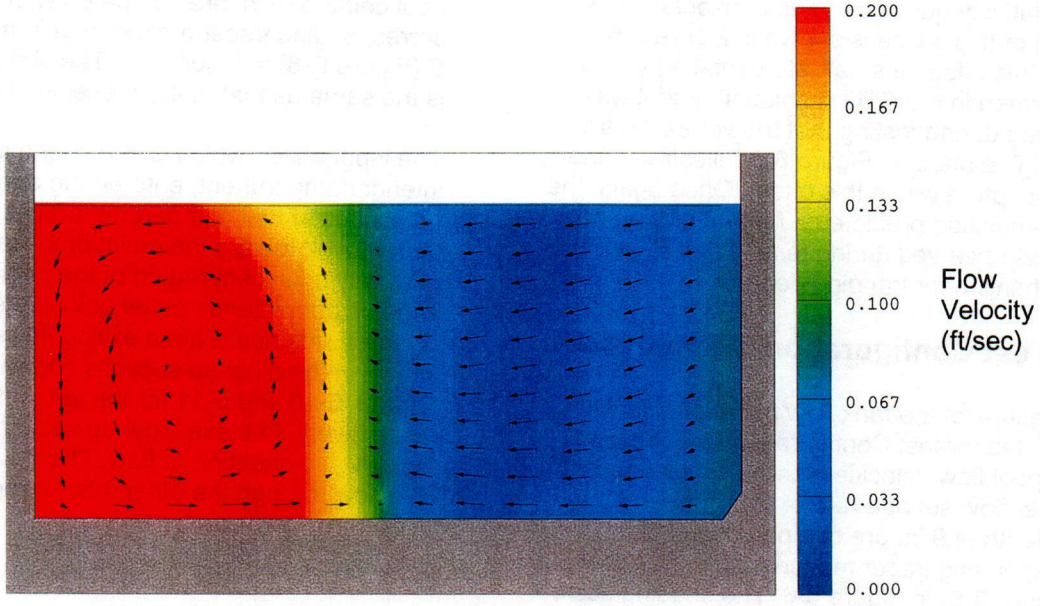

Figure 5-4 Vertical Cross Section of Configuration A CFD Simulation

C02

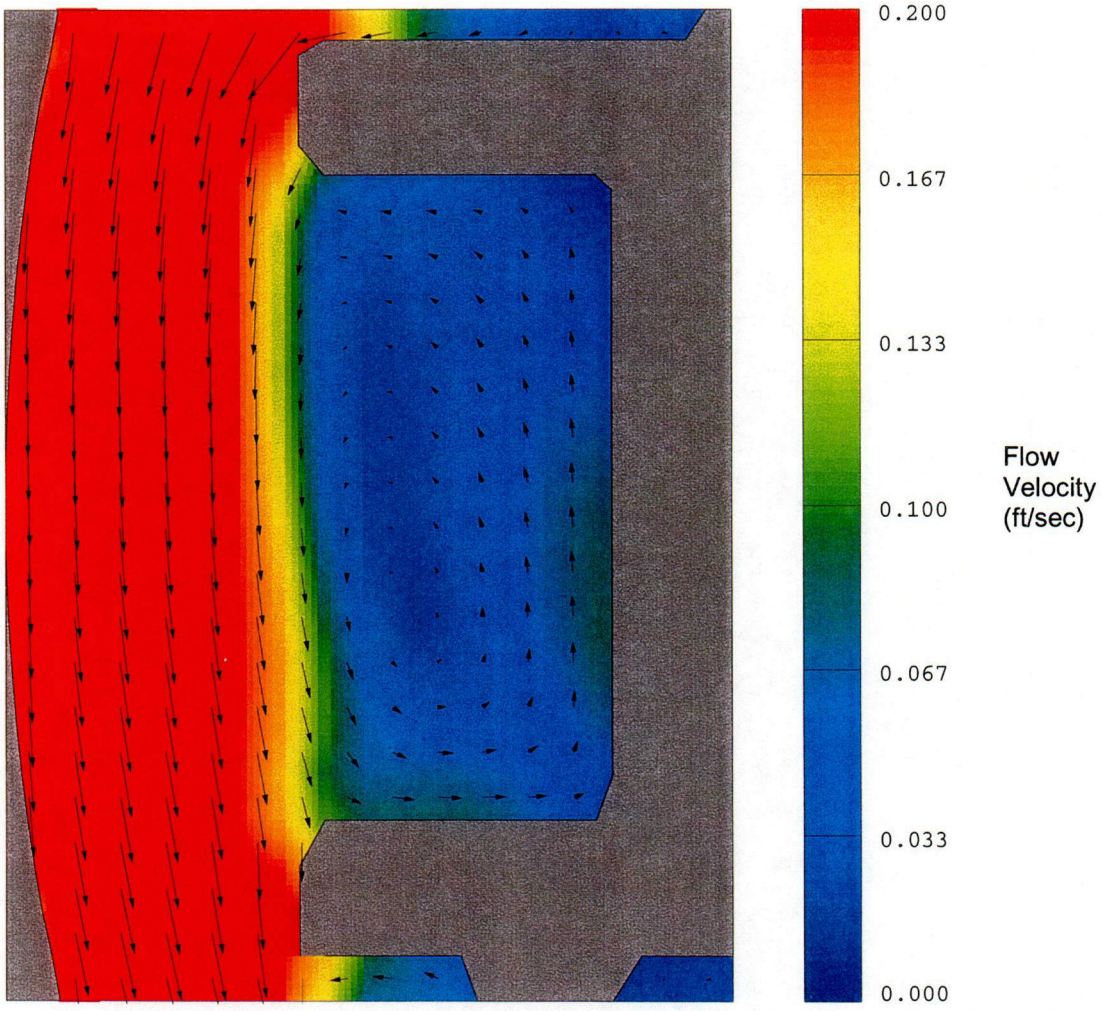

Figure 5-5 Horizontal Cross Section of Configuration A CFD Simulation

C03

INTENTIONALLY LEFT BLANK

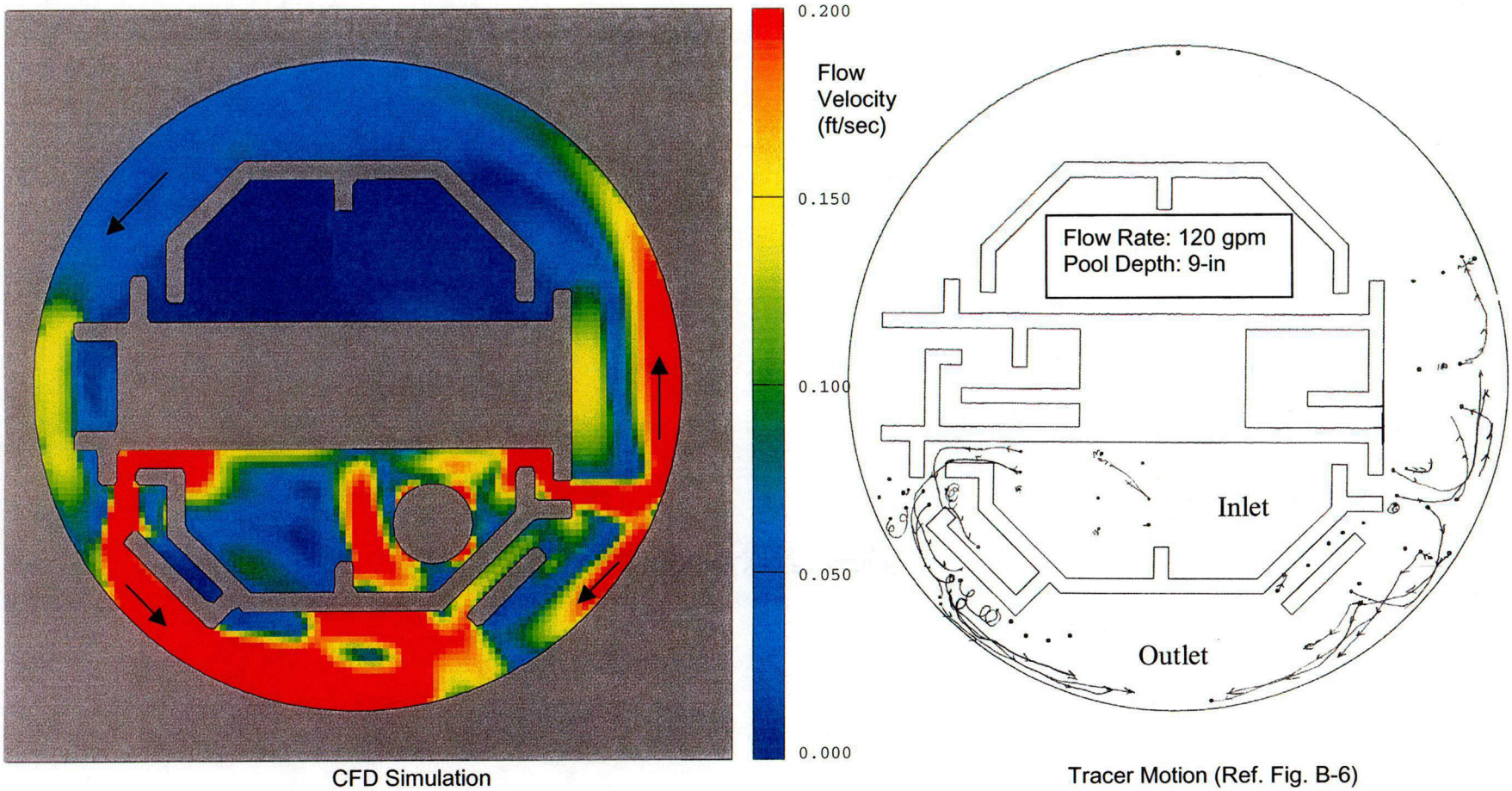

CFD Simulation

Tracer Motion (Ref. Fig. B-6)

Figure 5-6 Comparison of Configuration B CFD Simulation with Tracer Motion Map

C04

INTENTIONALLY LEFT BLANK

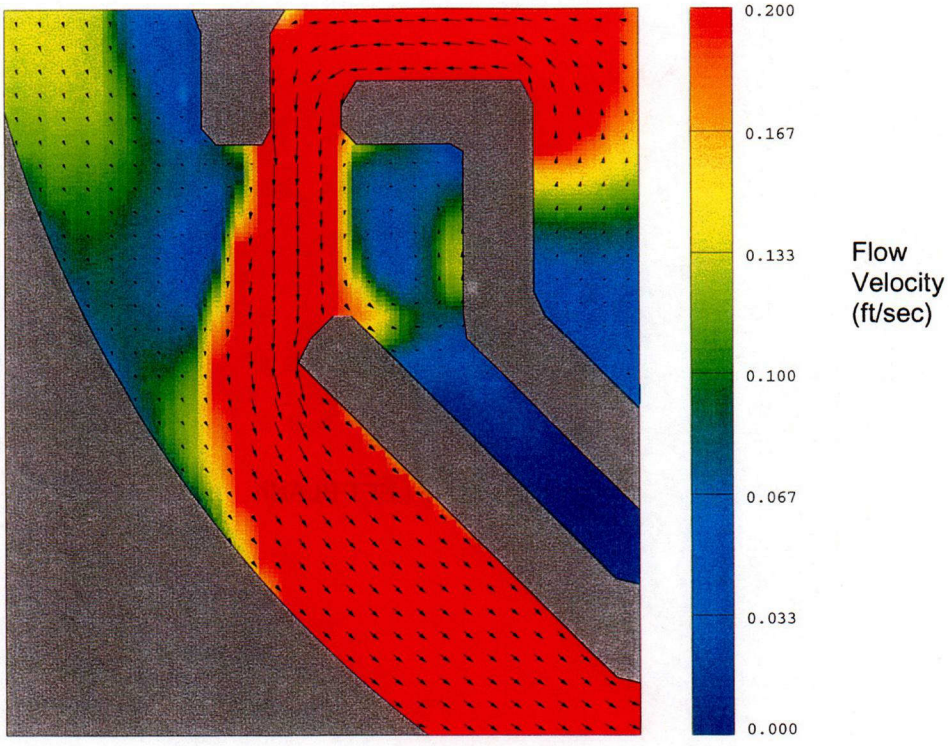

Figure 5-7 Blow-Up Section of Configuration B CFD Simulation (Left)

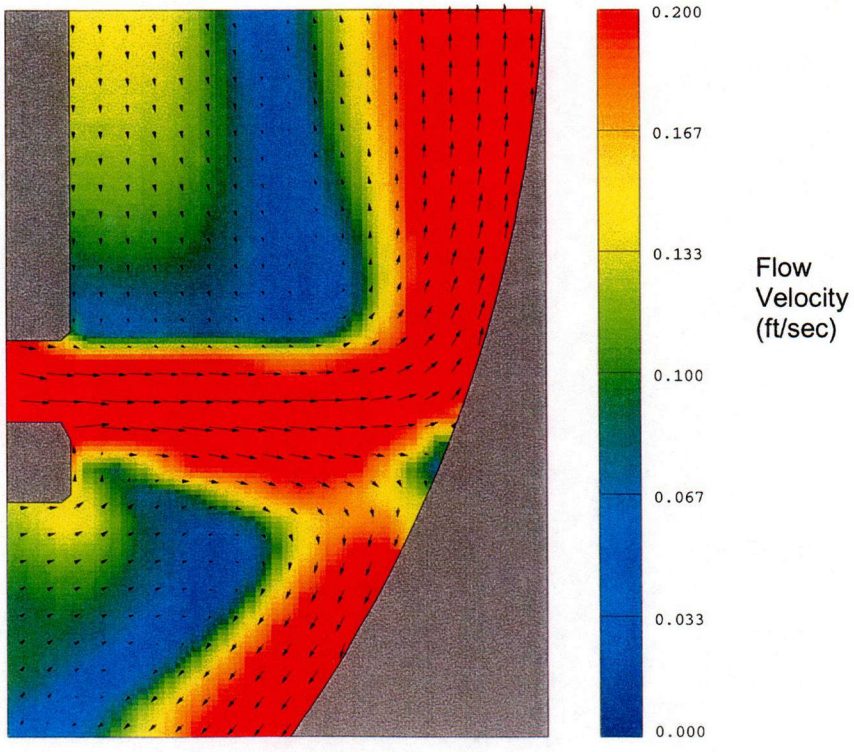

Figure 5-8 Blow-Up Section of Configuration B CFD Simulation (Right)

C05

INTENTIONALLY LEFT BLANK

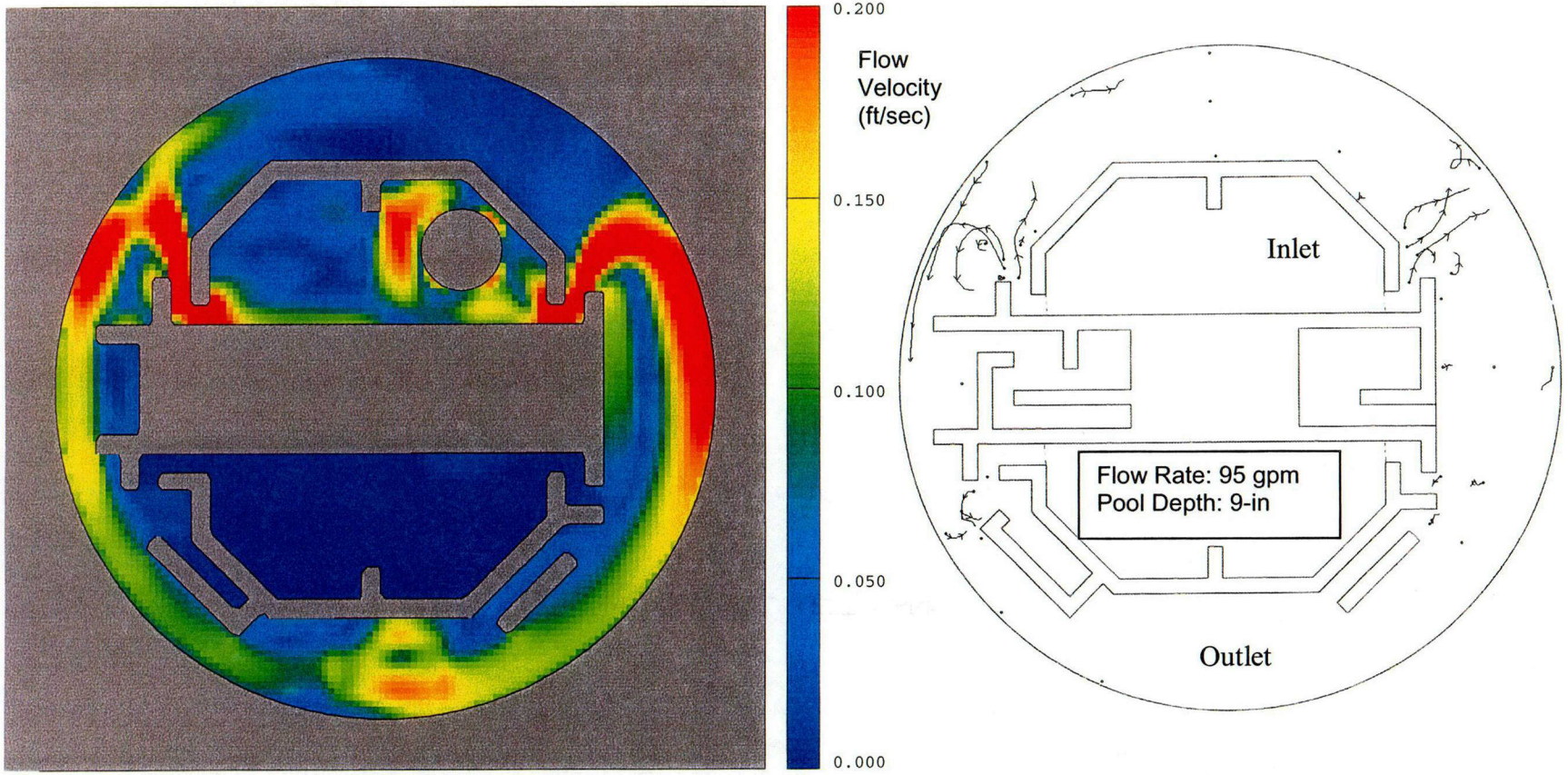

Figure 5-9 Comparison of Configuration C CFD Simulation with Tracer Motion Map

C06

INTENTIONALLY LEFT BLANK

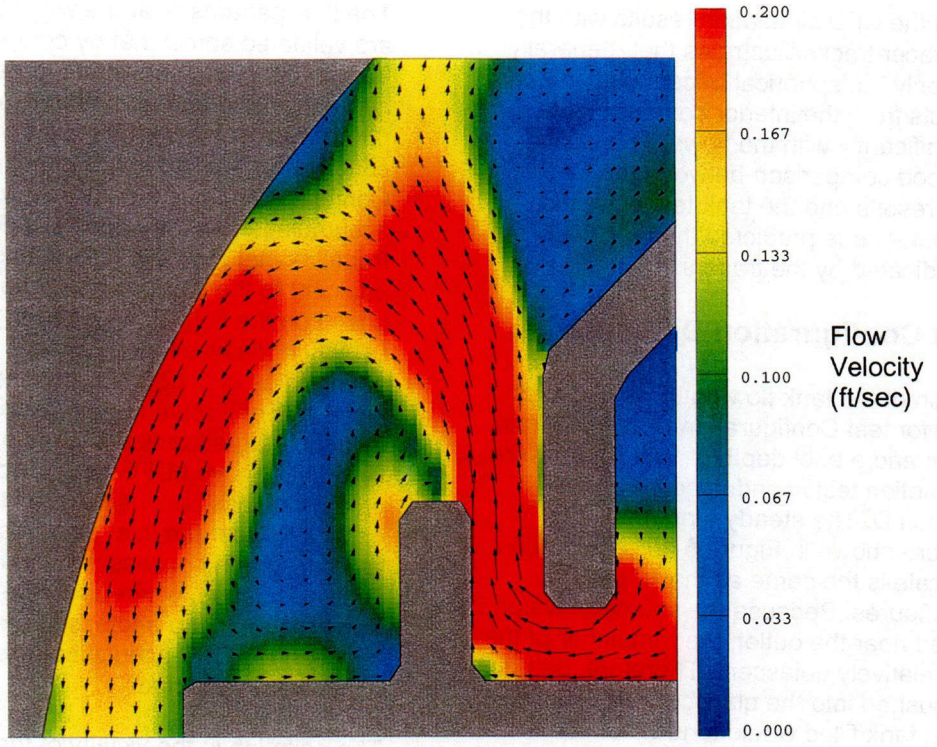

Figure 5-10 Blow-Up Section of Configuration C CFD Simulation (Left)

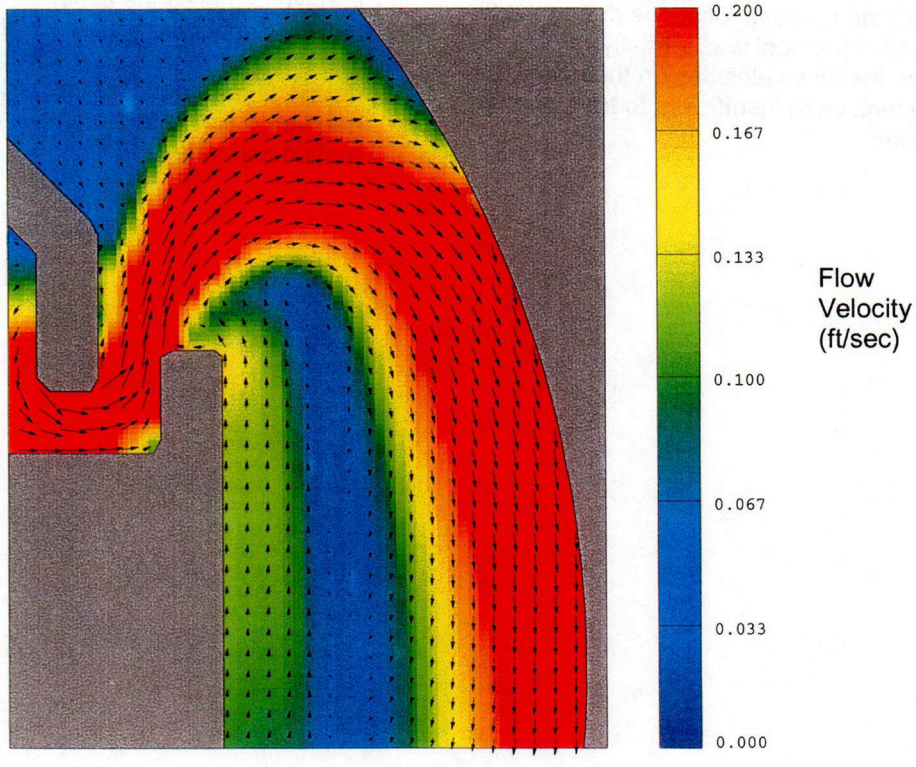

Figure 5-11 Blow-Up Section of Configuration C CFD Simulation (Right)

C07

Comparing the CFD simulation results with the spherical tracer tracks illustrates that, generally speaking, only the spherical tracers placed near the flow exits from the interior compartments moved significantly with the flows. This again shows a good comparison between the CFD simulation results and the tank test data; the CFD computer code predicted the tank flow patterns indicated by the tracers.

5.4 Test Configuration D Simulation

A simulation of the tank flow patterns also was completed for test Configuration D at a flow rate of 140 gpm and a pool depth of 9 in. There were no tracer motion tests conducted in Configuration D. The steady-state-pool flow velocities are shown in Figure 5-12. Again, the shading scale is the same as that of the preceding figures. Because the source of water was located near the outlet, the remainder of the tank was relatively quiescent. Therefore, debris that was pushed into the quiescent side of the tank as the tank filled would tend to remain there unless the debris was fine enough to be suspended. Example photos of debris remaining on the quiescent side of the tank are shown in Figures 6-3, 6-4, and 6-6. Note that this debris was transported to these locations during the fill-up phase; after the pool was partially established, the flow velocities on the quiescent side of the tank were insufficient to transport the debris further.

The flow patterns near the water inlet and outlet are validated somewhat by comparing Figure 5-12 with the photo shown in Figure 6-5. The pump flow rate and pool depth shown in this photo were approximately the same as the conditions specified in this simulation of test Configuration D. The photo shows LDFG debris accumulation on the opposite side of the tank from the inlet pipe and little debris near the wall adjacent to the pipe, as would be expected based on the CFD flow patterns. Note that LDFG debris was found to move along the floor at velocities of 0.12 ft/s or greater in water with low levels of turbulence (flume test data). In these integrated tank tests, the minimum flow velocity to move LDFG debris would be somewhat less because of pool turbulence, especially near the inlet pipe. Also note that the vertical screen box was not simulated in the CFD calculation, whereas the vertical screen was present in the photo, so some differences between the CFD simulation results and the photo were expected.

The agitation in the vicinity of the water inlet is illustrated further by a vertical CFD cross-section taken near the inlet that also passes through the outlet box (Figure 5-13). The CFD code appears to have captured the essence of the agitation that was observed with the water plummeting into the pool; however, a substantially more detailed input model of this region would be needed to simulate the details of this agitated motion accurately.

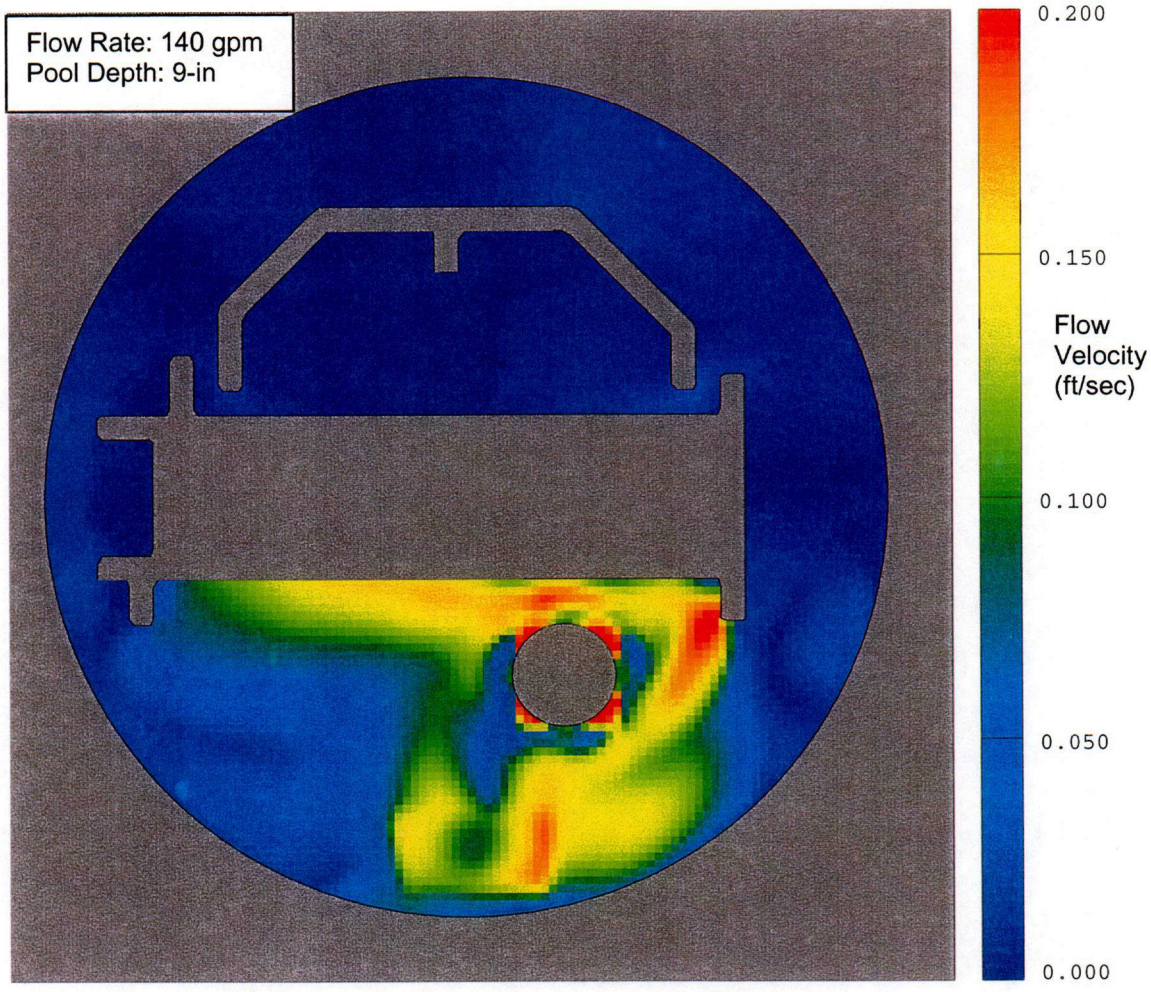

Figure 5-12 Configuration D CFD Simulation Result

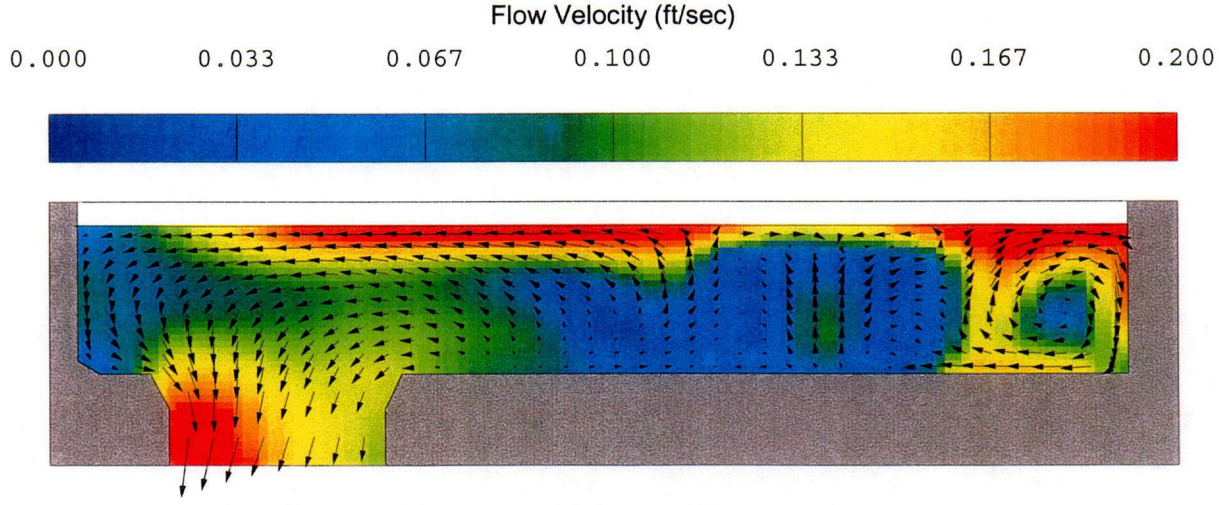

Figure 5-13 Configuration D CFD Simulation Inlet Region Agitation

C08

6.0 SUMMARY, CONCLUSIONS, AND RECOMMENDATIONS

Experiments were conducted to examine insulation-debris transport under flow conditions and geometric configurations typical of those found in PWRs. This work was part of a comprehensive research program to support the resolution of GSI-191, which addresses the potential for debris accumulation on the PWR sump screens and consequent loss of the ECCS pump NPSH following a LOCA. Among the GSI-191 program research tasks is the development of a method for estimating debris transport in PWR containments to estimate the quantity of debris that would accumulate on the sump screen for use in plant-specific evaluations. Predicting the transport of debris within the sump pool is a major part of that methodology. The analytical method proposed by LANL to predict debris transport within the pool is to use CFD combined with experimental debris-transport data to predict debris transport and accumulation on the screen. CFD simulations of actual plant containment designs would provide flow data for a postulated accident in that plant, e.g., 3-D patterns of flow velocities and flow turbulence. Small-scale experiments would determine the parameters defining the debris-transport characteristics for each type of debris. The integrated debris-transport test program was conducted to obtain debris-transport data under test conditions designed to simulate a variety of PWR containment and sump features.

The integrated debris-transport test program provided data that should support the development and/or validation of appropriate models designed to evaluate debris transport in a PWR containment sump; it is likely that such models will be developed to evaluate debris transport in a PWR plant on a plant-specific basis. For example, the tests developed data that could be used to benchmark CFD-based simulations supporting estimates of debris transport in water pools formed on PWR containment floors. The test data also provide insights that could support the development of simpler models, methods, or criteria for estimating debris transport. These insights specifically include the relative importance of the various debris-transport mechanisms and information regarding containment geometric features, such as the important features of the containment layout and sump positioning that affect debris transport and accumulation on the sump screen. The significant and important findings of the test program are summarized in Section 6.1 followed by conclusions and recommendations in Sections 6.2 and 6.3, respectively.

6.1 Summary of Test Findings

The test program provided data for various combinations of inlet conditions, four geometrical configurations, two screen configurations, and different debris types. The conditions of the tests established quiescent, turbulent, and rotational flow regimes within each test. Two phases of debris transport were examined: (1) debris transport during the period when the sump is filling with water and then (2) debris transport after the pool has filled. Important insights, observations, and findings from the test program are summarized below.

6.1.1 Effect of Buoyancy

Debris transport depended greatly on the buoyancy of each piece of debris. Preliminary testing of fragments of buoyant foam insulation confirmed that truly buoyant debris simply floated across the top of the water surface until it reached either a quiescent region, where it remained, or the outlet screen, even when subjected to the vortices of the rotational flows in the tests. If the outlet screen was fully submerged, the buoyant debris simply swirled above the outlet, but when the screen was submerged only partially, the buoyant debris partially blocked the screen at the water level. The separate-effects flume tests [4] indicated that this type of deposition likely does not cause significant head loss, but the buoyant debris was not tested in combination with other debris accumulation.

Buoyant debris also could include debris that normally would not be buoyant but had air trapped within it. Examples of such debris included partially torn fiberglass blankets and partially damaged RMI cassettes. These types of debris, when dry, move around partially submerged and easily could be transported with the water flow. Depending on the water temperature and the integrity of the encapsulation material, these types of debris

could become saturated with water and sink to the floor.[18] After they sink to the floor, these types of debris were found to be very difficult to transport, even at higher flow velocities. These types of debris potentially could block pathways connecting internal compartments (e.g., gratings on the doorways). Unsaturated blankets were observed that quickly moved closer to the sump screen during the fill-up phase and then sunk in front of the screen, thereby reducing the effective filtration area of the screen. Plant-specific analyses should consider these modes of transport.

Neutrally buoyant (or near neutrally buoyant) debris stayed suspended in the pool even when the water was relatively quiescent. Most notable were individual (or small bunches of) fibers from fiberglass insulation.[19] These fibers did not settle any place within the tank in the time frame of the tests. Rather, the fiber remained relatively well mixed in the tank until it was filtered from the outlet drainage water flow. Transport and deposition for this type of debris could occur over a period of several hours, and typically, the resulting head loss is higher than that compared with larger shreds.

Nonbuoyant debris sunk to the bottom of the pool, where its transport was a result of tumbling and sliding across the floor when the flow velocities were sufficient to move the pieces unless there was sufficient pool agitation, such as near the inlet pipe area, to keep the debris suspended and mixed. Floor-level obstacles, such as a shallow barrier placed across the annulus, affected floor debris transport. Floor debris ultimately ended up in areas where the velocity was not sufficient to move it further. These areas included regions of quiescent water, the centers of vortices, behind an obstacle, or on the outlet screen.

One exception was calcium-silicate debris. Larger pieces of calcium-silicate debris tended to sink to the floor after they became saturated with water. However, they disintegrated with time because of the combined effects of fluid turbulence and fluid temperature. After they were "dissolved," the pieces gave out fibrous residue that readily transported (similar to the neutrally buoyant materials described above). The chemical environment may accelerate this disintegration further.

6.1.2 Transport Phase

In these tests, debris transport occurred in two phases: (a) the fill-up transport phase, which is analogous to the pre-ECCS switchover containment sump fill-up phase, and (b) the steady-state transport phase, which is representative of post-switchover conditions. In the present test program, the fill-up phase began with the initiation of water flow into the tank and ended after a brief period of steady-state operation. Debris placed on the tank floor before pump flow was initiated underwent transport associated with the initial fast-moving flows as the tank began to fill, as well as steady-state pool transport after the tank reached steady state (and all intermediate flow conditions as well). This corresponds to debris entrapped on the containment sump floor during and shortly after completion of the primary system depressurization. In contrast, debris introduced after the steady-state pool was established was subjected simply to steady-state pool transport. This debris transport corresponds to deluge debris transport by the containment sprays and debris transport caused by water films draining down containment surfaces.

The tests repeatedly illustrated that as the initial inlet flow spread out across the tank floor during the fill-up phase, the flow pushed debris in front of the water flow as shown in Figure 6-1. This resulted in debris that initially was located near the inlet being pushed into the farther regions of the tank. This type of transport lessened with the

---

[18] A completely intact fiberglass blanket with a canvas cover takes approximately 15–20 min to sink to the floor when it is subjected to hot water (180°F). In colder water, the blanket tends to stay in suspension relatively indefinitely. RMI cassettes could stay afloat between 8 and 15 min, depending on whether they have slots on their sides. Al-RMI cassettes seem to stay afloat even longer. NUREG/CR-6772 [4] provides additional data.

[19] BWROG Air Jet Impact Tests (AJITs) [8] indicated that 5–10% of the generated debris from the destruction of LDFG insulation was made up of such smaller debris types. For mineral wool (European investigations) and aged-LDFG (NRC), this fraction could be larger. Some 15–25% of the LDFG insulation destroyed by an air jet during the Colorado Engineering Experiment Station, Inc. (CEESI) debris-transport tests [9] was in the form of very fine debris classified as non-recoverable because the debris either passed through a fine mesh screen to the environment or was too small to collect by hand.

distance from the inlet and as the tank water level rose. Upon completion of the fill-up phase, the debris generally had been relocated from its initial position. If the inlet was located near the outlet, substantial debris was relocated toward the rear of the tank (away from the outlet). This action tended to reduce the overall transport fraction. Conversely, if the inlet was located away from the outlet, the fill-up process relocated substantial debris toward the outlet, thereby tending to enhance the overall transport fraction. During the fill-up phase, substantial debris was pushed into inner compartments not directly associated with the inlet, where this debris tended to remain. The debris was pushed into regions of low velocity and low agitation, referred to here as quiescent regions.

In a PWR plant, another consideration for fill-up-phase transport would be the design of the sump. If the sump screen were physically below the floor level, debris that was pushed into the sump region during fill-up likely would become trapped in the sump, whereas with the sump screen above the floor (as it was in the tank tests), debris relocated to the sump was found later to partially drift away at the flow velocities typically tested. In addition, water flows preferentially toward the recirculation sump and/or the reactor cavity until these below-floor cavities are full. Therefore, this filling process and the time required to fill would affect debris transport. The effect of this filling process would be plant- and accident-sequence-specific.

In contrast to the fill-up phase, debris transport during steady state is much simpler. Here, debris simply followed the water and moved with the water if the local water velocity was sufficient to induce tumbling or sliding or settled out if the local water velocity was not sufficient to induce movement. Typically, steady-state transport is predictable and can be predicted by combining debris-transport data [4] with bulk-flow velocity information. The likely debris-entrapment mechanisms are (a) flow deceleration resulting from channel-width changes, (b) offset regions adjacent to the primary flow region resulting in the formation of eddies and quiescent regions, (c) cavities directly facing the approaching flow as a result of the Stokes effect, and (d) obstacles (e.g., curbs) on the sump floor.

6.1.3 Turbulent Mixing and Sump Location

Pool turbulence keeps most small debris near the inlet in suspension and rather well mixed. The turbulence associated with the inlet flow is shown in the photo in Figure 6-2. These conditions are conducive to keeping debris in suspension and further degrading the insulation fragments. RMI debris, as well as LDFG fibrous debris, was kept suspended close to the inlet. This mixing effect was demonstrated using numerous small polystyrene cylinders.[20] The effect of the turbulence lessens with distance from the inlet, and when the distance separating the sump and the inlet is sufficiently large, the debris transport away from the inlet turbulence likely would be relatively unaffected by the inlet turbulence. As turbulence subsides, all but the finer debris could settle to the sump floor before it reaches the sump.[21] In the experiments, when the inlet pipe is inside an inner compartment (as in many operating PWRs), most of that compartment remained relatively turbulent and the debris in that compartment remained in suspension (except for some in the corners). However, adjacent compartments separated from the inlet region by a relatively narrow entrance likely would be quiescent, allowing debris to settle. With the inlet in the outer annulus, the turbulence could tend to extend a good part of the way around the annulus, as observed during the integrated tests.

With the inlet near the outlet screen (Configuration D in these tests), the turbulence of the inlet flow affects the accumulation of debris on the screen. In addition to keeping the debris in suspension near the screen, the turbulence could remove accumulated debris from the screen. Debris could be returned the screen repeatedly, thereby increasing the residence time of the debris within the turbulence and enhancing further disintegration of the debris.

[20] During preliminary testing, numerous small polystyrene cylinders were released into the tank along with the inlet flow in an attempt to visualize flow patterns. Difficulties associated with data collection and recovering these cylinders precluded their use in further testing.

[21] The exception was fine fibrous debris consisting of individual fibers or small bunches of fibers, which essentially remained suspended until they were filtered from the pool by the outlet screen.

Figure 6-1 Photo of LDFG Debris Transport During Tank Fill-Up Phase

Figure 6-2 Photo Illustrating Pool Turbulence/Agitation Below Inlet Pipe (Configuration D)

6.1.4 Debris Entrapment

One of the most important insights gained from the integrated tank tests was related to the potential for debris entrapment offered by several containment features and structures. Examples of debris entrapment in the tests are shown in Figures 6-3 through 6-6. It is interesting to note that for each location where debris entrapment was observed in these tests, associated CFD simulation results indicated that debris entrapment likely would occur.

Typically, debris settling occurs in (1) quiescent regions in compartments away from the inlet that are shielded by rather narrow openings or behind barriers in regions offset from the main flow path and (2) the center of vortices formed by flow-path expansion. These locations depended on flow patterns that generally were rather complex. Further, these patterns depended on the depth of the water pool, which affected pool velocities and turbulence. The flow asymmetries, which are predictable using CFD computer codes, play a role in creating quiescent regions.

Floor barriers. The barriers are capable of stopping or redirecting floor-debris transport. Tests were performed to examine the effectiveness of barriers, and the results are consistent with the findings of the separate-effects study [4]. Debris stopped behind a barrier was likely to remain there if the flow velocities and turbulence were insufficient to lift it over the barrier. A barrier easily could redirect debris away or into the main channel flow, such as into a side compartment. However, if the barrier does not cover the entire cross section of the flow, its effectiveness could be reduced significantly.

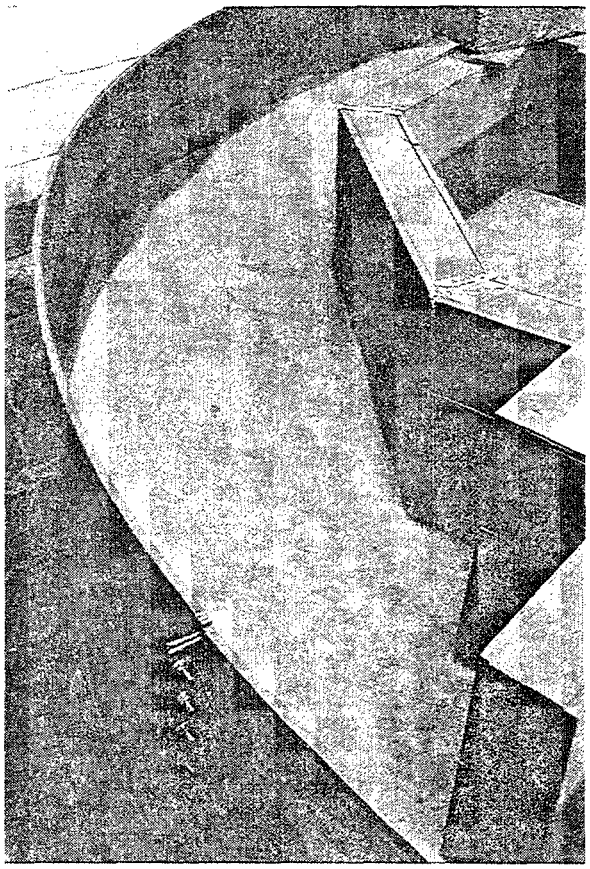

Figure 6-3 Debris Trapped in the Annulus Away from the Inlet

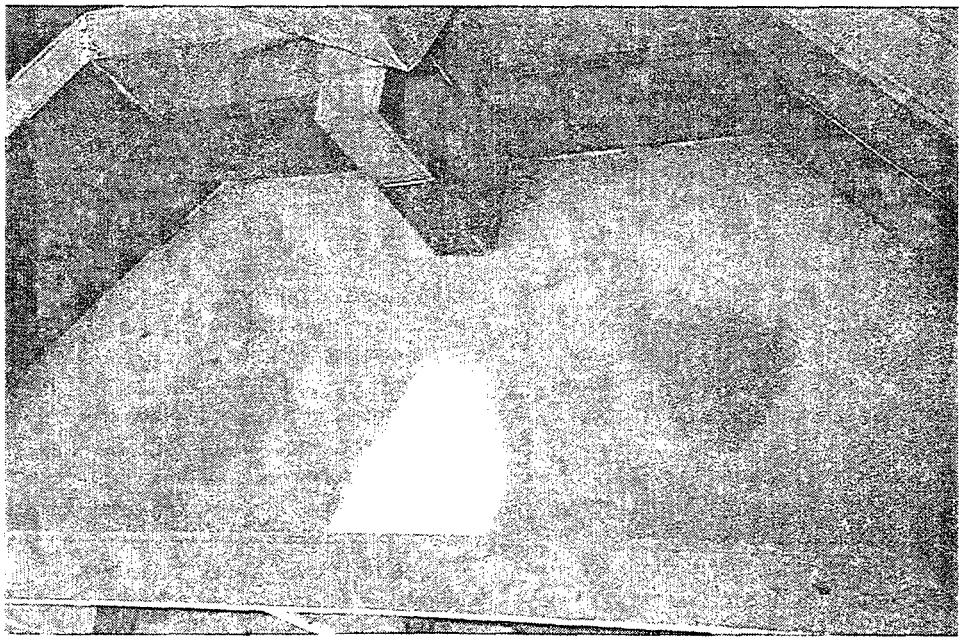

Figure 6-4 Debris Trapped in an Inner Compartment

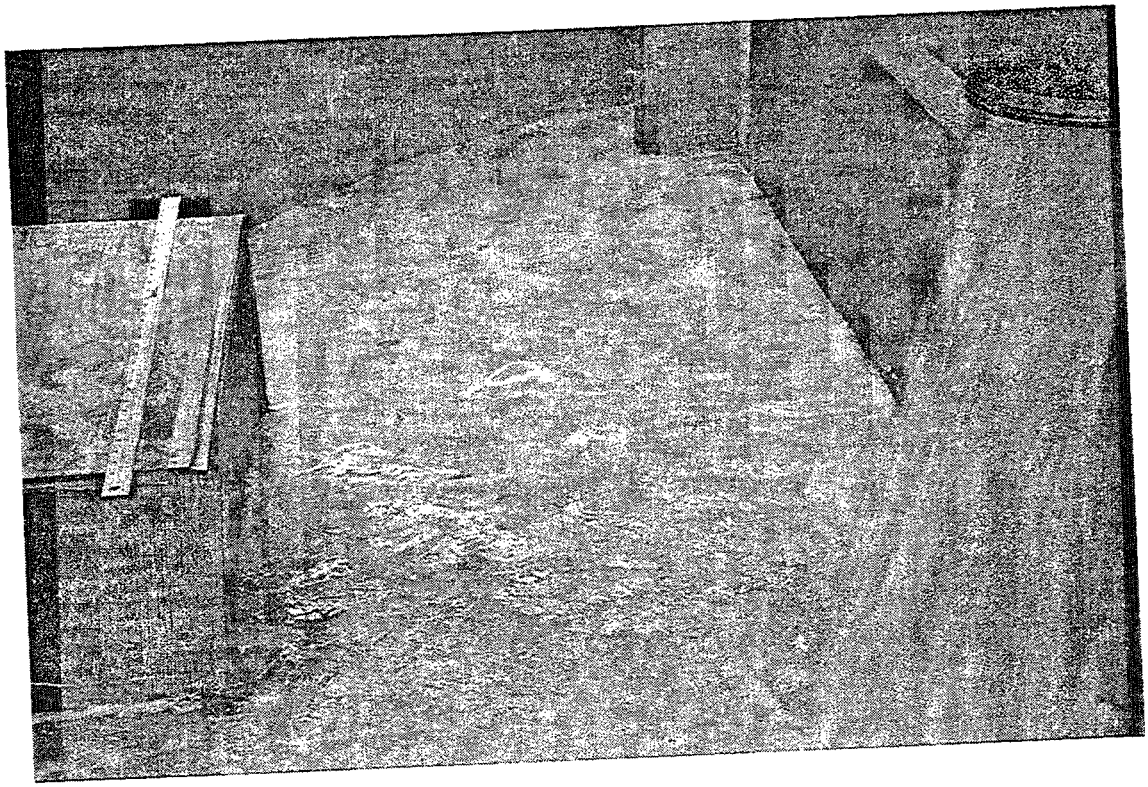

Figure 6-5 Debris Bunch to the Side of the Outlet Area

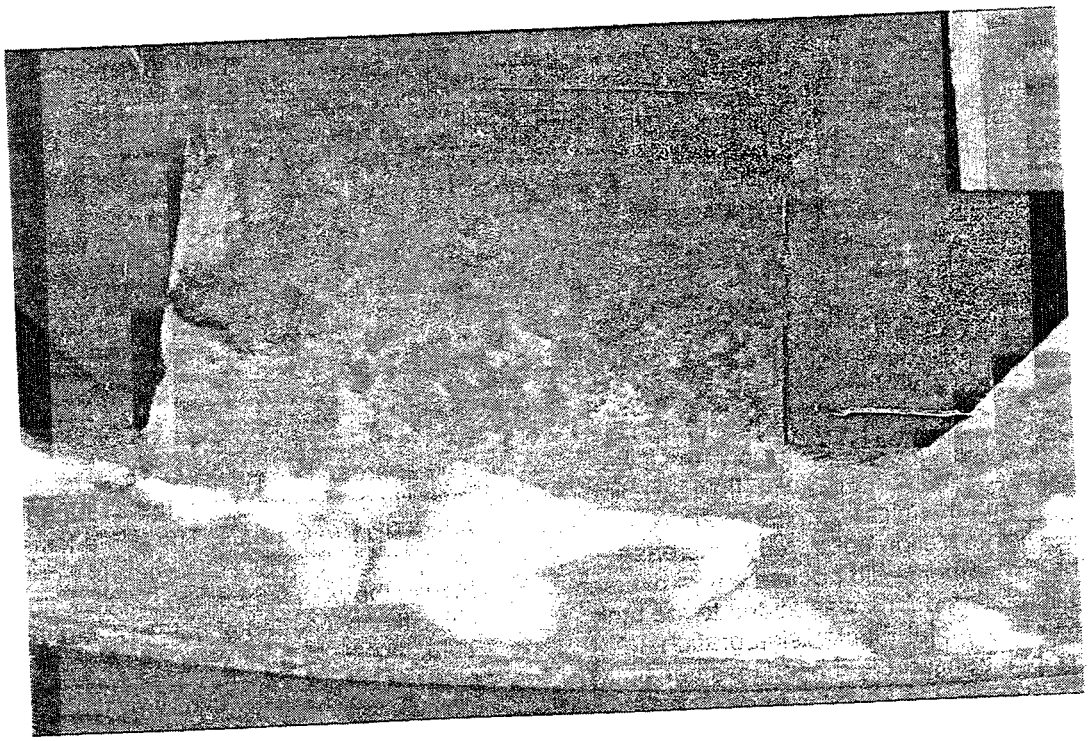

Figure 6-6 Debris Bunch in an Offset from the Annulus

Channel Expansion. Sudden expansion of the flow channel or bending of the flow paths caused rotational flows in the tests, where both relatively stable and unstable vortices were observed. Debris was found to reside in these vortices as shown in Figure 6-3. Close observations revealed how pieces of debris can be drawn into a vortex and how a debris piece trapped within a vortex can be affected by flow turbulence or pulsations, ejected from the vortex, and entrained in the bulk flow. LDFG debris inside a vortex (or in any quiescent region) frequently bunched together to form a "mat"-like structure. The trapped debris simply oscillated back and forth as a unit, and the "mat" appeared to barely touch the floor.

Quiescent Regions and Dead Regions. Examples of debris trapped in quiescent regions are shown in Figures 6-4, 6-5, and 6.6. Figure 6-4 shows debris trapped in an inner compartment relatively isolated from the inlet. Rotational flow inside the compartment tended to bunch the debris into the center of the compartment. Much of this debris was transported into the inner compartment from the inlet region during the tank fill-up phase. In Figure 6-5, the photo shows debris settled into a relatively quiescent area near the outlet box (top of the photo) despite the close proximity of the inlet. The debris scattered in front of the outlet was in motion but not necessarily moving toward the outlet. Often, debris was observed to move away from the outlet after having been trapped by the curb at the bottom of the outlet screen. In Figure 6-6, the debris is settled into a quiescent area offset from the annulus. With faster moving flows, the results would have been different.

6.1.5 Debris Disintegration Within the Tank

LDFG insulation debris was found to undergo significant additional fragmentation when it was subjected to the intense thrashing flow agitation associated with the inlet flow plummeting into the pool. Disintegration appeared to increase when the experiments did not use a flow diffuser and the insulation debris was added to the tank very close to the inlet. Such disintegration affects debris transport and head loss because it results in the generation of additional fine debris that remains suspended even at low levels of pool turbulence. In addition to LDFG, calcium-silicate insulation was found to undergo substantial disintegration. Calcium-silicate fragments were found to "dissolve," resulting in a fibrous residue that can be transported easily. The chemical environment may accelerate this disintegration further.

6.1.6 Screen Accumulation Observations

In the integrated tests of the transport of LDFG debris, the debris beds on the outlet screen were formed by the fine fibrous debris that normally remained suspended in the pool and by small pieces of debris that accumulated at the bottom of the screen and then occasionally "rolled up" onto the screen. Observations suggested that the accumulation of fine suspended debris dominated that of the floor transport debris. However, the actual contributions of the two processes could not be determined explicitly. It is believed that more than half of the accumulation was a result of the fine suspended debris.

Figure 6-7 is a photo of a typical debris bed formed when the tank pool was approximately 9 in. deep (about half the height of the screen). The fine debris tended to form a uniform layer across the entire cross-section of the screen that was under water, but the occasional "roll-up" pieces of debris contribute to its lumpiness. Because the fine debris remained suspended and reasonably well mixed in the tank pool, it accumulated uniformly as it essentially was filtered from the flow draining into the outlet box.

In some tests, small pieces of debris sometimes accumulated at the bottom of the screen. This type of buildup can be seen by looking closely at the bottom of the outlet screen in Figure 6-5. Most of the accumulation of the small pieces generally occurred within the first 30 min, after which the fine debris dominated debris accumulation.

The approach velocities to the screen for the majority of the integrated tests ranged from about 0.11 to 0.14 ft/s. The flume tests [4] found that pieces of small LDFG debris would tumble across the pool floor when the bulk flow velocities exceeded about 0.12 to 0.16 ft/s. Thus, the approach velocity in the integrated tank tests normally was fast enough to move pieces of LDFG along the floor to the outlet screen. However, these approach velocities generally were not sufficient to lift a piece of LDFG from the floor to a position higher on the screen. The flume test showed that the velocity had to exceed about 0.25 ft/s to lift a piece of

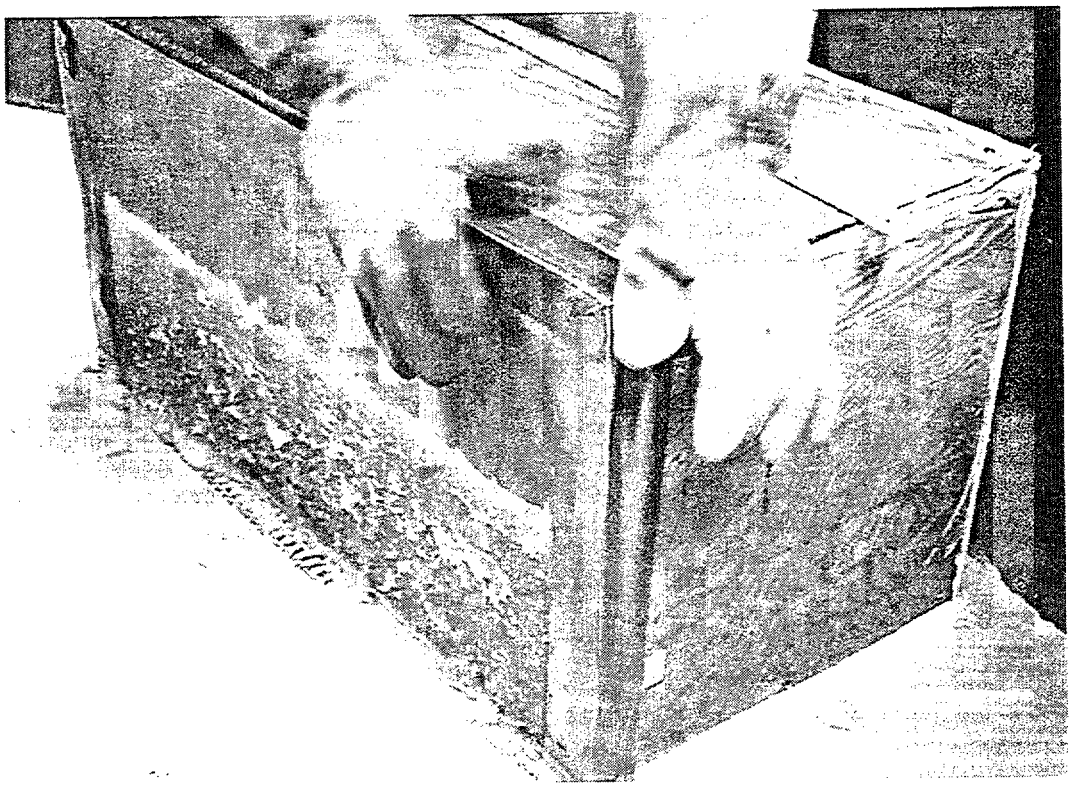

Figure 6-7 Typical Debris Buildup on Screen

LDFG over a 2-in.-high curb, which is why the small pieces tended to pile at the bottom of the screen. However, occasional pieces of small debris were observed to "roll up" onto the screen from the pile. It appears that occasional pulsations in the pool turbulence were lifting a piece of debris even though the average approach velocities were not fast enough to lift debris.

At the velocities tested, pieces of LDFG were seen drifting away from the debris pile at the bottom of the outlet screen. The flume tests showed that the velocity needed to keep a piece of LDFG on the screen was only about 0.05 ft/s, which was only about half the normal screen approach velocity. Apparently, the localized flow velocities at the bottom of the screen were somewhat less than the average screen-approach velocity, so pieces of debris were able to drift away from the screen.

The accumulation of LDFG debris created sufficient head loss to cause difficulties with draining the test tank. In fact, the debris usually had to be collected at intervals to keep the tank draining sufficiently to complete the tests. However, collecting the debris at intervals also provided time-dependent debris-accumulation data. In one of the first vertical screen tests, an unexpected blockage of an inner screen occurred, which forced the test to be terminated prematurely. This inner screen lay horizontally across the outlet box but inside the vertical screen box, and its purpose was to collect debris when the tank was cleaned at the end of the test after the vertical screen was removed. The outer vertical screen had been expected to filter virtually all the fibers from the flow stream. As it turned out, significant quantities of fibers passed through the vertical screen and collected on the finer mesh inner screen, which in turn filtered some sand[22] from the flow. When the inner screen was dried, this thin fiber/sand bed peeled off and looked like a layer of paper.

[22]Sand had contaminated the test facility reservoir.

6.1.7 RMI Transport

Tests were conducted to examine the transport of pieces of simulated RMI debris. During the fill-up phase, the pieces of RMI debris (both SS- and Al-RMI) were found to move readily with the water as it initially spread out across the tank floor. These tests were conducted with the inlet pipe located in Configuration A and the debris initially placed on the tank floor in the annulus a short distance from the inlet. In the test with Al-RMI, approximately 30% went to the outlet. In the test with SS-RMI, about 90% of the pieces went to the outlet. The transport of RMI during the fill-up phase depends greatly on the orientation of the inlet relative to the outlet and to the location of the debris. In some orientations, the inlet flow can push RMI toward the outlet, but in others, the inlet flow can push the debris away from the outlet.

After the tank became sufficiently flooded to slow the water flows, the RMI did not transport substantially at the tank velocities normally tested. The tumbling velocities for RMI, as measured in the flume tests, ranged from 0.2 to 0.25 for Al-RMI and 0.28 to 0.3 for SS-RMI. These tumbling velocities were larger than the tank velocities normally tested; hence, there was very little floor transport at steady-state flow conditions, i.e., an inlet flow ranging from 130 to 160 gpm. When the steady-state inlet flow was increased to 230 gpm, about half of the Al-RMI pieces on the pool floor moved from their original positions. At 440 gpm, all Al-RMI moved downstream except those pieces trapped in a quiescent region. RMI debris entering quiescent regions tended to stay in those regions (such as the inner compartments).

Pieces of RMI debris that were dropped into an established steady-state pool sometimes floated a significant distance before sinking because air was trapped within the debris. Some even floated to the outlet (horizontal screen configuration), where the piece swirled over the drain.

Probably the most important aspect of evaluating RMI debris transport is the transport during the fill-up phase. In some plants and some accident scenarios, the fill-up phase could push substantial RMI debris in the direction of the sump. Then, depending on outlet screen approach velocities, the RMI could accumulate on screen.

6.1.8 Intact Insulation Debris

It is possible for a relatively intact RMI cassette or an insulation pillow to be removed from the piping by the jet flow and deposited on the sump floor, where it could be transported to the sump screen. Fill-up-phase tests were conducted to examine the likelihood of these types of debris transporting across the floor. The tests considered a 1-ft by 1-ft SS-RMI cassette and a pillow of Thermal-Wrap fiberglass insulation. These fill-up tests were conducted with the inlet pipe in test Configuration A and either the cassette or the pillow placed a short distance from the inlet pipe. The pump flow rate required to move the item through the annulus then was determined. When the cassette or the pillow was initially dry, it moved through the annulus relatively easily at a pump flow of 120 gpm. However, when the cassette was filled or the pillow was saturated with water, it took a pump flow of 270 to 300 gpm to move it through the annulus. In a PWR plant scenario, these items could transport some distance during the fill-up phase until the item becomes saturated or the pool level deepens sufficiently to slow the fill-up flow velocity. These types of debris have a large potential to block pathways that connect internal compartments (e.g., gratings on the doorways). In some integrated tests, the unsaturated blankets quickly moved closer to the sump screen during the fill-up phase and then sunk in front of the screen, resulting in a lowering of the effective filtration area of the screen. Plant-specific analyses should focus on these modes of transport.

6.2 Conclusions

This test program provided data for various combinations of inlet conditions, geometrical configurations, screen configurations, and debris types. The conditions of the tests included the establishment of quiescent, turbulent, and rotational flow regimes within each test configuration. Preliminary comparisons of debris-movement data with CFD predictions provided a qualitative confirmation that CFD codes provide a necessary framework for modeling and analyzing debris transport.

The test program provided insights into the relative importance of the various debris-transport mechanisms and containment

geometrical features. Some of the important insights include the following.

1. Debris transport to the sump screen can occur in two-phases: the pre-ECCS switchover containment fill-up phase and the post-ECCS switchover steady-state phase. The importance of each of these phases is very plant-specific, but sump performance analyses should account for both phases explicitly.
2. The depth of the sump pool can have a pronounced effect on the fractions of debris transported to the sump screen, primarily because the bulk pool flow velocities are directly related to the pool depth, i.e., the deeper the pool the slower the water flow velocities, hence less debris would be transported. Debris transport during the pool fill-up phase could be more pronounced than during the steady-state phase. Plants with shallower pools would likely have higher pool debris transport fractions than plants with deeper recirculating sump pools.
3. Substantially more debris would typically be transported to the sump screen during the short-term as opposed to the longer-term transport. In the integrated debris transport tests, a majority of the debris is transported to the outlet screen during the first 30 min. Debris transport in the longer-term tends to consist of the finer debris that would remain in suspension during typical sump pool conditions.
4. The primary modes of debris transport depended upon the relative size and type of debris.
   a. Finer debris that remained suspended was simply transported with the water flow. The most notable example of suspended debris was individual fibers, which remained suspended even in relatively calm water flows for periods long enough for the fibers to be filtered from the pool by the sump screen.
   b. Non-buoyant debris typically sank to the pool floor where it would slide or tumble along the floor to the sump screen whenever and wherever the local pool flow velocities were sufficient to move the debris. For example, small pieces of fibrous insulation debris would typically saturate rather rapidly in hot water, sink to the bottom of the pool, and then tumble with the water flow in locations where the flow was fast enough.
   c. Truly buoyant debris floated along the pool surface until it reached the sump screen where it could accumulate on an exposed screen or hover over a completely submerged screen.
5. Transport of larger fragments (e.g., partially torn blankets of LDFG) should not be ruled out based solely on the fragments' characteristics after they are saturated with water. Instead, analyses should recognize that these debris types could transport to the screen or other narrow opening before they become saturated with water.
6. Debris entrapment in the quiescent or inactive regions is likely; however, refined plant-specific analyses may be needed to quantify the effect of such containment design features on debris transport.
7. The effects of various simulated containment features were observed to gain insights regarding their influence on debris transport.
   a. The position of sump relative to location of the break affects both debris transport near the sump screen and the accumulation of debris on the screen. The water plummeting from the break would create substantial to severe turbulence in the pool directly under the break. This turbulence keeps debris in suspension that would otherwise settle to the pool floor, which could relatively quickly transport the debris from that location. Turbulence near the sump screen would likely affect the accumulation of debris on the screen or even prevent accumulation of the larger debris. In a similar manner, turbulence associated with the drainage of containment sprays to the sump pool could affect debris transport and accumulation associated with the sump screens.
   b. An interior compartment can effectively isolate turbulent regions from the remainder of the sump pool, e.g., a break located in an interior steam generator compartment would isolate sump screens exterior to that compartment from most of effects of the break induced pool turbulence. Conversely, an interior compartment could be isolated rendering that compartment very quiescent so that debris located within the isolated compartment remains there.

c. The narrowing of flow channels accelerates flow and enhances debris transport within the channel but it also usually generates rotational flow regions where the channel widens and the flow de-accelerates.
d. Debris curbs and other floor level structures can both affect local flow and the forward motion of debris sliding or tumbling along the floor. Debris can be trapped or redirected by a structure. Debris can be lifted over a structure such as a curb if the flow velocities are sufficiently high.

8. For non-metallic debris, further disintegration of debris as a result of pool turbulence, particularly near the inlet flow, must be considered because the disintegration tends to generate more very fine debris that remains suspended even at low levels of pool turbulence. Nearly 100% of this very fine debris would transport to the sump screens.
9. Debris accumulation on the sump screen consisted of the filtration of suspended debris (e.g., individual or small groups of fibers) and small debris transported along the floor that may or may not roll-up onto the screen. The orientation of sump screen (i.e., horizontal versus vertical) primarily affects the accumulation of debris on the screen. Fine debris suspended in the water accumulated relatively uniformly regardless of the orientation of the screen. Debris that transported along the floor was affected by the screen orientation; this debris tended to accumulate near the bottom of a vertically orientated screen but more uniformly on a horizontally oriented screen.

6.3 Recommendations

The primary use of the data generated from the integrated test program should be to provide insights regarding the transport of debris and the accumulation of debris onto a sump screen. These insights should be valuable to the development of analytical debris-transport models. However, the measured transport fractions of the integrated tests should not be applied directly to plant-specific analyses because there is no apparent means of scaling those transport fractions from the test geometry to an actual plant. Rather, the CFD simulation models must apply the debris-transport phenomenology to all of the individual plant features for each specific plant. Another potential use of the integrated test data would be to use them to benchmark a specific debris-transport model, that is, show that the model can predict the measured transport fractions of the integrated tests.

The potential for pool turbulence to generate additional fine debris that would remain suspended in the pool was demonstrated; however, the tests did not provide a means of quantifying that disintegration as a function of turbulence levels. It is recommended that future test programs attempt to quantify this disintegration such that debris-transport models can account for the disintegration.

7.0 REFERENCES

1. D. V. Rao, B. Letellier, C. Shaffer, S. Ashbaugh, and L. Bartlein, "GSI-191 Technical Assessment: Parametric Evaluation for Pressurized Water Reactor Recirculation Sump Performance," NUREG/CR-6762, Volume 1, LA-UR-01-4083, 2002.

2. S. G. Ashbaugh, and D. V. Rao, "GSI-191 Technical Assessment: Development of Debris Transport Fractions in Support of the Parametric Evaluation," NUREG/CR-6762, Volume 4, LA-UR-01-5965, 2002.

3. B. E. Boyack et al., "PWR Debris Transport in Dry Ambient Containments – Phenomena Identification and Ranking Tables (PIRTs)," LA-UR-99-3371, Revision 2, December 14, 1999.

4. D. V. Rao, B. C. Letellier, A. K. Maji, and B. Marshall, "GSI-191: Separate-Effects Characterization of Debris Transport in Water," NUREG/CR-6772, LA-UR-01-6882, 2002.

5. A. W. Serkiz, "Containment Emergency Sump Performance," NUREG-0897, Revision 1, U.S. Nuclear Regulatory Commission, October 1985.

6. D. V. Rao, B. C. Letellier, K. W. Ross, L. S. Bartlein, and M. T. Leonard, "GSI-191; Summary and Analysis of US Pressurized Water Reactor Industry Survey Responses and Responses to GL 97-04," NUREG/CR-6762, Volume 2, LA-UR-01-1800, 2002.

7. G. Zigler, J. Bridaeu, D. V. Rao, C. Shaffer, F. Souto, and W. Thomas, "Parametric Study of the Potential for BWR ECCS Strainer Blockage Due to LOCA Generated Debris," NUREG/CR-6224 Final Report, U.S. Nuclear Regulatory Commission, October 1995.

8. "Utility Resolution Guidance for ECCS Suction Strainer Blockage," BWROG, NEDO-32686, Rev. 0, November 1996.

9. D. V. Rao, C. Shaffer, B. Carpenter, D. Cremer, J. Brideau, G. Hecker, M. Padmanabhan, and P. Stacey, "Drywell Debris Transport Study: Experimental Work," NUREG/CR-6369, Volume 2, SEA97-3501-A:15, September 1999.

APPENDIX A

FLOWMETER CALIBRATION

A Hoffer flowmeter (Model HIT-2-2-A-X-F) monitored the flow rate in the main pipes. The meter was calibrated several times to ensure its accuracy. The true volumetric flow rate was determined experimentally by measuring the time taken to fill the large flume (measuring 3 ft by 4 ft by 20 ft) to a designated water height and then comparing the time with the flowmeter data.

The recorded data are tabulated in Table A-1 and compared in Figure A-1, which shows the relationship between the meter readings and the measured volumetric flow rate. The calibration was checked periodically to ensure consistently accurate flow readings.

Table A-1 Flowmeter Calibration Data

Pump Frequency (Hz)	Volume Filled (gal.)	Time to Fill Volume (s)	Measured Flow Rate (gpm)	Flowmeter Reading (gpm)
33	74.8	46	98	111
34	112.2	49	137	142
35	149.6	55	163	169
36	149.6	43	209	199
37	224.4	53	254	260
38	224.4	47	287	299
39	299.2	51	352	341
40	288.2	42	427	424

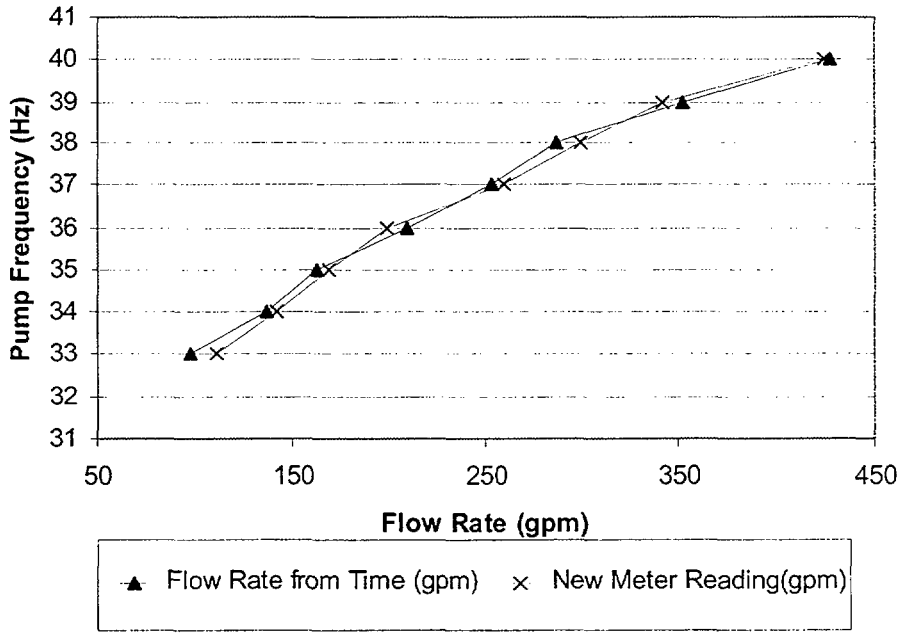

Figure A-1 Flowmeter Calibration Chart

APPENDIX B

SPHERICAL TRACER MOVEMENT TESTS

A series of exploratory tests was conducted that used spherical tracers placed on the pool floor to visualize flow patterns within the tank. After the tracers were placed on the floor of the tank, their motion was observed and charted over a period of time. Charts showing a multiple of these individual "motions tracks" then would, in effect, demonstrate the flow patterns within the tank. These tracks also provided some indication of the velocity of flow; however, these tracers could not be used to determine flow velocities accurately for a variety of reasons, including the uncertainty associated with floor friction effects and the slippage between the tracers and the flow. Nevertheless, these charts provide useful data that are documented in this appendix.

The tracers were small acrylic or nylon spheres (calibrated marbles) with a ¾-in. diameter. Section B.1 discusses the characteristics of these spheres and the measurement of those characteristics. Because the spherical tracers were found to start moving at about the same flow velocities as would typical debris under study, the spheres could be used as a surrogate for debris. The advantage of using the calibrated spherical tracers was their uniformity in contrast to actual pieces of debris, which varied from piece to piece.

The procedure was to place a spherical tracer at some initial location on the tank floor after steady-state flow was achieved. A 1-in.-diam PCV pipe was used to place the spherical tracer on the floor with minimal disturbance of the pool flow. The pipe (vertically oriented) simply was lowered to the bottom of the tank, the tracer was dropped through the pipe, and the pipe was lifted slowly out of the pool. As the water moved the tracer across the floor, the tracer's progress was charted and the time between two points was measured. In this manner, an average velocity of the tracer could be estimated. The process was repeated at numerous locations and for a variety of tank flow conditions. A few tests were conducted using actual insulation debris, but these debris tests produced little in the way of useful flow pattern measurements.

Neutrally buoyant balloons were considered first for these flow-pattern visualization tests; however, spherical tracers were found to work better than buoyant balloons because the tracers were smaller and would remain firmly against the floor. A few velocity measurements were taken using a neutrally buoyant, lead-weighted balloon. A balloon was inserted into the flow, and the time required for the balloon to traverse a measured distance provided the average flow velocity during that traverse. The balloon measurements yielded velocities ranging from about 0.05 to 0.1 ft/s in the annulus with a pump flow of 150 gpm and a water level of 11.5 in. (Configuration A). The slower velocities were measured in a region that was later designated a quiescent region where debris accumulated.

The test matrix and the results for these tests are provided in Sec. B.2.

B.1 Characteristics of Calibrated Spherical Tracers

The transport characteristics of the acrylic and nylon spherical tracers were measured before the tracers were used to determine pool flow patterns. Both the settling and tumbling velocities of the tracers were measured and compared with the corresponding velocities for typical debris. These velocities also were measured for some smaller glass spheres, but the characteristics of the glass spheres were found to be inadequate as a substitute for debris. Figure B-1 is a photo of the types of spheres tested. The specific gravities of the acrylic, nylon, and glass spheres (as provided by the vendors) were 1.39, 1.14 and 2.0, respectively.

The settling velocities were measured by dropping a tracer in a glass cylinder filled with water. The time required for the tracer to fall through 30 in. of water was used to calculate its settling velocity. The velocity was measured five times for each type of tracer. These settling velocities are shown in Table B-1.

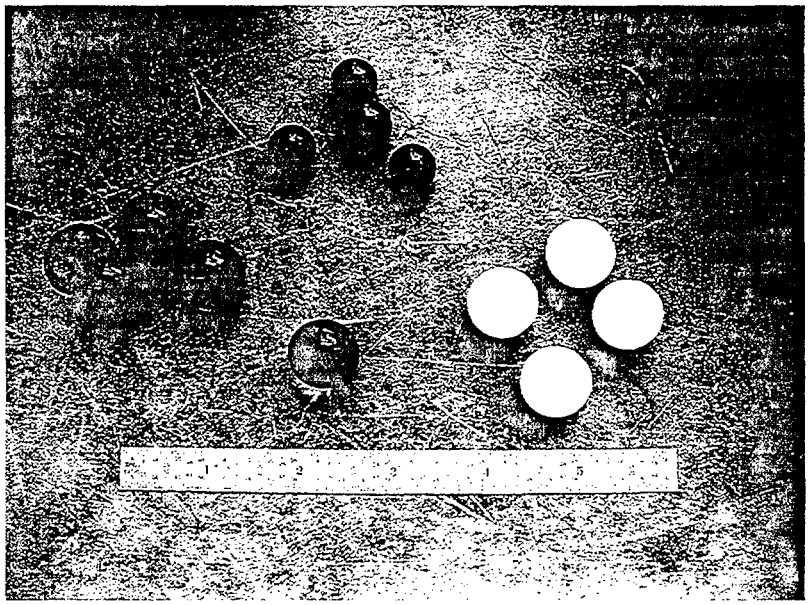

Figure B-1 Calibrated Acrylic (Left), Nylon (Right), and Glass (Top) Spherical Tracers

Table B-1 Settling Velocity of Calibrated Spherical Tracers					
Acrylic Spheres		Nylon Spheres		Glass Spheres	
Fall Time (s)	Velocity (ft/s)	Fall Time (s)	Velocity (ft/s)	Fall Time (s)	Velocity (ft/s)
3.10	0.806	4.32	0.579	1.84	1.359
3.34	0.749	4.03	0.62	1.72	1.453
3.28	0.762	3.81	0.656	1.60	1.563
3.21	0.779	3.94	0.635	1.72	1.453
2.85	0.877	4.57	0.547	1.98	1.263
Average	**0.795**	**Average**	**0.607**	**Average**	**1.418**

The tumbling velocities of the three types of tracers were measured in a linear flume under uniform flow conditions. A steady-state flow at a depth of about 18 in. was established in the flume at a low rate of flow. Several tracers were placed on the floor of the flume's test section. The flow then was increased gradually while the water level was kept constant until the tracers began to roll. The results are shown in Table B-2. The velocity at which some of the tracers moved was noted, and then the velocity where all of the tracers moved was noted.

The velocities measured for the spherical tracers are compared with velocities measured for typical types of debris in Table B-3. Because the tracers settled in water much faster than the typical debris, particularly LDFG, the tracers would not be suitable for testing where debris suspension was involved. However, for floor debris transport, the acrylic and nylon tracers made suitable surrogates for the purposes for which they were used. (Again, note that the glass spheres were not used.) The tumbling velocities for the acrylic and nylon tracers were nearly the same as the velocities for RMI but somewhat higher than the velocities for LDFG.

Table B-2 Incipient and Bulk Movement Tumbling Velocity of Calibrated Spherical Tracers			
Flow (ft/s)	**Acrylic Spheres**	**Nylon Spheres**	**Glass Spheres**
0.18	No Movement	No Movement	No Movement
0.20	No Movement	No Movement	No Movement
0.22	Some move	Some move	No Movement
0.27	**All move**	**All move**	No Movement
0.40			No Movement
0.45			Some move
0.53			**All move**

Table B-3 Measured Settling and Tumbling Velocities		
Test Item	**Settling Velocity (ft/s)**	**Tumbling Velocity (ft/s)**
Acrylic Sphere	0.76 to 0.88	0.22 to 0.27
Nylon Sphere	0.55 to0.66	0.22 to 0.27
Glass Sphere	1.26 to 1.56	0.45 to 0.53
LDFG	0.13 to 0.41	0.12 to 0.16
Al-RMI	0.08 to 0.21	0.20 to 0.25
SS-RMI	0.23 to 0.58	0.28 to 0.30

B.2 Spherical Tracer Motion Test Matrix and Test Results

Flow velocities within the tank were measured by timing the movement of an object through the water where the distance traversed could be estimated. After a steady-state flow and water level were established within the pool, spherical tracers were placed onto the tank floor one at a time and allowed to move with the flow. Their progress was charted for a period of 30 s. The distance traveled can be estimated using the charts from which the average velocity of the tracer can be estimated. More importantly, the tracks of the tracers yielded qualitative information regarding flow patterns. With many tracer motion tracks placed onto a single chart, the patterns of flow can be visualized. All of the spherical tracer motion tests were performed with 9 in. of water in the tank and steady-state flow conditions.

A total of 12 tests was conducted under this exploratory series; the test matrix is shown in Table B-4. The parameters varied included the location of the inlet pipe (test configuration), the pump flow rate, and the object tested. The number of individual tracks recorded for each test also is listed. Note that seven tests used spherical tracers and produced motion charts. The other five tests used insulation debris and provided only qualitative information regarding debris movement from its initial location and transport toward a quiescent region. Nine of the tests were conducted with the inlet pipe located in the annulus on the opposite side of the tank from the outlet box (Configuration A). In the other three tests, the inlet pipe was located in one of the interior compartments (Configurations B and C). These configurations are shown in Figures 2-5 through 2-7.

The results of the spherical tracer motion tests were recorded in charts in which the 30-s tracks of the tracers were sketched on a scaled drawing of the tank test apparatus. The beginning of each track is indicated by a black dot, and arrows indicate the direction taken by the tracer. When the tracer came to a rest within the 30-s period, the end point of the track is indicated by a black dot. However, when the tracer was still moving at the end of the 30-s period, an arrow at the end of the track indicates the end of the track.

Table B-4 Matrix of Spherical Tracer Motion Tests				
Test Number	**Test Objects**	**Test Configuration**	**Pump Flow (gpm)**	**Number of Sphere Tracks**
S1	Acrylic Spheres	A	150	13
S2	Acrylic Spheres	A	135	12
S3	Nylon Spheres	A	150	15
S4	Nylon Spheres	A	135	15
S5	Nylon Spheres	B	120	51
S6	Nylon Spheres	B	170	47
S7	Nylon Spheres	C	95	35
S8	LDFG	A	120	-
S9	LDFG	A	145	-
S10	Aluminum RMI	A	180	-
S11	Aluminum RMI	A	230	-
S12	Aluminum RMI	A	440	-

Tests S1 and S2. In the first test, Test S1, 13 30-s tracks using acrylic spherical tracers were recorded on the chart shown in Figure B-2. In Test S1, the inlet pipe was located in the annulus (Configuration A), and the pump flow was steadied at about 150 gpm with a tank level of 9 in. of water. Test S2 was conducted in the same manner as Test S1, except the pump flow rate was reduced to 135 gpm. The chart for Test S2 is shown in Figure B-3. Exploratory testing verified that a flow rate in this general range would provide the most useful range of flow conditions. At these flows, it was possible to identify areas where the tracers moved and areas where the tracers did not move. A comparison of Figures B-2 and B-3 shows less overall movement of the tracers in Test S2 than in Test S1. In fact, many of the spherical tracers in Test S2 did not move at all from their initial location, whereas all of the tracers in Test S1 moved regardless of their initial location in the annulus. Thus, it was observed that the relatively small variation in flow could alter floor debris transport significantly. The spherical tracer tracks in these tests indicate that the tracers were moving as fast as about 0.18 ft/s and as slow as no movement. The water was likely actually flowing a little faster than the tracers were moving. It must be kept in mind that when a tracer stopped before the 30-s period ended, this means that the tracer had a zero velocity during a portion of the 30 s.

Tests S3 and S4. Tests S1 and S2 essentially were repeated with the exception that the nylon spherical tracers were used rather than the acrylic tracers. The test results for Tests S3 and S4 are shown in Figures B-4 and B-5, respectively. The comparison of Tests S3 and S4 show the same general differences as Tests S1 and S2. However, the tests using nylon tracers indicated slightly less movement than did the tests using acrylic tracers. The reasons for this difference are not clear. The velocities for incipient tumbling were essentially the same, at least within the limits of the tests. Both types of tracers had the same diameter; however, the nylon tracers (with a specific gravity of 1.14) were slightly lighter than the acrylic tracers (with a specific gravity of 1.39). One might have expected the lighter nylon tracers to move more easily than the heavier acrylic tracers, not the other way around as indicated by the tests. More likely, uncertainty in test parameters such as the flow rate, water level, and the placement of the tracers were the cause of the difference found between the two types of tracers.

Tests S5 and S6. Two tests were conducted using nylon spherical tracers with the inlet pipe located in an inner compartment (Configuration B). Tests S5 and S6 were conducted at pump flow rates of 120 and 170 gpm, respectively, and the test results are shown in Figures B-6 and B-7, respectively. These flow rates were chosen to provide a distinct discrimination between areas of movement and no movement. As expected, the flow patterns were significantly more complex for Configuration B than for Configuration A. These two charts illustrate average tracer velocities ranging from no movement up to about 0.3 ft/s, with some track becoming rather convoluted.

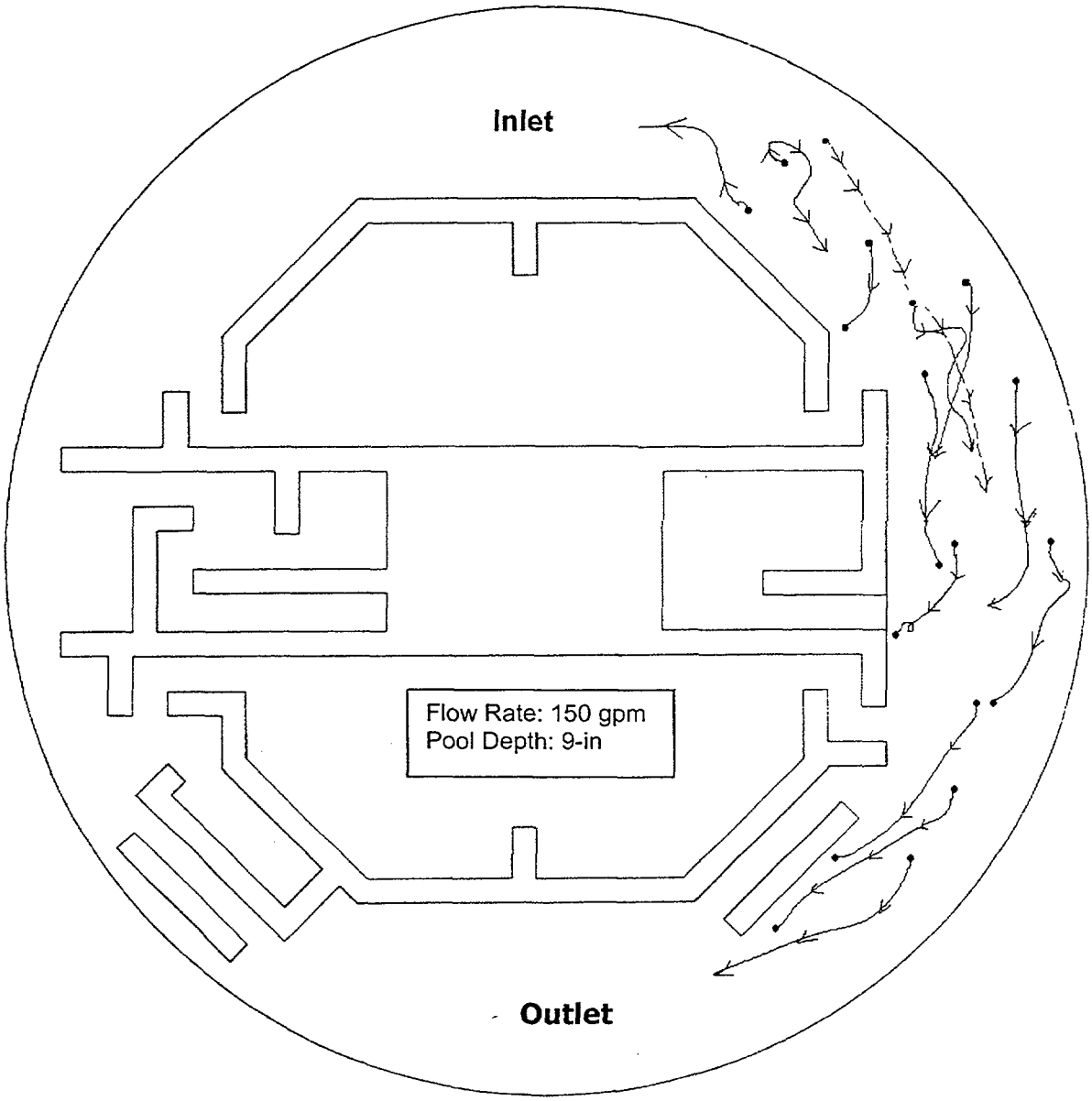

Figure B-2 Chart of Acrylic Spherical Tracer Motion Tracks for Test S1

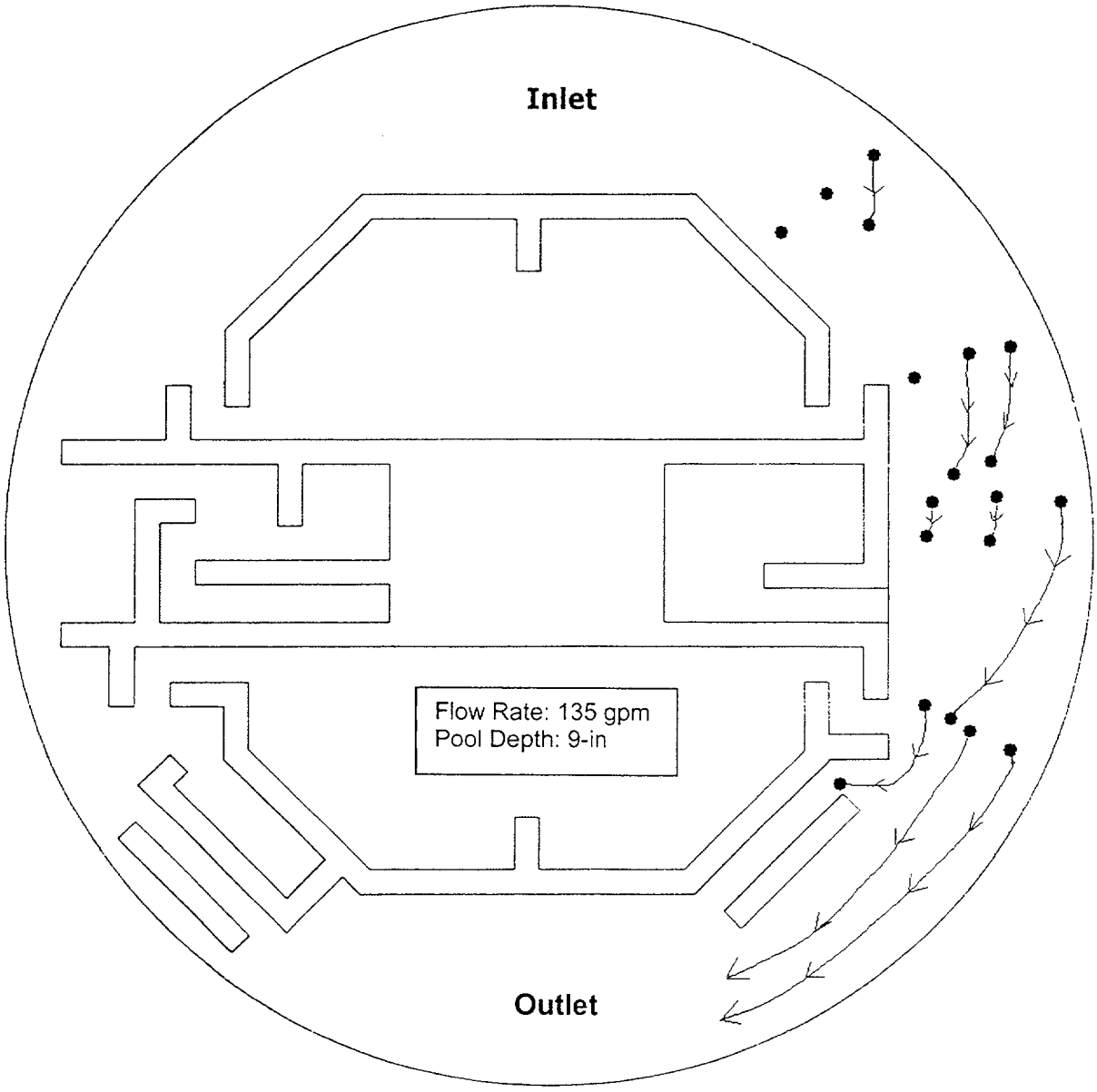

Figure B-3 Chart of Acrylic Spherical Tracer Motion Tracks for Test S2

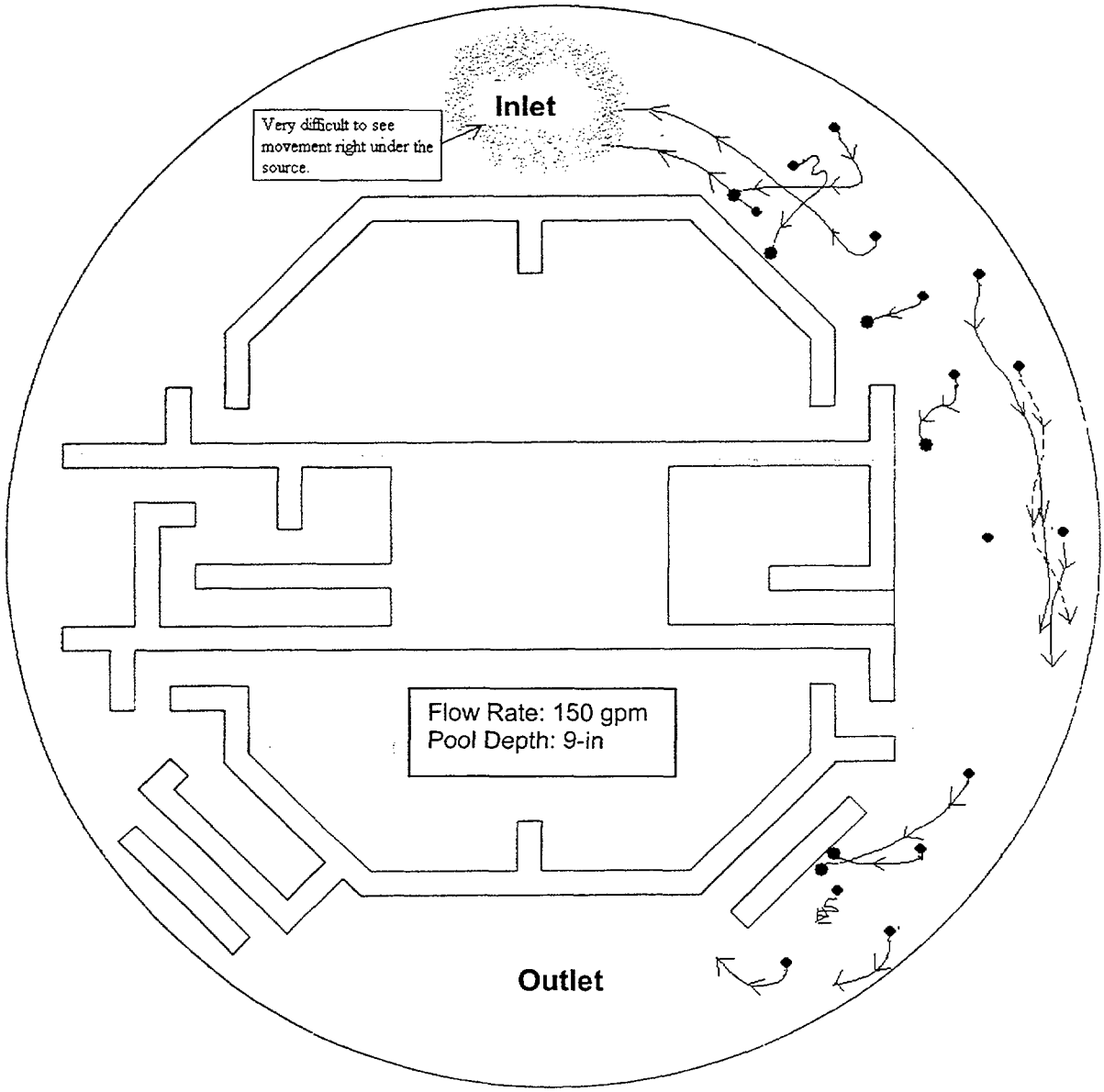

Figure B-4 Chart of Nylon Spherical Tracer Motion Tracks for Test S3

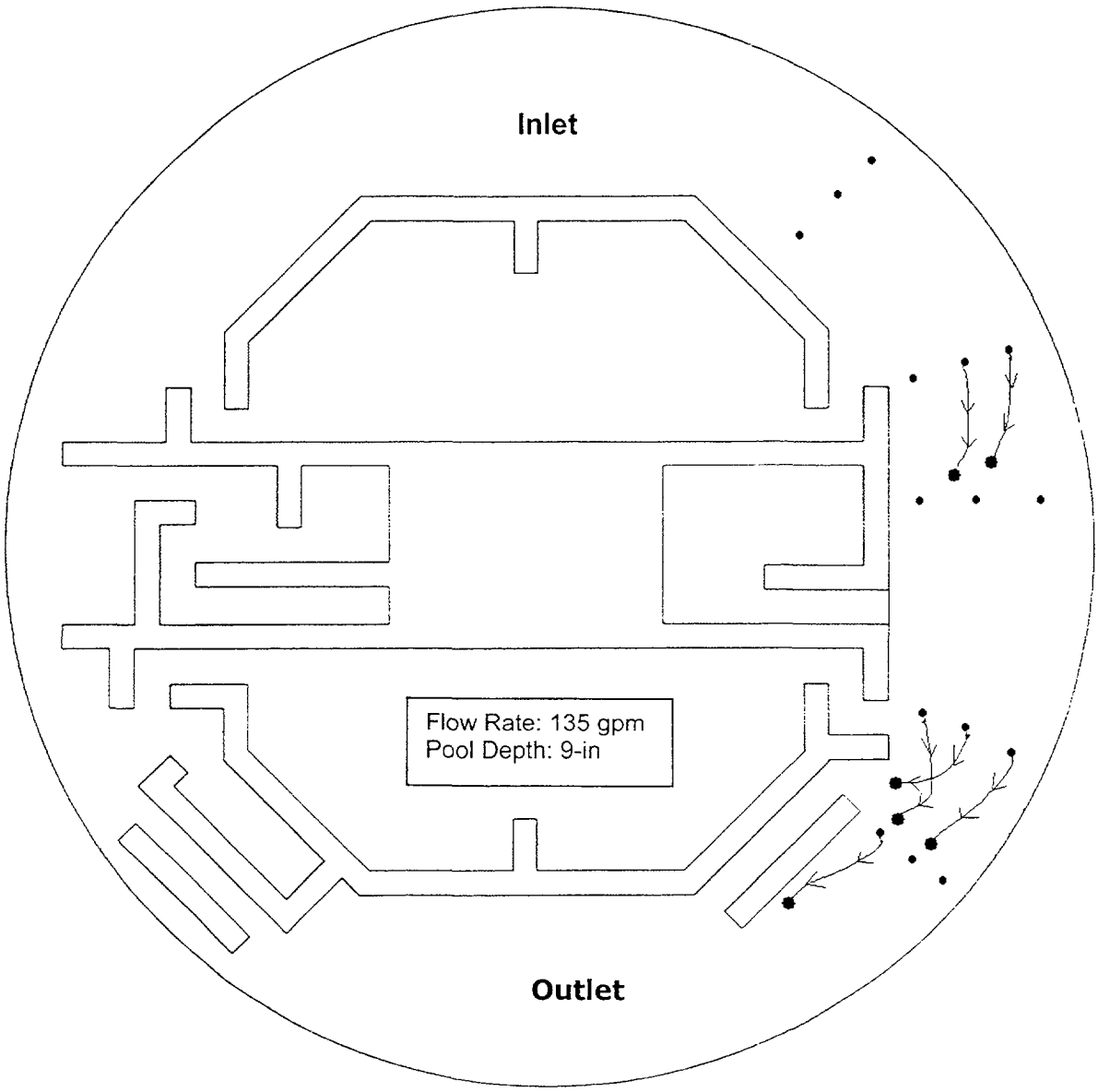

Figure B-5 Chart of Nylon Spherical Tracer Motion Tracks for Test S4

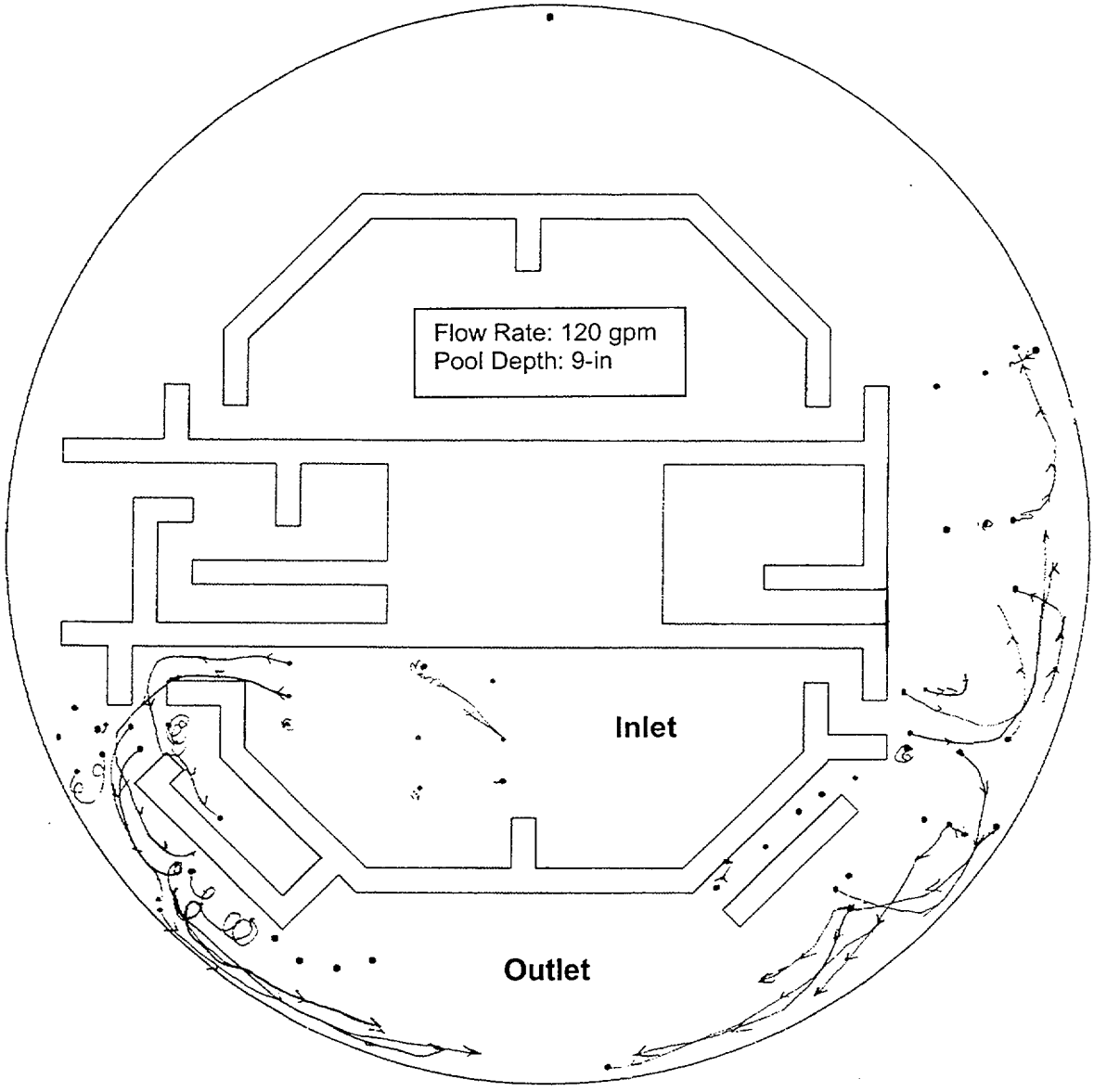

Figure B-6 Chart of Nylon Spherical Tracer Motion Tracks for Test S5

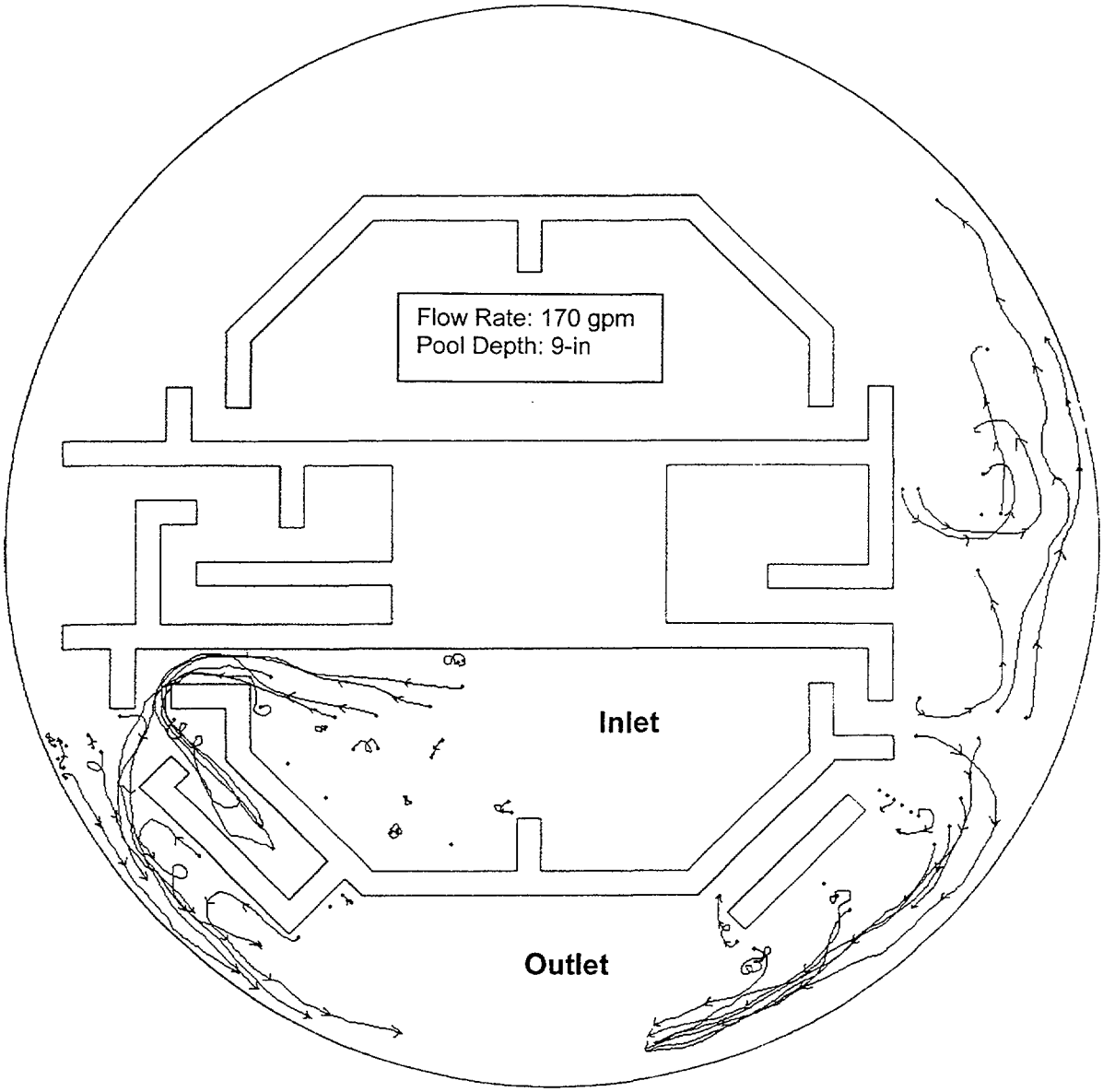

Figure B-7 Chart of Nylon Spherical Tracer Motion Tracks for Test S6

Test S7. One test was conducted with the inlet pipe located in a different inner compartment (Configuration C) and also using nylon tracers. Test S7 was conducted a pump flow rate of 95 gpm, and the test results are shown in Figure B-8. At this lower flow rate, the transport of the tracers basically was limited to the areas where the flow from the inner compartment was channeled through narrow exits to the annulus. In the annulus, transport to the outlet box was very limited.

Tests S8 through S12. Five tests were conducted using samples of LDFG and Al-RMI insulation debris, rather than spherical tracers. The debris was placed at various locations along the tank annulus floor. The areas are marked on the results chart (Figure B-9) with a circle to show the initial location of the debris. Figure B-9 applies to all five of these tests. A 4-in.-diam pipe was used to place the debris onto the floor. The chart simply indicates a couple of quiescent regions (the shaded areas are designated as dead zones) near the debris release points that collected substantial debris. Specific results included the following.

- At 120 gpm, LDFG did not move from drop Release Point 1, about 2/3 of sample moved from Point 4, and all LDFG moved from Point 5.
- At 145 gpm, LDFG moved from every release location, and significant quantities of the debris ended up in the quiescent regions. However, the Al-RMI did not move from any of the locations at this velocity.
- At 180 gpm, the Al-RMI still did not move from any location.
- At 230 gpm, about one-half of the Al-RMI moved from Release Points 1, 3, and 5.
- At 440 gpm, all of the Al-RMI moved downstream.

These tests clearly illustrated that it takes much higher flow velocities to move RMI debris than it takes to move LDFG debris. These results contributed to a decision to focus on LDFG debris and limit the testing of RMI debris. These tests also illustrated entrapment of debris within the quiescent regions, i.e., regions where flow agitation and velocities were not sufficient to move the debris further.

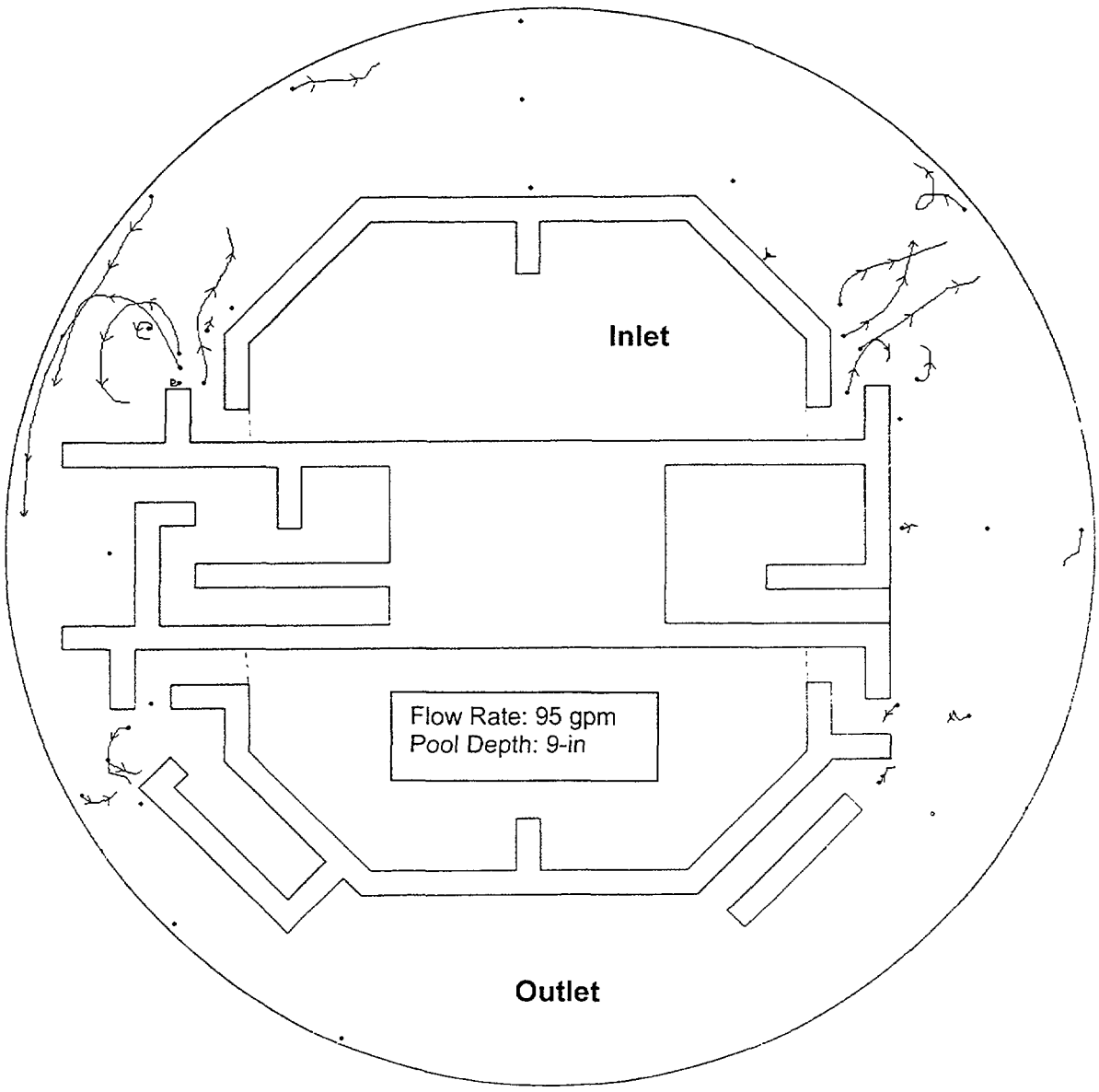

Figure B-8 Chart of Nylon Spherical Tracer Motion Tracks for Test S7

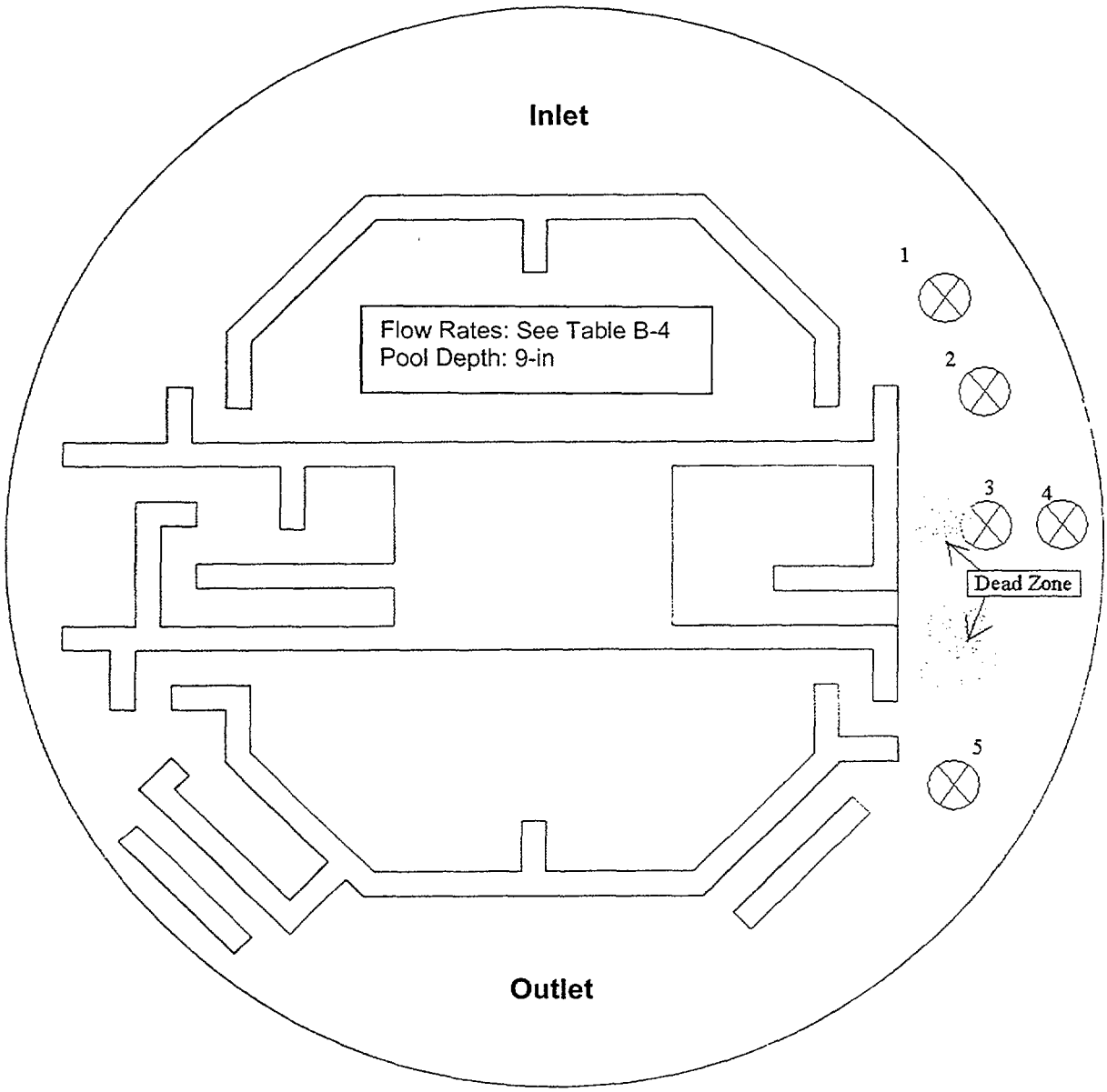

Figure B-9 Chart of LDFG and Al-RMI Debris Motion for Tests S8 through S12

NRC FORM 335 (2-89) NRCM 1102, 3201, 3202

U.S. NUCLEAR REGULATORY COMMISSION

BIBLIOGRAPHIC DATA SHEET

(See instructions on the reverse)

1. REPORT NUMBER (Assigned by NRC, Add Vol., Supp. Rev. and Addendum Numbers, if any.)
NUREG/CR-6773

2. TITLE AND SUBTITLE
GSI-191: Integrated Debris-Transport Tests in Water Using Simulated Containment Floor Geometries

3. DATE REPORT PUBLISHED
MONTH | YEAR
December 2002

4. FIN OR GRANT NUMBER
Y-6041

5. AUTHOR(S)
D. V. Rao, C. J. Shaffer (ARES Corporation, 851 University Blvd. S.E., Suite 100, Albuquerque, NM 87106), B. C. Letellier, A. K. Maji (University of New Mexico, Department of Civil Engineering, Albuquerque, NM 87110) and L. S. Bartlein

6. TYPE OF REPORT
Final

7. PERIOD COVERED *(Inclusive Dates)*
September 2000-December 2002

8. PERFORMING ORGANIZATION – NAME AND ADDRESS *(If NRC, provide Division, Office or Region, U.S. Nuclear Regulatory Commission, and mailing address; if contract, provide name and mailing address.)*

Probabilistic Risk Analysis Group (D-11)
Los Alamos National Laboratory
Los Alamos, NM 87545

9. SPONSORING ORGANIZATION – NAME AND ADDRESS *(If NRC, type "Same as above"; if contract, provide NRC Division, Office or Region, U.S. Nuclear Regulatory Commission, and mailing address.)*
Division of Engineering Technology, Office of Nuclear Regulatory Research, US Nuclear Regulatory Commission, Washington, DC 20555-0001

10. SUPPLEMENTARY NOTES
B. P. Jain and M. L. Marshall, NRC Project Managers

11. ABSTRACT *(200 words or less)*

This report documents the results of experiments conducted to examine insulation debris transport under flow and geometry configurations typical of those found in pressurized water reactors (PWRs). This work was part of a comprehensive research program to support the resolution of Generic Safety Issue (GSI)-191. GSI-191 addresses the potential for debris accumulation on PWR sump screens and consequent loss of the emergency core cooling system pump net positive suction head following a loss-of-coolant accident. Among the GSI-191 program research tasks is the development of a method to estimate debris transport in PWR containments and the quantity of debris that would accumulate on the sump screen for use in plant-specific evaluations. Predicting the transport of debris within the sump pool is an essential part of that methodology.

The analytical method proposed by the Los Alamos National Laboratory to predict debris transport within the pool is to use computational fluid dynamics combined with experimental debris transport data to predict debris transport and accumulation on the screen. The three-dimensional tank tests were conducted to test debris transport under conditions that simulate flow regimes relevant to a typical PWR plant. These tests provided insights into the relative importance of the various debris-transport mechanisms and are directly applicable to creating or validating models capable of estimating debris transport within a PWR plant containment sump.

12. KEY WORDS/DESCRIPTORS *(List words or phrases that will assist researchers in locating this report.)*

Emergency Core Cooling System, Recirculation Sump, Loss of Coolant Accident, Thermal Insulation Debris Blockage, ECCS Net Positive Suction Head, ECCS Performance, Sump Clogging, Testing

13. AVAILABILITY STATEMENT
unlimited

14. SECURITY CLASSIFICATION
(This Page)
unclassified
(This Report)
unclassified

15. NUMBER OF PAGES

16. PRICE

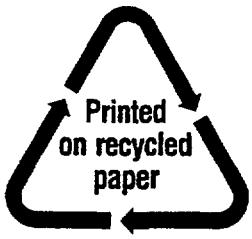

Federal Recycling Program